Centre of Excellence in Engineered Fibre Composites
Faculty of Engineering and Surveying

DEVELOPMENT OF HEMP OIL BASED BIORESINS FOR BIOCOMPOSITES

A dissertation submitted by

Nathan William Manthey

BE (Mechanical) (Hons I)

For the award of

DOCTOR OF PHILOSOPHY

2013

Principal supervisor

Dr. Francisco Cardona

Associate supervisor

Prof. Thiru Aravinthan

Abstract

Within the civil engineering and construction industries fibre composites are now being adopted in certain applications in place of more traditional building materials such as timber and steel. Although, fibre composites possess certain advantages over traditional building materials they are predominately produced from non-renewable resources. Of particular concern is the petro-chemical based polymer resins commonly used such as epoxy, vinylester and polyester. It is due to this dependence on finite petro-chemicals and the negative environmental impact associated with their production and uses that alternative, competitive options are sought. Plant oil based bioresins are one such option. Although in its infancy, research suggests that biocomposites produced with plant oil based bioresins and plant based fibres offer the potential to be used as a sustainable replacement option to traditional fibre composites.

The research work presented within this dissertation is to the best of the author's knowledge a world-first overall investigation pertaining to the concept of synthesising hemp oil based bioresins and applying them to biocomposites. In this work hemp oil based bioresins, specifically epoxidized hemp oil (EHO) and acrylated epoxidized hemp oil (AEHO) were synthesised and characterised and proposed as a potential replacement to their equivalent synthetic polymer resins (epoxy and acrylated resins) and also as an alternative to other commercially available bioresins. The synthesised bioresins were also applied as matrices in the production of suitable biocomposites. Hemp oil was epoxidized in a solvent free process using peracetic acid and an acid ion exchange resin (AIER) catalyst via *in situ* epoxidation. From ^{1}H-NMR spectroscopy analysis, oxirane oxygen content was calculated as approximately 8.6% and a relative conversion to oxirane of 92% with approximately 5.1 epoxy groups per triglyceride. AEHO was synthesised from EHO via *in situ* acrylation. According to the ^{1}H-NMR analysis of AEHO, acrylate peaks were apparent and were of the magnitude of approximately 4.1 acrylates per triglyceride. Some

epoxide homopolymerisation was observed limiting conversion to AEHO to approximately 81%. Curing analysis and cure kinetic modelling were also performed for both EHO and AEHO. The kinetics of curing of both bioresin systems were able to be accurately modelled using a modified expression of Kamal's autocatalytic model.

The synthesised bioresins were applied to biocomposites and characterised in terms of mechanical, dynamic mechanical and moisture absorption properties. Scanning electron microscopy (SEM) was also performed to investigate the fibre-matrix interfacial adhesion. EHO based bioresins and jute fibre reinforced biocomposites were manufactured and compared with commercially produced epoxidized soybean oil (ESO) and synthetic epoxy based samples. It was found that EHO based bioresins when applied to jute fibre reinforced biocomposites can compete with commercially produced ESO in terms of mechanical performance, dynamic mechanical properties and water absorption characteristics. Although it was shown that EHO can be used in higher concentrations than ESO when blended with synthetic epoxy thereby resulting in more sustainable biocomposites.

AEHO based bioresins and jute fibre reinforced biocomposites were manufactured and compared with commercially produced vinylester (VE) based samples. AEHO based samples exhibited higher fibre-matrix interfacial adhesion compared with the VE based samples.

Finally the mechanical performance, dynamic mechanical properties and moisture absorption properties of 100% hemp based biocomposite panels were investigated and compared to those of a VE hybrid composite. Results showed that, except for the flexural modulus that was 23% higher in the case of the hybrid composite, no significant differences exist in the mechanical performance of both tested materials. The higher fibre-matrix compatibility of the biocomposites led to stronger fibre-matrix interfaces compensating the lower mechanical performance of the neat bioresin with respect to the synthetic VE resin.

All of the biocomposite sample types displayed lower dynamic mechanical properties compared with their synthetic counterparts. As, expected moisture absorption was also found to be higher in the biobased specimens although fibre transport was the dominate mechanism rather than resin type.

Overall from this research work it can be concluded that hemp oil based bioresins can effectively compete with commercially available bioresins and their equivalent synthetics in biocomposite applications. An enhanced understanding of the synthesis, characterisation and performance of hemp oil based bioresin and biocomposites for use in engineering applications is a key outcome of this investigation.

Certificate of dissertation

I certify that the ideas, experimental work, results, analysis and conclusions reported in this dissertation are entirely my own effort, except where otherwise acknowledged. I also certify that the work is original and has not been previously submitted for any award, except where otherwise acknowledged.

_____ Date: / /

Signature of Candidate

ENDORSEMENT

_____ Date: / /

Signature of Principal Supervisor

Dr. Francisco Cardona

_____ Date: / /

Signature of Associate Supervisor

Prof. Thiru Aravinthan

Acknowledgments

I would like to thank my supervisors, Dr. Francisco Cardona and Prof. Thiru Aravinthan for taking on the responsibility of supervising this PhD. Francisco, thank you for your patience, encouragement, guidance, persistence, expert advice and friendship throughout the past four years, your contribution to the completion of this work cannot be understated. I will always be indebted to you. Thiru, thank you for your patience, expert advice and help, especially with the scholarship application processes, without your support this work would not have been possible.

I would also like to take this opportunity to acknowledge the support provided by the Faculty of Engineering and Surveying (FoES), the Centre of Excellence in Engineered Fibre Composites (CEEFC) and the University of Southern Queensland (USQ). I would also like to thank the Queensland State Government's financial contribution in the form of a Smart Futures PhD Scholarship. Martin Geach, thank you for always ensuring that I received what I needed and for putting up with my many requests. Wayne Crowell, thank you for proving expert advice and assistance with sample preparation and testing. Your advice saved me numerous headaches throughout this work. Juanita Ryan, thanks for providing administrative support. Kim Larsen thanks for always coming through with any laboratory equipment when I was in need. Sandra Cochrane, thanks for your encouragement and helping out with all of my queries and requests. Dr. Steven Goh, thanks for being a mentor to me and for providing opportunities and advice regarding professional development.

Thank you to my friends Tyson Cooney and Dr. Gaston Francucci that directly supported me throughout this work. Tyson and Gaston, sharing an office with you both made my time at the CEEFC far more enjoyable. Thank you both for your friendship, advice, guidance and support. I would also like to thank all of my dear friends who have helped me throughout my life and indirectly with this PhD. Thank you, Luke Hildred, Glenn Moore, Chris Pickford, Megan Pickford, Jeff Pickford and Mustafa Jamal Eddine. Each of you have provided me with

encouragement and stuck with me throughout my life, even though I was not easy to deal with and at times was, no doubt a prick. I am indebted to each of you.

Finally I wish to thank my family. Mum and dad thank you both from the bottom of my heart for all of your love, endless patience, continuous support and encouragement throughout my life. It is because of you both that I am where I am today. Thank you to my brothers and my two best friends, Quinton and Byron. Quinton, thank you for helping me relax and take my mind off of work when required. Byron, thank you for helping me get through some of the hardest times in my life during the past three years. To my two beautiful 'sisters', Amy and Jackie. Amy, thank you for your encouragement and kindness. Jackie, thank you for putting up with my 'moods', making my life less stressful and for having Lilly.

To those whom I have not mentioned but have been a part of this endeavour, I thank you.

Disclaimer

This research is proudly supported by the Queensland Government's Growing the Smart State PhD Funding Program and may be used to assist public policy development. However, the opinions and information contained in this research do not necessarily represent the opinions of the Queensland Government or carry any endorsement by the Queensland Government. The Queensland Government accepts no responsibility for decisions or actions resulting from any opinions or information supplied.

This dissertation is dedicated to anyone suffering from depression.
I hope it serves to encourage you to never give in to the darkness, but instead to push through, live your life, pursue your passions and never ever give up.

Beyondblue

Phone: 1300 22 4636

Email: infoline@beyondblue.org.au

Web: www.beyondblue.org.au

"*I've missed more than 9000 shots in my career. I've lost almost 300 games. 26 times, I've been trusted to take the game winning shot and missed. I've failed over and over and over again in my life. And that is why I succeed.*"

Michael Jordan

Associated publications

The following publications were produced as a direct result of this PhD candidature:

Journal articles

N. W. Manthey, F. Cardona, T. Aravinthan, T. Cooney, "Cure kinetics of an epoxidized hemp oil based bioresin system," Journal of Applied Polymer Science, vol. 122, pp. 444-451, 2011.

N. W. Manthey, F. Cardona, T. Aravinthan, "Cure kinetic study of epoxidized hemp oil cured with a multiple catalytic system," Journal of Applied Polymer Science, vol. 125, pp. E511-E517, 2012.

G. Francucci, F. Cardona, **N. W. Manthey**, "Cure kinetics of an acrylated epoxidized hemp oil (AEHO) based bioresin system," Journal of Applied Polymer Science, vol. 128, No. 3, pp. 2030-2037, 2012.

N. W. Manthey, F. Cardona, G. Francucci, T. Aravinthan, "Thermo-mechanical properties of acrylated epoxidized hemp oil biocomposites," Journal of Composite Materials, 2013.
doi: 10.1177/0021998313488155

G. Francucci, **N. W. Manthey**, F. Cardona, T. Aravinthan, "Processing and characterization of 100% hemp based biocomposites obtained by vacuum infusion," Journal of Composite Materials, 2013.
doi: 10.1177/002199831485266

N. W. Manthey, F. Cardona, G. Francucci, T. Aravinthan, "Thermo-mechanical properties of epoxidized hemp oil based bioresins and biocomposites," Journal of Reinforced Plastics and Composites, 2013.
(Accepted – In production)

Refereed conference proceedings

N. W. Manthey, F. Cardona, T. Aravinthan, H. Wang, T. Cooney, "Natural fibre composites with epoxidized vegetable oil (EVO) resins: a review" In: SREC 2010: Southern Region Engineering Conference, 11-12 Nov 2010, Toowoomba, Australia.

N. W. Manthey, F. Cardona, T. Aravinthan, H. Wang, T. Cooney, "Natural fibre composites with QLD based fibres and vegetable oils" In: ACMSM 21: Incorporating Sustainable Practice in Mechanics of Structures and Materials, 7-10 Dec 2010, Melbourne, Australia.

N. W. Manthey, F. Cardona, T. Aravinthan, "Mechanical properties of epoxidized hemp oil based biocomposites: preliminary results" In: eddBE2011: 1st International Postgraduate Conference on Engineering, Designing and Developing the Built Environment for Sustainable Wellbeing, 27 -29 Apr 2011, Brisbane, Australia.

N. W. Manthey, F. Cardona, G. Francucci, T. Aravinthan, "Green Building Materials: Hemp Oil Based Biocomposites", ICACE2012: International Conference on Architectural and Civil Engineering, 24-25 Oct 2012, Bali, Indonesia.

Table of contents

List of figures

Chapter 2 **Biocomposites using plant oil based thermosetting resins: A review**

Chapter 3 **Synthesis and characterisation of hemp oil based bioresins**

Chapter 5 Thermo-mechanical properties of hemp oil based bioresins and biocomposites

Appendix A

List of tables

Chapter 2 **Biocomposites using plant oil based thermosetting resins: A review**

Chapter 3 **Synthesis and characterisation of hemp oil based bioresins**

Chapter 4 **Cure kinetics of hemp oil based bioresins**

Chapter 5 Thermo-mechanical properties of hemp oil based bioresins and biocomposites

Chapter 6 Production and characterisation of 100% hemp based biocomposites

Acronyms and abbreviations

AAMSO	Acetic Anhydride Modified Soybean oil
AEHO	Acrylated Epoxidized Hemp Oil
AELO	Acrylated Epoxidized Linseed Oil
AESO	Acrylated Epoxidized Soybean Oil
AEVO	Acrylated Epoxidized Vegetable Oil
AIER	Acid Ion Exchange Resin
C-C	Carbon-Carbon Bond
C=C	Carbon-Carbon Double Bond
CCC	Carbon-Carbon Composites
CMC	Ceramic Matrix Composites
CNSL	Cashew Nut Shell Liquid
DGEBA	Bisphenol A Diglycidyl Ether
DMA	Dynamic Mechanical Analysis
DSC	Dynamic Scanning Calorimetry
E’	Storage Modulus
EAS	Epoxidized Allyl Soyate
ECO	Epoxidized Canola Oil
EEW	Epoxy Equivalent Weight
EHO	Epoxidized Hemp Oil
ELO	Epoxidized Linseed Oil
EMS	Epoxidized Methyl Soyate
EPO	Epoxidized Palm Oil
ESO	Epoxidized Soybean Oil
ESOA	Epoxidized Soybean Oil Acrylate
EVO	Epoxidized Vegetable Oil
FTIR	Fourier Transform Infrared Spectroscopy
HF	Hemp Fibre
^{1}H-NMR	Proton Nuclear Magnetic Resonance
ILSS	Interlaminar Shear Strength
IMC	intermetallic matrix composites
IPD	Isophorone Diamine
IV	Iodine Value
KF	Keratin Fibre
LCM	Liquid Composite Moulding
LO	Linseed Oil
MEKP	Methyl Ethyl Ketone Peroxide
MMC	Metal Matrix Composites
MMSO	Methacrylic Anhydride Modified Soybean oil
MSO	Methacrylated Soybean Oil
MUFA	Monounsaturated Fatty Acid

OO	Oxirane Oxygen
PAN	Polyacrylonitrile
PMC	Polymer Matrix Composites
PPE	Personal Protective Equipment
PUFA	Polyunsaturated Fatty Acid
RTM	Resin Transfer Moulding
SFA	Saturated Fatty Acid
SEM	Scanning Electron Microscopy
SFO	Sunflower Oil
TAG	Triglyceride
TETA	Triethylenetetramine
T_g	Glass Transition Temperature
THC	delta-9-tetrahydrocannabinol
TMS	Tetramethylsilane
UP	Unsaturated Polyester
VARTM	Vacuum Assisted Resin Transfer Moulding
v_e	Crosslink Density
VE	Vinyl Ester
VI	Vacuum Infusion
VO	Vegetable Oil

Chapter 1

INTRODUCTION

1.1 General

Queensland's economy is heavily reliant on mining, agriculture, tourism and financial services. According to the Queensland Government, agriculture contributes more than $10 billion to the economy annually (Queensland State Government 2012). In Queensland there is government interest and support into the development and commercialisation of biobased industrial products for both industrial and consumer applications (Gillard 2010). Currently this biobased market is dominated by biofuels involving the utilisation of corn and sugar-cane.

To achieve and sustain growth within this area of biobased products it is imperative that novel high value added outputs must replace traditional low value outputs. Diffusion of these new technologies and products is a central component to regional Queensland's global technological future. Southern Queensland is an area with significant economic potential as it has the proven ability to grow plant oils such as sunflower, canola and industrial hemp for use as sustainable biobased polymers (Van Erp, G & Rogers 2003). These plant oils are directly applicable to the growing civil engineering and construction based fibre composite market.

Fibre composites have risen to prominence throughout civil engineering and construction industries due to their inherent design flexibility and relative low

whole-of-life-costs (Wool, R. & Sun 2005). Fibre composites consist of a petrochemically derived polymer resin matrix reinforced with synthetic fibres such as glass, aramid and carbon. Increasing environmental awareness to their use within the fibre composite industry is propelling the development of bioresins based on renewable natural materials. Bioresins are an emerging sustainable material often derived from plant oils and due to their biological origin represent a sustainable, low environmental impact option to existing petrochemically derived resins. They may be reinforced with natural or synthetic fibres thereby creating a class of materials termed, natural fibre composites or biocomposites.

Plant oil based bioresins, such as those studied within, offer a potential alternative to petrochemical based polymer resins. Moreover, the required plant oil feedstocks are readily available in Queensland with several main types of oilseed crops, namely soybeans (20000 tonnes/annum) and sunflowers (31700 tonnes/annum) being harvested (Australian Oilseeds Federation 2010). An extensive collection of research involving plant oil based bioresins in terms of synthesis, characterisation and in biocomposite applications has been conducted by many authors (Adekunle, Åkesson & Skrifvars 2010a, 2010b; Bouchareb & Benaniba 2008; Can et al. 2006a, 2006b; Chandrashekhara, K et al. 2002; Czub 2006a, 2006b; Dweib et al. 2006; Espinoza-Pérez, Haagenson, et al. 2009; Espinoza-Pérez et al. 2008; Espinoza-Pérez, Wiesenborn, Kristi, et al. 2007; Espinoza-Pérez, Wiesenborn, Tostenson, et al. 2007; Espinoza-Pérez, Wiesenborn, et al. 2009; Hong & Wool 2005; Jin & Park 2008; Khot et al. 2001; Meyer et al. 2008; O'Donnell, Dweib & Wool 2004; Park, Jin & Lee 2004; Petrovic et al. 2002; Takahashi et al. 2008; Wool, R. & Sun 2005; Zhu, Jiang et al. 2004). This research encompasses numerous different plant oil feedstocks with the chief focus being on soybean, canola and linseed oils. However these oils are also used in food production which may pose ethical issues should demand for biobased feedstocks to service the civil engineering and construction industries increase. Therefore, to alleviate this conflict of interest it is imperative to focus on using fast growing, non-food oil crops for use as bioresin feedstocks. One

such type of oil crop that has shown initial promise as a bioresin feedstock, is industrial hemp.

At the Centre of Excellence in Engineered Fibre Composites (CEEFC) research into the development of novel hemp oil based bioresins, such as epoxidized hemp oil (EHO) and acrylated epoxidized hemp oil (AEHO) for biocomposite applications is being conducted. Industrial hemp is able to produce both fibre and oilseeds although the majority of industrial applications and research has focused on using the fibre with hemp oil being viewed essentially as a by-product of fibre production. Therefore, one of the main driving motivations for this research is investigating the development of high commercial value solutions to this 'waste' hemp oil. Worldwide production of industrial hemp fibre and oilseed was 66325 and 30265 t respectively with the main producers of oilseed being China, France and Chile (Anwar, Latif & Ashraf 2006). Investigations into the chemical functionalization of hemp oil have not been undertaken and reported in the literature which is rather surprising given hemp oil's unique fatty acid profile; high in both linoleic and linolenic acid which offers considerable potential as a bioresin feedstock.

1.2 Aim and objectives

It is the overlying aim of this thesis to assess the viability of using hemp oil to produce biobased polymer resins and use these bioresins for the production of biocomposites. Within this overall aim, the following specific research objectives were targeted and met:

1. Synthesise and characterise hemp oil based bioresins; epoxidized hemp oil (EHO) and acrylated epoxidized hemp oil (AEHO).

2. Investigate the curing behaviour and develop curing kinetic parameters and models for EHO and AEHO based bioresins.

3. Determine and investigate the thermo-mechanical properties of neat cured EHO and AEHO based bioresins.

4. Determine and investigate the thermo-mechanical properties of EHO and AEHO based biocomposites with natural fibre reinforcement.

5. Study the moisture absorption behaviour of EHO and AEHO based bioresins and biocomposites and determine the effect of bioresin content on moisture diffusion and saturation moisture content.

1.3 Scope of thesis

As limited prior research has previously been conducted with hemp oil based biopolymers and biocomposites, this study concentrates on the synthesis and characterisation of hemp oil based thermosetting bioresins, specifically EHO and AEHO for use as biocomposite matrices. The objectives of the study were constrained as follows:

1. Review the literature on plant oil, biocomposite matrices and biocomposites.

2. Determine whether hemp oil was a suitable plant oil from which to produce bioresins for biocomposite applications, synthesis of EHO and AEHO were examined. Characterisation of the synthesised EHO and AEHO was performed to investigate the 'quality' and to ascertain their performance to similar resins, be they synthetically derived or biobased.

3. Classify the curing behaviour of hemp oil based bioresins, curing kinetic studies limited to 100% hemp oil based bioresins.

4. Determine the thermo-mechanical properties of the neat bioresins, by conducting flexural, impact and dynamic mechanical analysis (DMA). The

measured properties were compared with commercial synthetic and biobased equivalents.

5. Determine the thermo-mechanical properties of the biocomposites, by conducting flexural, impact and DMA. The measured properties were compared with commercial synthetic and biobased equivalents.

6. Understand the moisture absorption behaviour of the hemp oil based bioresins and biocomposites by conducting moisture absorption analysis. The rate of moisture diffusion and saturation moisture content were investigated and compared with commercial synthetic and biobased equivalents.

1.4 Structure of dissertation

This dissertation is comprised of seven chapters which describe the different investigations conducted in this study.

Chapter 1 provides a general introduction, scope, overall research aim and specific objectives of this study.

Chapter 2 presents a comprehensive literature review related to the work in this thesis. The current status of natural fibre or biocomposite research with a particular emphasis on plant oil based thermosetting polymers is provided. An introduction to fibre composites and thermosetting polymers is presented with attention given to commonly utilised composite processing techniques. Research into the field of biocomposites, specifically research pertaining to utilising plant oil based thermosetting polymer resins is investigated and reviewed. Oleochemistry is discussed with an emphasis on plant based oils and the synthesis of plant based polymers, with a focus on epoxidation and acrylation for use in biocomposites. A review into natural fibres is also presented with a focus on plant based fibres including natural fibre structure

and composition. Factors affecting their use in composite applications are also investigated. Industrial hemp, its origins and current climate within Australian agriculture is reported. Finally the chapter concludes with a review into the leading research regarding the development of biocomposites and the associated applications.

Chapter 3 presents the synthesis and characterisation of hemp oil based thermosetting polymers, EHO and AEHO.

In Chapter 4 the curing kinetics of EHO and AEHO thermosetting polymer resins is presented. Specifically the curing kinetics study and a model for the curing behaviour of EHO based bioresin cured with triethylenetetramine (TETA) are discussed. In addition to this, the curing kinetics of EHO based bioresin cured with a combination of isophorone diamine (IPD) and TETA is reported and compared with the curing kinetics and curing behaviour of EHO based bioresin cured with TETA. Finally the curing kinetics and developed model for the curing behaviour of AEHO based bioresin is reported.

Chapter 5 presents the study on the thermo-mechanical properties of hemp oil based bioresins and biocomposites. Firstly, the effect of EHO concentration on the thermo-mechanical behaviour (glass transition temperature, storage modulus and crosslink density), flexural properties and moisture absorption (saturation moisture level and diffusion coefficient) of EHO based bioresin epoxy blends is reported. Comparisons with commercial epoxidized soybean oil (ESO) based bioresin epoxy blends and a control synthetic epoxy resin were also performed. EHO based bioresin epoxy blends applied to jute fibre based biocomposites are also presented and compared in terms of mechanical properties, thermo-mechanical behaviour (glass transition temperature, storage modulus and crosslink density) and moisture absorption (saturation moisture level and diffusion coefficient) with biocomposite samples prepared using commercially available ESO based bioresins.

Chapter 6 presents the study of 100% hemp based biocomposites, prepared with an AEHO based bioresin reinforced with untreated hemp fibre random mat and compares it to that of hybrid composites prepared with VE resin reinforced with the same hemp fibre mat. Mechanical properties (tensile, flexural, Charpy impact and interlaminar shear), dynamic mechanical properties (glass transition temperature, storage modulus and crosslink density) and moisture absorption properties (saturation moisture level and diffusion coefficient) were investigated and reported.

Chapter 7 provides a summary of the results and the major findings obtained in Chapters 3 to 6. Recommendations and areas for future work based on this thesis are also presented.

1.5 Summary

Fibre composites and thus polymer resins are now being widely utilised in the civil engineering and construction industries to replace existing traditional materials such as timber and metals. However fibre composites, particularly the polymer matrices used within are principally non-renewable petrochemical based materials. Growing interest among the general community in sustainability is driving therefore driving the development and production of environmentally friendly alternatives. Furthermore this has been the key motivation and justification for this research. One avenue of research with the possibility of offering a potential sustainable substitute or alternative is the development of plant oil based thermosetting polymers such as those based on hemp oil as presented within this study.

Chapter 2

BIOCOMPOSITES USING PLANT OIL BASED THERMOSETTING RESINS: A REVIEW

2.1 General introduction

The implementation of composites is often perceived to be a relatively new occurrence, however the reality is that they have been utilised for centuries. Some of the earliest evidence of the existence of composite materials can be traced back to biblical times with the book of Exodus describing the Israelites being forced to find their own straw to make clay bricks and the Mongols producing archery bows from tendons, horns, bamboo, silk and pine resin (Beckermann 2007). Composites also exist in nature in numerous forms for example; bone (protein-calcium-phosphate matrix reinforced with collagen) and wood (lignin matrix reinforced with cellulose). However in civil engineering and construction terms composites represent a relatively young material group.

Over the last several decades there has been an increasing use of composite materials in the civil engineering and construction industries. Reasons for this movement are focused on exploiting the advantages that composite materials can bring to these industries. According to Goldsworthy (1995) and Goldstein (1996), composites offer economic advantages in terms of initial construction

and whole-of-life costs. Karbhari (1997) also reasons that the lower mass (i.e. density), of composites can lead to benefits namely; higher load capacities for the same supporting structure, the use of smaller supporting structures and finally greater ease of placement without the requirement for heavy equipment. Increases in life span may also be realised through the use of composite materials and due to the deterioration and failure of existing post-war structures throughout Australia, composites present a viable replacement option (Van Erp, G. & Ayers 2004).

Composites are a lightweight, strong, stiff material that consists of two main components, fibre reinforcement and matrix. Fibre serves to provide reinforcement to the composite. The fibres are stiff and brittle and are encased within a polymer matrix. The polymer matrix transmits any applied loads and or stresses to the fibre reinforcement within the composite. It also helps to hold the fibres in position and protect them from any environmental damage.

Composites have inherent flexibility in that the constitutes (fibre reinforcement and matrix) may be selected in order to design a material with specifically desired properties. It is the synergy of the combined selected constituents that ensures the final composite material has superior material properties for the required application than each of the individual material elements alone. Harper (2002) has classified composites into five different types by primary phase; fibre, particulate, filler, flake and laminar (Figure 2.1). Furthermore according to Beckermann (2007) there are numerous different categories of composite materials separated by matrix type for example; ceramic matrix composites (CMC), metal matrix composites (MMC), intermetallic matrix composites (IMC), carbon-carbon composites (CCC) and polymer matrix composites (PMC). The focus of this research is on the development of laminated PMCs, distinctively natural fibre composites or biocomposites utilising both biobased reinforcement and matrix systems.

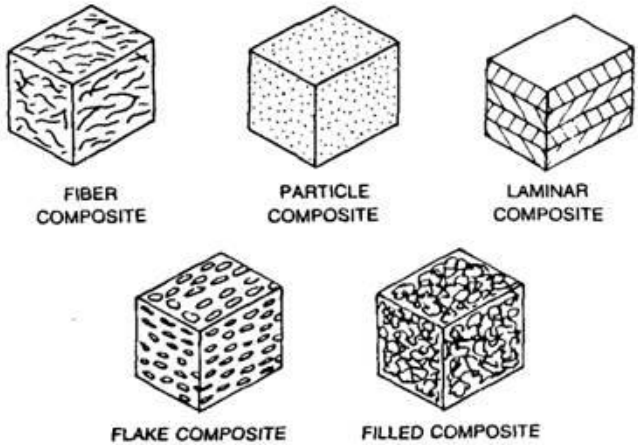

Figure 2.1. Composite classifications (Harper 2002).

2.2 Thermosetting polymers

Polymers are by definition large molecules that are produced through covalently bonded smaller units called monomers (Flory 1953). A thermosetting polymer or thermoset is a polymeric material that undergoes irreversible curing. Thermosets are characterised as being in liquid form at room temperature, which enables the easy addition of fibres and or other additives before being cured. Curing of the thermosets is achieved by the addition of a catalyst/hardener and often through heat or by a combination of the two methods. Unlike a thermoplastic, once cured thermosets remain in the solid phase and are unable to return to a liquid phase. This phenomenon can be attributed to crosslinking of the molecules whereby a rigid three dimensional network is formed through the reaction of the active sites within the molecules. The cross linking permanently increases the molecular weight and viscosity of the polymer, even upon reheating.

Thermosetting polymers are the most common type of resin used in the composite industry within civil engineering and construction. Generally these resins are of relatively low viscosity and are therefore appropriate for typical composite production. Compared with thermoplastics, significant advantages are offered by thermosets such as processing at ambient temperature and low

pressures. Ultimately this results in simplification of production requirements and enables flexibility in terms of fabrication of composite parts. Some of the most common types of thermosets used throughout industry are unsaturated polyesters, epoxies, phenolics and vinylesters. Of these thermosets the two of interest in this work are epoxy and vinylester.

2.2.1 Epoxy polymers

Epoxies are high performance oligomers that contain epoxide groups and have traditionally been widely used in aerospace and marine applications. However, epoxies are increasingly being considered as the high-performance option for fibre composite matrix systems for use within civil engineering. In terms of processing, epoxies are characterised as having low shrinkage thereby enabling the production of large composite parts without distortion. Moreover, they have high mechanical properties, high temperature resistance, good resistance to chemical attacks and offer excellent fibre-matrix adhesion properties necessary for durability and structural performance. The most prevalent type of epoxy in use is diglycidyl ether of bisphenol A (DGEBA), Figure 2.2. DGEBA is formed through the reaction of bisphenol A and epichlorohydrin. Bisphenol A is formed through the reaction of phenol and acetone.

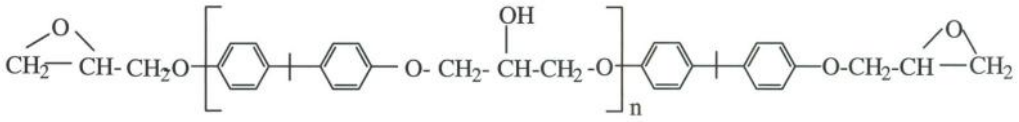

Figure 2.2. Chemical structure of DGEBA epoxy.

In terms of chemical reactivity, epoxies tend to be versatile which leads to different curing options and conditions. Curing of epoxies is achieved in several different ways; reaction with themselves through homopolymerisation or through reacting with amines, anhydrides thiols and alcohols (Klempner et al. 2004). Typically, in civil engineering applications epoxies are cured with amine

or anhydride type hardener. When mixed, the epoxy and hardener react to form a crosslinked polymer network. In this work an amine in the form of triethylenetetramine (TETA) is used, Figure 2.3.

Figure 2.3. Chemical structure of triethylenetetramine.

2.2.2 Vinylester polymers

Although epoxies may be considered as the high performance option in terms of polymers for civil engineering composite applications, vinylester (VE) offers another suitable option. As VE polymers utilise a base oligomer and reactive monomer they may be considered analogous to unsaturated polyesters (UP) as the formation of the final polymer network is achieved via a free-radical crosslinking cure mechanism.

VE is formed by reacting a base epoxide with an unsaturated carboxylic acid such as acrylic or methacrylic acid. Most commonly, DGEBA is used as the base epoxide. Figure 2.4 presents the chemical structure of a DGEBA epoxy based vinylester oligomer. Examining this chemical structure it is evident that a molecule with terminal unsaturation is yielded due to DGEBA epoxy possesing only terminal functional groups.

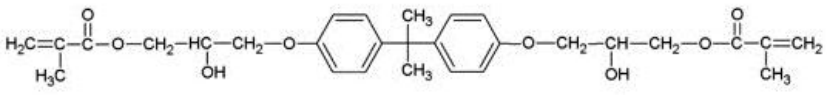

Figure 2.4. Chemical structure of a DGEBA epoxy based vinylester oligomer.

Vinylester is less expensive than epoxy systems predominatly due to the cost offset associated with the use of a reactive monomer such as styrene. Styrene is less expensive than the DGEBA epoxy before it is converted into VE and usually accounts for approximately 30-50% of the final volume of the resin system

(Davey 2004). It is possible to use lower quantities of styrene although the result is an increase in viscosity and lower workabilty which may pose difficulties in composite processing techniques. As a styrenated system VE displays similar shrinkage behavior to UP systems.

VE are cured via similar mechanisms to UP systems namely, free radical addition reactions. Both the VE and styrene molecules combine to form the final cured network. Different combinations of accelerators, promotors, initiators and inhibitors are utilised in the curing of VE systems. Most commonly an Methyl ethyl ketone peroxide (MEKP) based initator in combination with a cobalt accelerator is employed in the curing of VE.

2.3 Synthetic fibres

Traditional synthetic fibre reinforcements that are commonly used in engineering applications can be categorised into three main groups; glass, carbon and aramid fibres. Each of these classes of fibre reinforcements are commonly used in advanced industry applications. Figure 2.5 shows that these three different fibre groups make up approximately 31% of the fibre composite market.

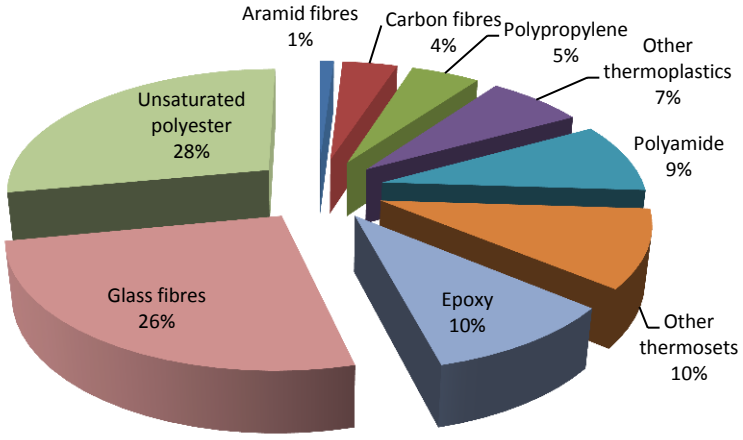

Figure 2.5. Percentage value of fibre reinforced fibre composite market (Bunsell & Renard 2005).

2.3.1 Glass Fibres

Glass fibres have been in use since the 1940's and are the most widely used reinforcements in the current fibre composite industry. The uses of glass fibre reinforced composites are wide ranging and encompass civil to military applications. Glass fibres are produced by an extrusion process whereby the molten glass is heated to temperatures of up to 1200 °C and extruded through fine spinnerets. The filaments are then drawn to produce fine uniform fibres with diameters of between 5 and 15 μm (Bunsell & Renard 2005). There are numerous different types of glass fibres throughout the glass category with silica (SiO_2) being the most common base. The composition of the most common types of glass, along with their associated mechanical properties is shown in Table 2.1 (Bunsell & Renard 2005).

From the five different types of glass fibre listed in Table 2.1, the most common form is E-glass. E-glass was developed for electrical applications as it displays high electrical resistance, S and R glass fibres are known to display superior mechanical properties. Glass fibres can be used as short fibres or can be woven into a mat or made into a non-woven mat depending on the application.

Glass fibres exhibit several properties that make them advantageous for use in composites. They are inexpensive compared to other fibres, they are easy to manufacture as there is a wealth of existing knowledge, and they are compatible with a range of various different materials.

The main disadvantages with glass fibres are their low elastic modulus compared with other fibres and their potential to be a health risk with regards to skin irritation (Matthews & Rawlings 1999). Although these health risks can be minimised through the use of the correct personal protective equipment (PPE) such as long sleeve shirts and eye protection when machining or cutting the fibres. The typical price for E-glass fibre is approximately 2 to $4 per kilogram, with the price of R and S-glass fibre being approximately 24 to $40 per kg.

Table 2.1. Composition and mechanical properties of the most common types of glass (Bunsell & Renard 2005).

Glass type	**E**	**S**	**R**	**C**	**D**
SiO_2	54	65	60	65	74
Al_2O_3	15	25	25	4	
CaO	18		9	14	0.2
MgO	4	10	6	3	0.2
B_2O_3	8			5.5	23
F	0.3				
FeO_3	0.3				
TiO_2					0.1
Na_2O				8	1.2
K_2O	0.4			0.5	1.3
Density	2.54	2.49	2.49	2.49	2.16
Strength (*GPa*)	3.5	4.65	4.65	2.8	2.45
Elastic modulus (*GPa)*	73.5	86.5	86.5	70	52.5
Failure strain	4.5	5.3	5.3	4.0	4.5

2.3.2 Carbon Fibres

Carbon fibres are often associated with high performance fibre composites such as aerospace and motorsport applications. They are a lightweight fibre that exhibits high stiffness and high strength that is due in part to the strongest covalent bond in nature (carbon-carbon bond) (Bunsell & Renard 2005). Carbon has two different crystalline forms (diamond and graphite), with graphite being the most important form for use in fibre composites (Matthews & Rawlings 1999).

Carbon fibres are manufactured from several different precursors with the majority being made from polyacrylonitrile (PAN) precursors (Bahl et al. 1998). The process involves the PAN fibres being heated to approximately 250 °C while being held under tension. The structure is made infusible due to the presence of cross linking and is further heated to approximately 1000 °C in a nitrogen rich atmosphere so that the nitrogen level decreases. The fibres are then reheated to around 1500–1600 °C (Bunsell & Renard 2005). Ultimate strengths of PAN precursor based carbon fibres range from 3000 MPa to above 6000 MPa.

Carbon fibres offer advantages such as:

- High fibre stiffness
- High fibre strength
- Low density
- High public marketability

However there are disadvantages such as:

- High cost (~30 to $80 per kg)
- Resin incompatibility
- Fibre availability

2.3.3 Aramid Fibres

Aramid fibres are a type of organic fibre that is used in a range of diverse applications ranging from military, aerospace and transport infrastructure. They are an aromatic polyamide that is typically manufactured by spinning a solid fibre from a liquid chemical blend (Bunsell & Renard 2005). Aramid fibres are more widely known by their trademarked names such as Kevlar and to a lesser extent Twaron.

Aramid fibres are used in continuous reinforcement applications such as bullet proof vests because of their high impact strength characteristics. They are also suitable for applications such as gaskets due to their high temperature properties. A disadvantage is that they have a propensity to degrade after being exposed to ultraviolet light. The typical price for high quality aramid fibre is approximately 30 to $50 per kg.

2.4 Biocomposites

Biocomposites are defined as natural fibre reinforced polymer composites. They are similar to synthetic fibre composites except that the materials that compromise

one or more phases, be it reinforcement or matrix are of biological origin instead of synthetic origin. The polymer matrix may be derived from plant oils instead of synthetic epoxies or VE for example. The reinforcing phase may be hemp, flax or jute fibres instead of glass, carbon or aramid fibres.

The key 'selling point' if you will is that they are more sustainable than synthetic composites. Although throughout the literature biocomposites are produced utilising plant based natural fibre reinforcement and petrochemically derived matrices and the opposite, in the authors view these may be more aptly termed hybrid composites. For the production of true biocomposites it is imperative that both the fibre and the matrix system be produced from biobased sources. This dissertation is only concerned with thermoset based biocomposites.

Biocomposite research is frequent throughout the literature with valuable research compilations provided. For instance Wool and Sun (2005) present a book on bio-based polymers, natural fibres and biocomposites. In particular, fibre separation processes, plant oil based polymer production and manufacturing of biocomposites are discussed in detail. A number of high quality review articles have also been produced throughout the literature. Puglia et al. (2005) reviews natural fibre based composites with an emphasis on the processing behaviour and final composite properties of natural fibres with polymeric matrices ranging from thermosets, thermoplastic and biodegradables. The use of chemical and physical fibre treatments for improving fibre-matrix adhesion is also reviewed. Saheb and Jog (1999) reviewed natural fibre polymer composites with an emphasis on fibre type, matrix polymers, natural fibre treatments and the fibre-matrix interface. Although they report that natural fibres have similar specific properties to synthetic fibres, namely glass they note that problems abound in terms of fibre-matrix incompatibility and composite processing being limiting. John and Thomas (2008) reviewed various aspects of biofibres and biocomposites throughout the literature. They classified biocomposites into green, hybrid and textile and highlighted applications of said biocomposites. Finally they discuss that the material revolution of this century may be realised through the use of

green composites. Fowler et al. (2006) reviews biocomposites, natural fibres and polymers with an emphasis on developing non-food markets for plant based fibres and polymers. Processing of biocomposites is also discussed. Future prospects of using biocomposites are also outlined with potential uptake barriers such as quality and consistency of base resources and supply reliability discussed.

Although the majority of the literature is dominated by research into plant based natural fibres using petrochemical based resins research is growing with regard to utilising plant oil based polymer resins for biocomposite matrices.

Adekunle et al. (2010a) synthesised novel soybean oil based matrices; methacrylated soybean oil (MSO), methacrylic anhydride modified soybean oil (MMSO), and acetic anhydride modified soybean oil (AAMSO) and used them as a matrices for flax fibre reinforced biocomposites. Hong and Wool (2005) developed a novel bio-based biocomposite material from soybean oils and keratin feather fibres (KF), suitable for electronic as well as automotive and aeronautical applications. They found that keratin feather fibres significantly improved the storage modulus compared to neat resin samples and that the final composite material was acceptable in terms of mechanical performance for composite applications. Furthermore Morye and Wool (2005) studied biocomposites and hybrids using a modified soybean oil matrix material reinforced with different glass/flax fibre ratios and different fibre arrangements. The fibre arrangement was varied to make symmetric and unsymmetrical composites. It was found that fibre arrangement resulted in different mechanical properties with unsymmetric composites exhibiting lower tensile strengths than symmetric composite samples. O'Donnell et al. (2004) utilised vacuum-assisted resin transfer moulding to produce composite panels out of plant oil-based resin acrylated epoxidized soybean oil (AESO) and natural fibre mats made of flax, cellulose, pulp and hemp. It was found that these composites displayed suitable mechanical properties for applications such as housing materials, furniture and automobile components. Takahashi et al. (2008) investigated the use of epoxidized soybean oil (ESO) cured with

Terpene-based acid anhydride reinforced with cellulose fibres. The produced biocomposites showed promise for use as structural building materials and are able to be biodegraded at the end of their lifecycle.

From the literature it is apparent that plant oil based bioresins are indeed being used in biocomposite applications. Section 2.5 discusses and reviews the literature regarding plant oil triglycerides, oilseed production within Australia, technical background of plant oils and synthesis of plant oil thermosetting polymers.

2.5 Plant oil triglycerides

Considerable work has been conducted into producing polymers from naturally derived sources (Imam, Greene & Zaidi 1999). Indeed the impetus for this research is to supplement or replace the petrochemically derived varieties that are dominant in the market. Of the most successful of these naturally derived polymers are those produced from plant oil based triglycerides. While supply issues and therefore cost have prevented other natural based thermoset polymers from becoming widely used, plant based plant oil based polymers have a large supply base (Liu 1997). Accordingly, plant oils offer a suitable feedstock alternative to petrochemicals for the production of polymers for civil engineering and construction applications. In addition, the plants themselves may be genetically modified to produce oils and therefore polymers with differing properties, targeted to different applications.

2.5.1 Oilseed production on Australia

Australia currently produces approximately 2-3 million tonnes of oilseed annually of which over 90% is comprised of canola and cotton seed (Australian Oilseeds Federation 2010). Sunflower and soybean comprise the majority of the remaining 10% with minor contributions being from sunflower, peanut, linseed

(Australian Oilseeds Federation 2010) and recently industrial hemp. Total oilseed production in Australia is forecasted to increase over the next 5 years, reaching 4996 kt in 2016 (ABC 2012).

Queensland produces several main types of oilseed crops, namely soybeans (20000 tonnes/annum) and sunflowers (31700 tonnes/annum) (Australian Oilseeds Federation 2010). Other oilseed crops such as cottonseed, peanut and industrial hemp are produced in smaller quantities. The majority of oilseed production is used for food products (cooking oils, shortening and other edible products) and livestock meal. A potential problem posed by using food based plant oils for industrial uses is the fact that it may diminish the supply for food sources. Therefore a focus on using fast growing non-food crops, such as industrial hemp for use as bioresins is required. Current Queensland and Australian legislation does not allow the use of industrial hemp in food products thereby making it a suitable candidate for a bioresin feedstock (Cowles 2013). Although the production of industrial hemp is still in its infancy after being previously banned, it is currently being grown in southern QLD with oilseed yields of 250-500 kg/ha and also in Tasmania and NSW (Plate 2006). In comparison due to research and development, Canada has yields of ~900-1500 kg/ha (Laate 2012).

2.5.2 Chemical structure of plant oil

Plant or vegetable oils are lipids derived from plants and are differentiated from fats in that they are liquid form at room temperature. The majority of plant oils are extracted from oil seeds (e.g. such soybean, sunflower, hemp and linseed) although some oils may be extracted from different plant sources such as pulp (e.g. palm, avocado and olive). Chemically, plant oils consist of triglyceride molecules which can be categorised as comprising of a glycerol molecule attached to three fatty acid chains. The glycerol molecule ($C_3H_5(OH)_3$) consists of a chain of three carbon atoms that are connected to three hydroxyl groups (-OH). Moreover triglycerides are formed via the esterification of three fatty acid

carboxyl groups to a single glycerol molecule. A triglyceride molecule is shown in Figure 2.6.

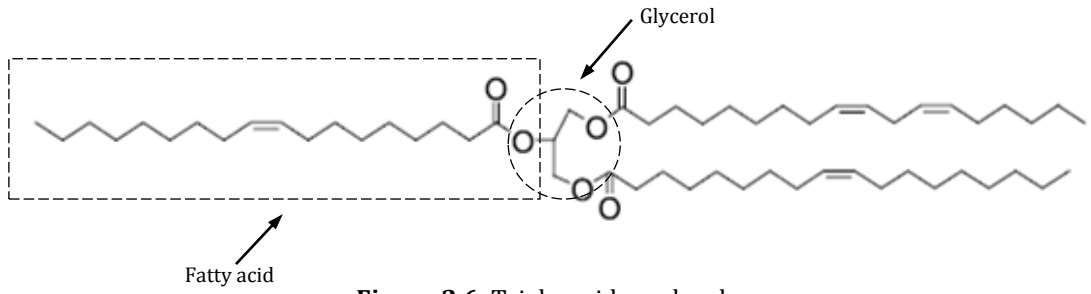

Figure 2.6. Triglyceride molecule.

A fatty acid is a carboxylic acid attached to a long unbranched aliphatic carbon chain. Although variations in length do occur, the majority of common fatty acids found in plant oils are usually between 14-22 carbons atoms in length (Wool, R. & Sun 2005). Plant oil based fatty acids are also typically comprised of even numbers of carbon atoms.

Fatty acids can be characterised as being saturated fatty acids (SFA), monounsaturated fatty acids (MUFA) and polyunsaturated fatty acids (PUFA). SFA occur when all of the carbon atoms are fully saturated by hydrogen atoms. Therefore there are only carbon-carbon single bonds (C-C) and no carbon-carbon double bonds (C=C) in SFA chains. MUFA are similar to SFA except that there is one (mono) position where there is a (C=C) instead of all (C-C). PUFA differ further in that they contain two or more (C=C) inside the fatty acid chain.

A multitude of different types of SFA and USFA exists. Although plant oil based triglycerides contain both SFA and USFA they are predominately comprised of the following USFA; oleic acid, linoleic acid and linolenic acid. Different plant oils show variations in both the quantity and the type of fatty acids and subsequently variations in both the quantity and the type triglycerides. Certain types of branched fatty acids of interest to the polymer industry occur naturally. Examples of these include vernolic acid which is a naturally occurring epoxidized fatty acid obtained from the seeds of the Ironweed plant (*Veronica galamensis L.)* and ricinoleic acid which is obtained from the castor plant

(*Ricinus communis L.*) and is a naturally occurring hydroxylated fatty acid (Gunstone 1996).

An overview of the structures of some types of fatty acids is shown in Figure 2.7. C=C are represented as parallel lines, for example in Figure 2.7 it can be observed that oleic acid (1) has C=C between the ninth and tenth carbon atoms. Table 2.2 outlines the fatty acid composition of some common plant oils. In the Table the name of the fatty acid is given, the length in carbon atoms and the position of the C=C within the fatty acid chain.

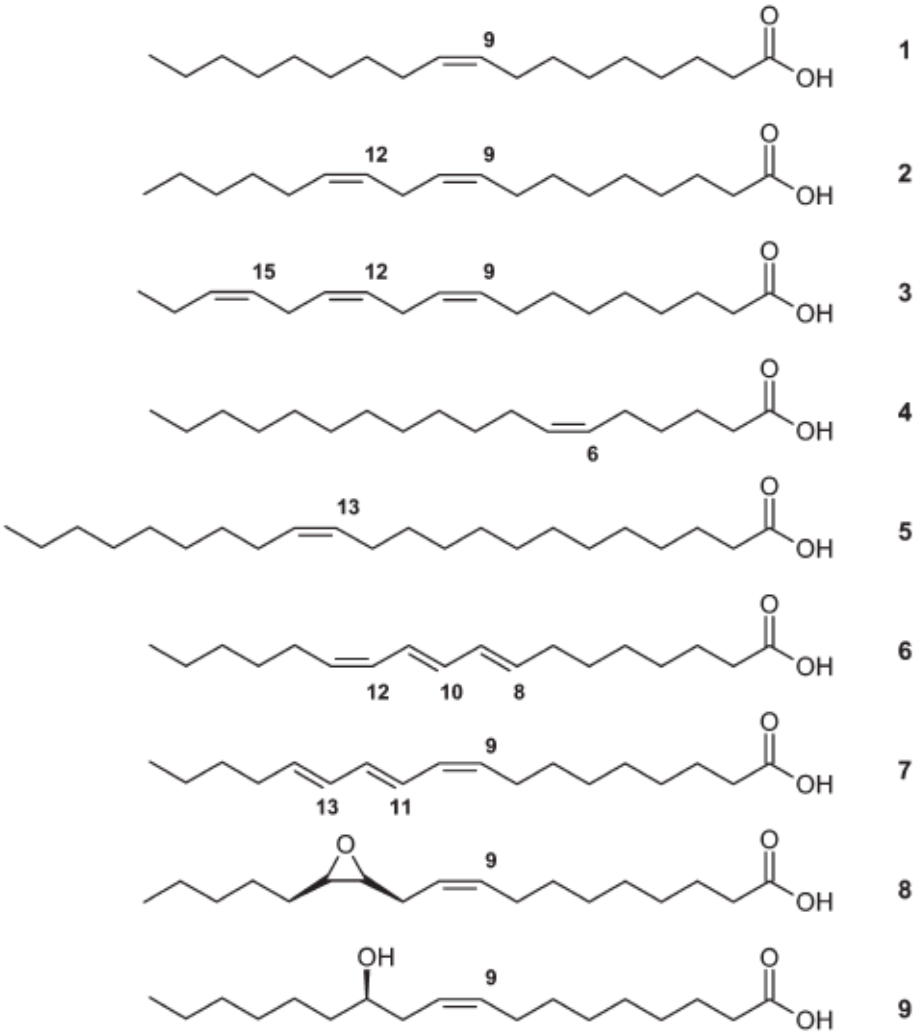

Figure 2.7. Structures of unsaturated fatty acids: (1) oleic (2) linoleic (3) linolenic (4) petroselinic (5) erucic (6) calendic (7) α-eleostearic (8) vernolic (9) ricinoleic (Meier, Metzger & Schubert 2007).

The C=C that are present in UFA are used as one of the primary reaction sites in the formation of epoxides, which in the case of epoxidized vegetable oils (EVO) are used in crosslinking. To achieve plant or vegetable oil based bioresins such as EVO and later acrylated epoxidized vegetable oils (AEVO) with satisfactory performance it is therefore desirable to begin with plant oils that exhibit high levels of PUFA as opposed to oils with high levels of SFA or to a lesser extent MUFA. This can be explained by examining the fatty acid structures of some UFA. For example linolenic acid has a C=C situated three, six and nine carbon atoms from the end of its fatty acid chain; in contrast with oleic acid that exhibits a C=C nine carbon atoms from the end of its fatty acid chain. Epoxidized linolenic acid should theoretically result in a polymer with greater stiffness due to there being less fatty acid chain left to 'wiggle' about and not contribute to the overall structural enhancement. From the fatty acid composition of the plant oils in Table 2.2 oils with higher potentials for functionalization such as linseed and hemp can be identified.

Table 2.2. Fatty acid profiles of various plant oils (%)
(Callaway 2004; Ecofibre 2010; Wool, R. & Sun 2005).

Fatty acid	#C: DB[a]	Canola	Linseed	Olive	Palm	Soybean	Hemp
Myristic	14:0	0.1	0.0	0.0	1.0	0.1	0.0
Palmitic	16:0	4.1	5.5	13.7	44.4	11.0	6.0
Palmitoleic	16:1	0.3	0.0	1.2	0.2	0.1	0.0
Margaric	17:0	0.1	0.0	0.0	0.1	0.0	0.0
Stearic	18:0	1.8	3.5	2.5	4.1	4.0	2.0
Oleic	**18:1**	**60.9**	**19.1**	**71.1**	**39.3**	**23.4**	**12.0**
Linoleic	**18:2**	**21.0**	**15.3**	**10.0**	**10.0**	**53.2**	**57.0**
Linolenic	**18:3**	**8.8**	**56.6**	**0.6**	**0.4**	**7.8**	**21.7**
Arachidic	20:0	0.7	0.0	0.9	0.3	0.3	0.0
Gadoleic	20:1	1.0	0.0	0.0	0.0	0.0	0.0
Behenic	22:0	0.3	0.0	0.0	0.1	0.1	0.0
Eurcic	22:1	0.7	0.0	0.0	0.0	0.0	0.0
Lignoceric	24:0	0.2	0.0	0.0	0.0	0.0	0.0
Avg. # DB/TAG		**3.9**	**6.6**	**2.8**	**1.8**	**4.6**	**5.6**

N.B. Double bonds (DB), Triglycerides (TAG)

2.5.3 Thermosetting polymers from plant oils

Quantitatively, polymers represent one of the most important products of the chemical industry and are used in a numerous range of applications. Currently

the majority of polymers are produced from petrochemical feedstocks. As such they represent a large contribution to the increasing problem of unsustainability that is apparent within the fibre composite and engineering construction industries. Although from a civil engineering perspective there is a necessary requirement that construction materials do not biodegrade there are still issues surrounding recycling and end-of-life incineration. These issues are required to be considered with regards to economic and environmental perspectives.

Recently there has been a heightened awareness regarding sustainability in the general community. As such a push to develop biobased polymers, such as plant oil based thermosets for use within the civil engineering and construction industries is also apparent (Dweib et al. 2004; Dweib et al. 2006; Hu et al. 2007). These plant oil based polymers offer a sustainable and with growth of scale, potentially a cost competitive option to petrochemically derived polymers.

As previously mentioned, triglycerides contain active sites acquiescent of chemical functionalisation and or reactions. According to Puig (2006) these sites allow triglycerides to be directly polymerised or for the triglyceride structure to be modified with polymerisable groups using techniques developed and widely used for petrochemical based polymers. Of these two different pathways the interest of this research lays with chemical modification and polymerisation rather than direct polymerisation.

2.5.4 Synthesis of plant oil based polymers

Chemical functionality is able to be added to the triglyceride at the unsaturation sites, the sites allylic to these unsaturation sites, the ester groups and the carbons alpha to the ester groups (La Scala, JJ 2002). Of utmost importance is the realisation of increased molecular weight, crosslink density and stiffness of the polymer. Numerous different chemical pathways leading to polymers from triglyceride molecules have been discovered, Figure 2.8 (Wool, R. & Sun 2005).

Once modified these triglycerides are liquid at room temperature and due to their high functionality are able to crosslink. Of the pathways presented in Figure 2.8 the two relevant to this work are six and seven, which represent acrylation and epoxidation respectively.

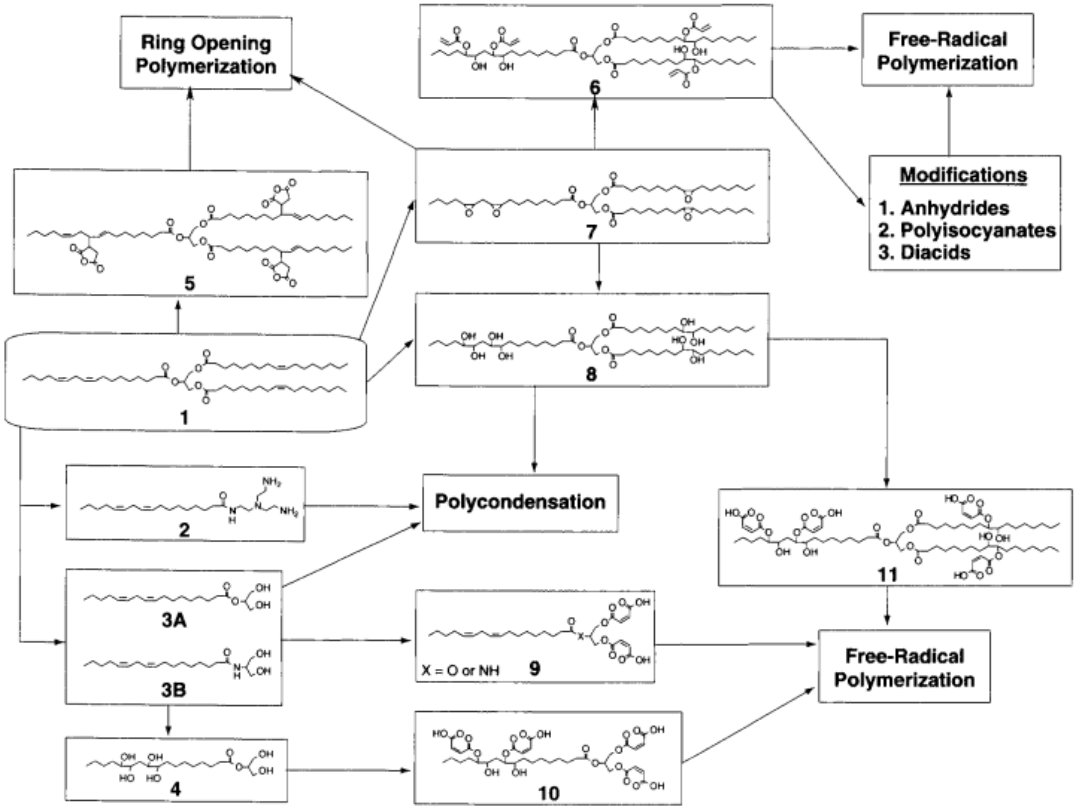

Figure. 2.8. Chemical pathways leading to polymers from triglyceride molecules (Wool & Sun 2005).

Epoxidation of plant oils

Epoxy groups are able to be incorporated into the triglycerides through the process known as epoxidation. Epoxidation represents one of the most important fundamental reactions involving the triglyceride and specifically involves functionalising the C=C. Epoxidation of plant or vegetable oils leads to polymers that are known as epoxidized vegetable oil (EVO). According to Puig (2006) traditionally EVO has been used as predominantly as plasticisers (Gibbons, Patel & Kusy 1997), reactive diluents (Czub 2006a, 2006b) and tougheners (Parzuchowski et al. 2006; Zhu, Jiang et al. 2004) for synthetic

epoxies. One drawback of EVO is that due to the structure of the triglyceride the hydroxyl and epoxy functional groups are not as reactive as those of synthetic petrochemically derived epoxies (La Scala, JJ 2002).

Epoxidation of a plant or vegetable oil occurs through the formation of a cyclic ether at the ethylenic unsaturation, C=C sites positioned along the fatty acid chains through the addition of an oxygen atom, Figure 2.9. Epoxidation is an important reaction because the formed epoxides are intermediates that are able to be converted into numerous products. Numerous different plant oil types have been epoxidized as shown in Table 2.3.

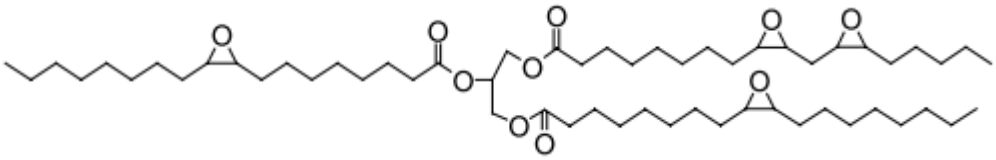

Figure 2.9. Epoxidized triglyceride molecule (Lu, J, Khot & Wool 2005).

Campanella and Baltanás (2005) studied the influence of processing variables namely stirring speed, temperature, hydrogen peroxide concentration, particle diameter and amount of catalyst added on oxirane ring opening using soybean oil. Petrovic et al. (2002) epoxidized soybean oil in a toluene solution with *in situ* formed peroxoacetic and peroxoformic acid. The kinetics of the reaction and the extent of the side reactions were studied at 40, 60 and 80 °C. Side reactions were found to be minimal with peroxoacetic acid throughout the temperature range however with peroxoformic acid side reactions were found to increase at 80 °C.

Sinadinović-Fišer, et al. (2001) studied the kinetics of *in situ* epoxidation of soybean oil in bulk catalyzed by an ion exchange resin. Of specific interest was the effect of the different reaction variables on the epoxidation reaction. Espinoza-Pérez et al. (Espinoza-Pérez, Haagenson, et al. 2009; Espinoza-Pérez et al. 2008; Espinoza-Pérez, Wiesenborn, et al. 2009) performed epoxidation of canola and soybean oils and studied the process parameters of both. The produced resins were then applied to composite samples.

Mungroo et al. (2008) epoxidized canola oil (ECO) using hydrogen peroxide catalysed by acidic ion exchange resin (AIER). Optimisation of processing parameters was specifically studied to identify the optimum reaction conditions. Optimised parameters included temperature (65 °C), acetic acid to ethylenic unsaturation molar ratio (0.5), hydrogen peroxide to ethylenic unsaturation molar ratio (1.5), and AIER loading (22%). Goud et al. (Goud, V et al. 2007; Goud, V, Pradhan & Patwardhan 2006; Goud, VV et al. 2010; Goud, VV, Patwardhan, AV & Pradhan, NC 2006) performed epoxidation on different plant oils such as Jatropha, Mahua and Karanja.

Dinda et al. (2008) studied the kinetics of epoxidation of cottonseed oil by peroxyacetic acid generated in situ from hydrogen peroxide and glacial acetic acid in the presence of liquid inorganic acid catalysts. In this study acetic acid was found to be superior to formic acid. Cooney et al. (Cooney, T 2009; Cooney, T., Cardona & Tran-Cong 2011) studied the epoxidation of hemp oil and studied the reaction kinetics in order to optimise the reaction conditions. These studies are used as the base point for the work in this thesis.

Table 2.3. Research conducted on the epoxidation of different plant oils.

Oil	Reference
Soybean	(Campanella & Baltanás 2005; Petrovic et al. 2002; Sinadinović-Fišer, Janković & Petrović 2001)
Canola	(Espinoza-Pérez, Haagenson, et al. 2009; Espinoza-Pérez et al. 2008; Espinoza-Pérez, Wiesenborn, et al. 2009; Mungroo et al. 2008)
Jatropha	(Goud, VV et al. 2010; Goud, VV et al. 2007)
Mahua	(Goud, VV, Patwardhan, AV & Pradhan, NC 2006)
Cottonseed	(Dinda et al. 2008)
Karanja	(Goud, V, Pradhan & Patwardhan 2006)
Hemp	(Cooney, T 2009; Cooney, T., Cardona & Tran-Cong 2011)

There are four established techniques acknowledged in the literature regarding the conversion of plant oils into EVO. These are epoxidation with organic and inorganic peroxides using a transition metal catalyst, epoxidation using halohydrines, epoxidation via molecular oxygen and epoxidation *in situ* with percarboxylic acid.

The most widely reported technique throughout the literature for the epoxidation of plant oils is epoxidation *in situ* (Cooney, T 2009; Espinoza-Pérez,

Haagenson, et al. 2009; Espinoza-Pérez et al. 2008; Espinoza-Pérez, Wiesenborn, Kristi, et al. 2007; Espinoza-Pérez, Wiesenborn, Tostenson, et al. 2007; Espinoza-Pérez, Wiesenborn, et al. 2009; Goud, V, Patwardhan, A & Pradhan, N 2006; Goud, VV, Patwardhan, AV & Pradhan, NC 2006; Mungroo et al. 2008). This involves reacting peroxycarboxylic acid with triglycerides. Peroxycarboxylic acid is used as an oxygen donor in formation of the epoxides. After this donation, carboxylic acid is returned to the mixture. The formation of peroxycarboxylic acid occurs *in situ* through the reaction of carboxylic acid and hydrogen peroxide in the presence of an acidic ion exchange resin (AIER) catalyst (Campanella & Baltanás 2005; Espinoza-Pérez, Haagenson, et al. 2009; Espinoza-Pérez et al. 2008; Goud, V et al. 2007; Goud, V, Patwardhan, A & Pradhan, N 2006; Mungroo et al. 2008; Sinadinović-Fišer, Janković & Petrović 2001). Epoxidation *in situ* was chosen for this study as it is safe, relatively environmentally friendly and the chemistry is well established in the literature.

Acrylation of plant oils

Although EVO polymers by themselves may be suitable as a polymeric matrix for biocomposites if blended with synthetic epoxies, further modifications can be made on the chemical structure to modify functionalities. One such modification involves acrylation of the epoxides. Reaction of epoxy functional triglycerides with acrylic acid incorporates acrylate chemical groups onto the triglyceride, attaching vinyl functionalities to its structure, Figure 2.10 (La Scala, J & Wool 2005; Wool, R. & Khot 2001). During the addition of the acrylate groups, the triglycerides are able to undergo polymerisation (Wool & Sun 2005). La Scala and Wool (2005) found that the reaction of acrylic acid with epoxidized soybean oil was found to have first order dependence with regards to epoxy concentration and second order dependence with regard to acrylic acid concentration.

After this modification, a polymer in the form of an acrylated epoxidized vegetable oil (AEVO) is obtained. The conversion of EVO to AEVO allows, lower curing temperatures, shorter curing times and improved material properties to

be achieved. This new monomer can be blended with a suitable, reactive comonomer such as styrene and cured by a typical free radical polymerization mechanism. The addition of the reactive comonomer (styrene), also serves to lower resin viscosity thereby making the bioresin suitable for most liquid composite processing techniques (Malik, Choudhary & Varma 2000).

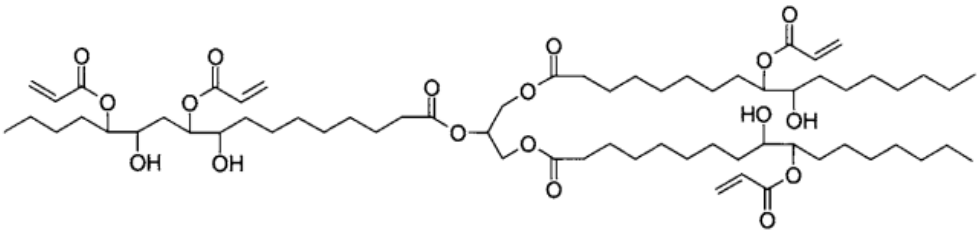

Figure 2.10. Acrylated epoxidized triglyceride molecule (Wool & Sun 2005).

Predominantly, AEVO research has focused on the acrylation of soybean (Khot et al. 2001; La Scala, J & Wool 2005; Li, Y et al. 2010; Lu, J, Khot & Wool 2005; Pelletier, Belgacem & Gandini 2006; Scala, JL & Wool 2005; Wool, R. & Khot 2001) and linseed oils (Lu, J & Wool 2006). Acrylated epoxidized soybean oil (AESO) has widespread use within the surface coating industry and also for ink applications and has also been commercially produced by Aldrich Chemicals (Borden 1975; Trecker, Borden & Smith 1976a, 1976b). In terms of research pertaining AEVO within to the composite industry the majority of the research conducted on these AEVO bioresins has been conducted at the University of Delaware, USA (Khot et al. 2001; La Scala, J & Wool 2005; Lu, J, Khot & Wool 2005; Lu, J & Wool 2006; Scala, JL & Wool 2005; Wool, R. & Sun 2005). Wool and the associated research group have studied the synthesis of epoxidized soybean oil (ESO) and epoxidized linseed oil ELO into AESO and epoxidized linseed oil (AELO). Specifically the free-radical polymerisation of the AEVO and its subsequent blending with styrene and other reactive diluents was performed with the aim of obtaining polymeric materials suitable for use in composite structural applications.

Li et al. (2010) conducted research into the acrylation of ESO containing different epoxy contents. ESO was synthesized by *in situ* epoxidation of soybean oil and the AESO was obtained by the reaction of ring opening of ESO using acrylic acid as a ring opener. They found that the thermal properties of these

synthesised polymers were dependent upon the epoxy value with the glass transition temperature increasing with increasing epoxy value.

Pelletier et al. (2006) synthesised and studied the polymerisation of AESO via free-radical photo-polymerization. The results suggested that AESO responded well to the photo-polymerization giving high yields of crosslinked materials within a few seconds. Compared with ESO, AESO the study showed that acrylation leads to an improvement in photo-activity under UV radiation.

Subsequent to the acrylation reaction the triglyceride may still contain some residual unreacted epoxides (Puig 2006). These unreacted epoxides may be used to impart further functionalisation to the triglyceride and may improve polymer performance. Further modifications of the AEVO include reactions with diacids, diamines, anhydrides and isocyanates and have been performed with varying levels of success (Wool, Richard. et al. 2000). According to Wool et al. (2000), of these modifications, maleinization appears to be the most effective with a reported increase in flexural modulus of ~723 MPa for AESO to ~2000 MPa for MAESO. However the maleinization reaction results in a large increase in viscosity which may affect the processability of the bioresin. Due to this reason no maleinization was undertaken in this work.

In conclusion, polymers have indeed been produced through the epoxidation and subsequent acrylation of numerous different plant oils. The success of these polymers for use as matrix systems is mixed and is heavily reliant on the fatty acid composition of the oils. Moreover a high proportion of the plant based oils that have been subjected to epoxidation and acrylation throughout the literature are also used within the food supply chain. This, in the author's opinion represents a conflict of interest and as such the focus of this work is on utilising non-food based oil crops, such as industrial hemp oil for the production of plant based polymers.

2.6 Natural fibres

Natural fibres are sustainable renewable materials and are able to be used as reinforcement for polymer matrices thereby leading to biocomposites. There are numerous categories of natural fibres however they are predominately sourced from plants, animals or minerals as outlined in Figure 2.11 (Bunsell & Renard 2005). Plant based natural fibres can be further classified as leaf, bast, fruit, seed (O'Donnell, Dweib & Wool 2004), wood, cereal straw, and other grass fibres (John & Thomas 2008). Table 2.4 outlines the most significant natural fibres in terms of global production. Generally plant based bast fibres are used to reinforce polymer matrices. These plant based fibres are also increasingly being used or positioned as potential replacements for glass fibre reinforcement in fibre composites within the civil engineering and construction industries.

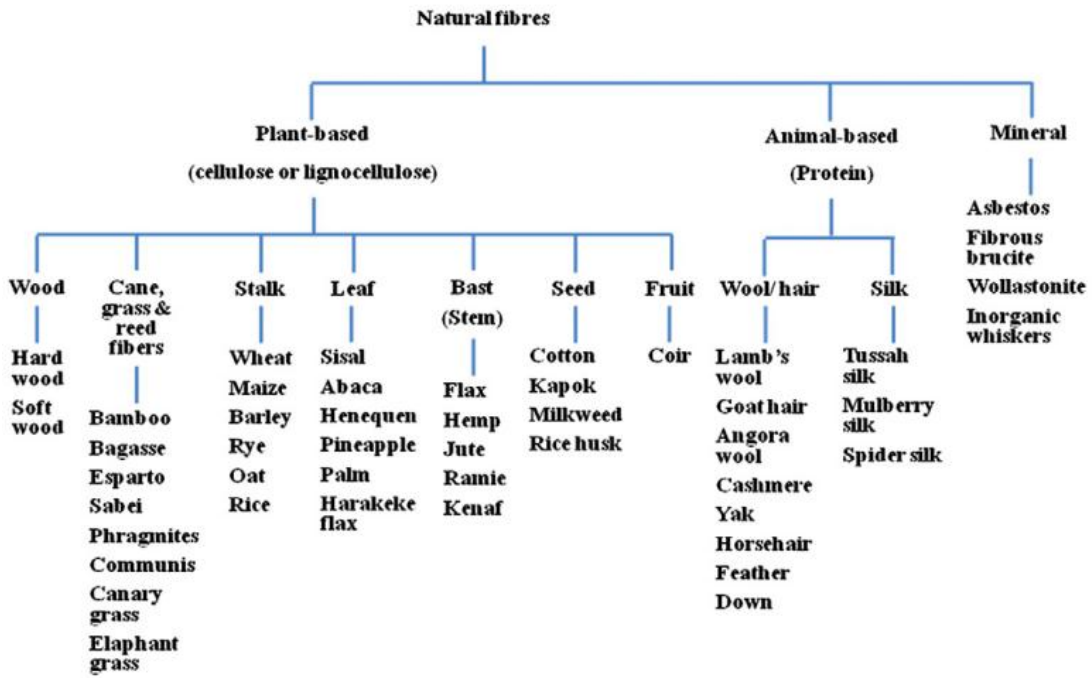

Figure 2.11. Natural fibre classifications (Ho et al. 2012).

Table 2.4. Global commercially significant fibre production (Islam, Mohammad Saiful 2008; Takahashi et al. 2008).

Fibre source	Species	World production (000' tonnes)	Origin
Wood	> 10000	1750000	Bast
Cotton	*Gossypium sp.*	18450	Fruit
Bamboo	> 1250	10000	Bast
Jute	*Corchorus sp.*	2300	Bast
Kenaf	*Hibiscus Cannabinus sp.*	970	Bast
Flax	*Linum Usitatissimum*	830	Bast
Sisal	*Agave Sisilana*	378	Leaf
Roselle	*Hibiscus Sabdariffa*	250	Bast
Hemp	*Cannabis Sativa*	214	Bast
Coir	*Cocos Nucifera*	100	Fruit
Ramie	*Boehmeria Nivea*	100	Bast
Sunn hemp	*Crorolaria Juncea*	70	Bast

Plant based natural fibres demonstrate numerous advantages over synthetic fibres. They signify an inexpensive, renewable fibre with sound end-of-life recyclability (Agrawal et al. 2000; Canché-Escamilla et al. 1999; O'Donnell, Dweib & Wool 2004). Natural fibres offer processing flexibility as they are less susceptible than synthetic fibres to machine tool damage and health hazards associated with manufacturing (Ho et al. 2012). Other advantageous properties of plant based natural fibres are a reduced carbon footprint from the growing of the plants, and enhanced energy recovery at the end of their lifecycle (Joshi et al. 2004). Furthermore natural fibres also exhibit high specific material properties compared with E-glass for instance. Table 2.5 summarises the mechanical properties of natural and commonly used synthetic fibres.

Table 2.5. Mechanical properties of natural fibres compared with E-glass (Bos, Van Den Oever & Peters 2002; Ho et al. 2012; Mohanty, Misra & Hinrichsen 2000; Wambua, Ivens & Verpoest 2003).

Fibre	Specific gravity	Tensile strength (MPa)	Young's modulus (Gpa)	Specific strength (MPa)	Specific modulus (GPa)
Hemp	1.14	550-900	50-70	482-790	44-62
Jute	1.46	600-1100	10-30	411-753	7-21
Cotton	1.55	287-597	5.5-12.6	191-398	4.0-8.0
Coir	1.20	175	4.0-6.0	146	3.0-5.0
Kenaf	1.30	930	53	715	41
Sisal	1.20	600-700	38	500-583	32
Flax	1.20	800-1500	60-80	667-1250	50-67
Wool	1.30	120-174	2.3-3.4	92-134	2.0-3.0
E-Glass	2.60	2000-3400	75	1308	29
Carbon	1.40	4000	235	2857	168
Aramid	1.40	3000	65	2143	46

2.6.1 Structure and composition of plant fibres

Plant fibres can be thought of as being a natural form of composite material with the main constitutes being cellulose fibres reinforced in a lignin and hemi-cellulose matrix (John & Thomas 2008). Figure 2.12 shows the structure of a plant fibre. The basic structure of a plant fibre is a primary cell wall surrounding a secondary wall. The primary cell wall is responsible for providing structural and mechanical support, controlling growth rate and direction and cell-cell interactions. The secondary wall consists of three layers that provide the bulk of the mechanical strength of the fibre (John & Thomas 2008). The outmost layer of the fibre is called the middle lamella and it serves to provide stability by fixing adjacent cells together.

The components of common plant based fibres are displayed in Table 2.6 with the main components shown to be, cellulose, hemi-cellulose, lignin and pectin. Cellulose is a naturally occurring polysaccharide and is directly related to the strength, stiffness and reinforcing ability of the natural fibre. An increase in cellulose content can be correlated with an increase in tensile strength and Young's modulus (John & Thomas 2008). The cell walls of all plants contain hemi-cellulose which is comprised of 5 and 6 carbon ring sugars that support the cellulose microfibrils through a matrix arrangement. Lignin is a chemical compound located in the secondary cell wall of plants. According to John & Thomas (2008) lignin is a thermoplastic polymer with a glass transitional temperature of 90 °C and a melting temperature of 170 °C. Ultraviolet (UV) degradation of natural fibres can be related to lignin content. Pectin is a polysaccharide and due to the carboxylic groups in its structure, is the most hydrophilic compound in plant fibres. The mechanical strength of the plant fibre is related to the distribution of lignin between hemi-cellulose and cellulose, causing binding and stiffening of the plant fibres to occur.

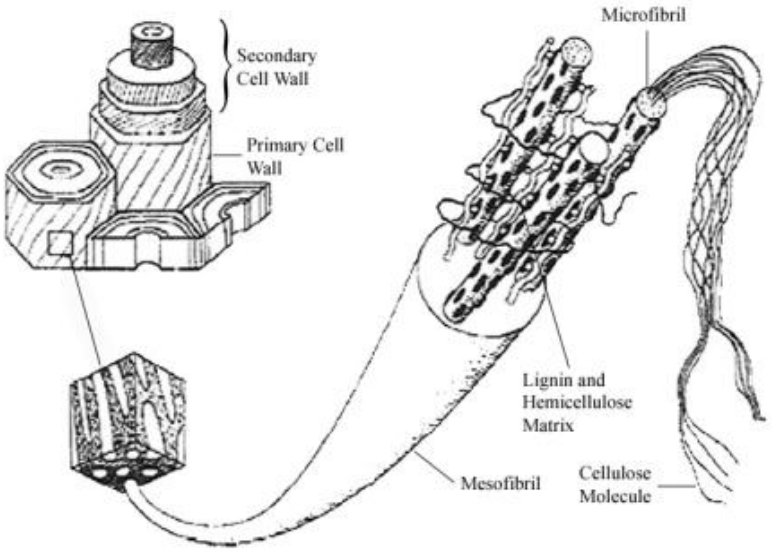

Figure 2.12. Structure of a plant fibre (Dickison 2000).

Table 2.6. Composition of some common plant fibres (wt%)(Bogoeva-Gaceva et al. 2007).

Fibre	Cellulose	Hemi-cellulose	Lignin	Pectin	Other
Jute	61-71	13.6-20.4	12-13	0.2	0.5
Flax	71-78	18.6-20.6	2.2	2.2	5.5
Hemp	70.2-74.4	17.9-22.4	3.7-5.7	0.9	7
Kenaf	53-57	15-19	5.9-9.3	-	7.9
Sisal	67-78	10-14.2	8-11	10	3

2.6.2 Factors affecting natural fibres in composite applications

Although natural fibres possess some advantageous properties they also have certain disadvantages such as the propensity to form aggregates during processing, inconsistencies due to different growing conditions, thermal instability and low resistance to moisture absorption (Joseph, Thomas & Pavithran 1996; Saheb & Jog 1999). Of all of these issues the most problematic is the hydrophilic nature of the natural fibres. This characteristic may lead to poor matrix-fibre compatibility and therefore compromise overall composite performance.

As discussed in section 2.6.1 plant fibres are comprised of cellulose, hemicelluloses, lignin and pectins. Of these constituents it is the hemicelluloses and pectins that are problematic regarding moisture absorption due to their

hydrophobic characteristics. Hydrogen bonds, specifically hydroxyl (-OH) groups act as active sites for the sorption of water molecules. As a result when natural fibres are used within a hydrophobic polymer matrix poor fibre-matrix interfacial adhesion may occur resulting in compromised mechanical performance of the end composite (Zakaria & Kok Poh 2002). Understandably in order to maximise composite properties it is imperative to improve the moisture absorption of the natural fibres.

Reducing the moisture content involves simply heating the natural fibres at elevated temperatures and in essence dries them out. Furthermore, modifications of the natural fibre's surface in the form of chemical treatments aim to facilitate improved fibre-matrix interfacial adhesion. Chemical treatments such as alkali, acetylation, silane, benzoylation and peroxide treatments have been studied throughout the literature (Jacob, M., Varughese & Thomas 2006; Joseph, Thomas & Pavithran 1996; Le Troedec et al. 2008; Li, X, Tabil & Panigrahi 2007; Mehta et al. 2006; Rong et al. 2001; Thomsen et al. 2006; Tripathy et al. 2000; Valadez-Gonzalez et al. 1999). The main premise behind the chemical treatments entails exposing a larger quantity of reactive sites on the fibre surface thereby facilitating fibre-matrix adhesion (Dash et al. 1999). Interestingly, according to Joseph (1996) via Islam (2008) thermosetting polymers such as epoxies or phenolics are able to form covalent crosslinks to the plant fibres by way of the –OH groups. It is this premise that may prove to negate the need for natural fibre chemical modifications if a –OH 'rich' plant oil based polymer, such as AEHO is also utilised as the matrix.

2.7 Industrial hemp

Industrial hemp (*Cannabis sativa* L.) Figure 2.13, is one of the oldest crops known and used by humans. It is believed to have originated from China and numerous hemp based products such as canvas and ropes for example have been discovered dating back as far as 800 BC. Although sharing the same species as marijuana, industrial hemp contains low levels of the psychoactive

compound delta-9-tetrahydrocannabinol (THC). It was the largest crop in the world in the early 19th century (O'Donnell, Dweib & Wool 2004) and was being projected as the first 'billion dollar crop' in the 1930's. The production of hemp decreased due to marijuana prohibition and the dawn of the synthetic fibre industry. Although banned in the past in Australia industrial hemp is now being cultivated under license for industrial uses (Murphy 2012).

Industrial hemp is an annual herbaceous plant of the Mulberry genus with a maximum height of ~5 m and between 4-60 mm in diameter depending on the plantation density (Beckermann 2007; Olsen 2004). The plants are known to have a deep, well developed root system with the stem of the hemp plant is comprised of the bast and the hurd. Industrial hemp is largely diocious although monoecious varieties do exist.

Although there is no such national policy regarding the production of industrial hemp is limited. Licensing programs to allow the cultivation of industrial hemp first began in Tasmania, Australia in 1991 followed by Victoria, Australia in 1997. In Queensland, Australia the Drugs Misuse Act 1986 was amended in 2002 thereby facilitating the production of industrial hemp. Western Australia, Australia passed legislation in 2004 allowing the production of industrial hemp for commercial uses. New South Wales, Australia allows only field trials and the other states and territories have not yet proceeded with legislative changes (Olsen 2004).

Figure 2.13. Mature industrial hemp plants (left). Hemp stem, leaf and plant top (right) (Thygesen 2006).

Industrial hemp is able to produce both fibre and oilseeds, Figure 2.14. However the majority of industrial applications and research has focused on using the fibre with hempseed oil being viewed essentially as a by-product of fibre production. Currently the main use for industrial hempseed oil is in personal care products (Anwar, Latif & Ashraf 2006). Worldwide production of industrial hemp fibre and oilseed was 66325 and 30265 t respectively, with the main producers of oilseed being China, France and Chile (Mooleki et al. 2006). The oil is extracted using a typical 'two-step' process of extraction and filtration. Industrial hemp oil has an oil content typically ranging from 25-35% of which is comprised of a high level of MUFA and PUFA (Leizer et al. 2000; Sanders & Lewis 2007). It is this unique fatty acid structure of hempseed oil that makes it a suitable candidate as a bioresin feedstock.

Figure. 2.14. Industrial hemp fibre (left) and oilseed (right).

2.8 Applications for biocomposites

According to Beckermann (2007) several billions tonnes of reinforcing fibres and fillers are used annually within the plastics industry. This coupled with the extensive use of petrochemically derived polymers presents a large potential market for sustainable biobased supplementary materials such as biocomposites. According to Mohanty et al. (2004) although the main use of biocomposites are currently automotive, medical and packaging industries bioresins and biocomposites have enormous potential within the civil engineering and construction industries. Currently however, biocomposites manufactured with natural plant fibres or natural/synthetic hybrid fibre blends

in a plant oil based matrix or a blends have shown the potential to be used as an alternative to glass fibre composites in entry-level structural engineering applications.

Large scale biocomposite 'unit beams' of sandwich construction were successfully manufactured at the University of Delaware (UD) from flax mat, chicken feathers, recycled paper and structural foam using AESO and a modified vacuum assisted resin transfer moulding (VARTM) process (Czub 2006b; Dweib et al. 2006; Hu et al. 2007; Zhu, Jiang et al. 2004). Similar work undertaken at UD focused on the development of biocomposite bridges using recycled paper, sisal and jute twine, jute fabric and AESO and VARTM (Parzuchowski et al. 2006). The overall goal of this study at UD is the development of an all-natural monolithic roof system for residential construction (Shenton & Wool 2004).

Other researchers have undertaken research into natural fibres with synthetic resins and/or glass fibres with plant oil based bioresins. Chandrashekhara et al. (2002) and Zhu et al. (2004) from the University of Missouri-Rolla have conducted research into pultruded composite structural beams using ESO based resins and glass fibres. They demonstrated that ESO resins showed significant promise for use in structural composite applications.

Singh and Gupta (2005) produced biocomposite panels from jute, coir and sisal using a polyester matrix. They also produced biocomposite sandwich panels using a jute honeycomb core with jute and glass fibre faces. Performance was found to be similar to commercially sourced fibreboard. In addition, roofing sheets, doors, door frames and door shutters were also produced from sisal, jute and polyester. In a similar study Singh et al. (2000) produced jute reinforced phenolic biocomposite door frames via pultrusion.

A body of work from Burgueno et al. (Burgueño, Quagliata, Mehta, et al. 2005; Burgueño et al. 2004; Burgueño, Quagliata, et al. 2005a, 2005b) has primarily focused on developing structural hierarchical natural fibre composite beams and panels. Numerous materials were used ranging from chopped hemp, flax

mat, E-glass and jute mat with unsaturated polyester resins (UPE). Results from these studies found that hierarchical designs can improve the performance of natural fibre composite beams and plates thereby allowing them to potentially compete with synthetic fibre composites. From this body of reviewed literature it is evident that for biocomposites to be used as structural elements they require to be shaped so as to maximise stiffness and strength.

2.9 Conclusions

This chapter has reviewed the current status of biocomposites using plant oil based bioresins. From this review it is apparent that fibre composites are gaining acceptance within the civil engineering and construction industries despite their sustainability issues. Although at a relatively early stage of research and implementation, plant oil based bioresins applicability to biocomposite matrices need to be further studied and developed. In particular, as these thermosetting biopolymers are heavily dominated by soybean, canola and linseed oils alternative plant oils need to be examined. An ideal plant oil feedstock has been suggested in the form of hemp oil. The present project, therefore studies the development of hemp oil based bioresins for biocomposite matrices for the production of biocomposites.

Chapter 3

SYNTHESIS AND CHARACTERISATION OF HEMP OIL BASED BIORESINS

3.1 Introduction

In fibre reinforced composites, the polymer matrix ensures that the fibres remain in position, transfers applied loads to the fibre reinforcement and protects the fibres from mechanical damage and other environmental factors. Fibre composites are categorised as biocomposites when either the fibre or matrix is sourced from natural origins. However, the manufacture of true biocomposites demands that both the fibre and the matrix be made predominantly from renewable resources. In terms of naturally derived matrices, vegetable or plant oils can be used as the building blocks of naturally derived thermosetting resins. Typically, these oils are chemically modified to form cross-linkable molecules such as the epoxides and acrylated forms of hemp oil that is presented in this chapter.

This chapter presents the full characterization of the bioresins obtained through the chemical functionalization of hemp oil. Hemp oil feedstock is converted into epoxidized and acrylated bioresins through the process of epoxidation and acrylation, which are termed, epoxidized hemp oil (EHO) and Acrylated

epoxidized hemp oil (AEHO) respectively. EHO are akin to epoxy resins, and similar to other epoxidized vegetable oils (EVO) are inexpensive and can be primarily used as plasticisers or toughening additives for synthetic epoxy resins. Further functionalization of EHO and EVO can be used to create acrylated epoxidized vegetable oil (AEVO) that can be categorised as being analogous to vinylesters. In general AEVO demonstrate improved mechanical and visco-elastic performance in comparison with EVO.

3.2 Materials for synthesis and characterisation of bioresins

Cold pressed raw industrial hemp oil supplied by Ecofibre (Maleny, Queensland, Australia) with a fatty acid profile consisting of the following acids; palmitic = 6.0%; stearic = 2.0%; oleic = 12.0%; linoleic = 57.0%; linolenic = 20.7%; other = 2.3% was used to synthesis EHO. The provided hemp oil has an iodine number = 165 (g I/100 g oil) and saponification value = 193. Analytical grade glacial acetic acid and hydrogen peroxide with minimum concentrations of 99.7% and 30% respectively were used as received from LabServ (Biolab, Australia). Amberlite IR-120 the ionic H^+ form was used as received from Fluka (Sigma-Aldrich, Australia). Anhydrous sodium sulphate (Ajax Chemicals, Australia) was used as received. For the synthesis and characterisation of AEHO; hydroquinone inhibitor (≥ 99%, Sigma-Aldrich), acrylic acid (≥ 99.5%, Acros Organics), AMC-2 catalyst (Ampac Fine Chemicals), 0.5% solution phenolphthalein (Chem Supply) and sodium hydroxide (0.5 N) were used as received.

3.3 Synthesis of epoxidized hemp oil

As each reactor is often different in terms of volume, temperature control accuracy and achievable stirring speed the optimisation study performed by Cooney (2009) on the epoxidation of hemp oil forms the basis of the

epoxidation reaction conditions such as time, temperature and reactant concentrations used throughout this study. EHO was synthesised through the epoxidation of cold pressed raw industrial hemp oil (156.25 g, 1 mol) by peroxyacetic acid, formed *in situ* by the reaction of hydrogen peroxide (113.4 g, 1 mol) and acetic acid (40.04 g, 0.67 mol) in the presence of an acidic ion exchange resin, Amberlite IR-120 H^+ (15% by weight of hemp oil) as the catalyst, as shown in Figure 3.1. The constituents were added to a four-necked reaction vessel equipped with a mechanical stirrer and thermometer, Figure 3.2. Stirring was initiated and the reactor temperature was increased until the mixture reached 40 °C. Thereafter hydrogen peroxide was added drop over a period of one hour. Temperature and stirring speed were then increased to operational values of 75 °C and 110 rpm respectively. These parameters were maintained for a period of 7 h.

On completion of the reaction the catalyst was filtered off and the reactor contents were cleaned in a separation funnel by washing with distilled water three times (cool (~20 °C), hot (~85 °C), cool (~20 °C)) to remove the aqueous phase. Next the resin was centrifuged and aerated to remove any remaining water. The resin was then further dried through the addition of anhydrous sodium sulphate in the proportion of 0.15 g per 1 g of resin. Following the addition of anhydrous sodium sulphate, the resin was placed in an oven at 70 °C for 12 h and subsequently filtered through Whatman No. 4 filter paper. Oxirane oxygen content was determined by titration to be 8.3%. The yield of EHO bioresin recovered after washing and separation from the catalyst and reactants was approximately 75% by volume in relation to the initial volume of hemp oil. Inevitably some bioresin was lost during this process of washing and purification. At room temperature EHO is a yellow coloured liquid with a slight vegetable oil odour.

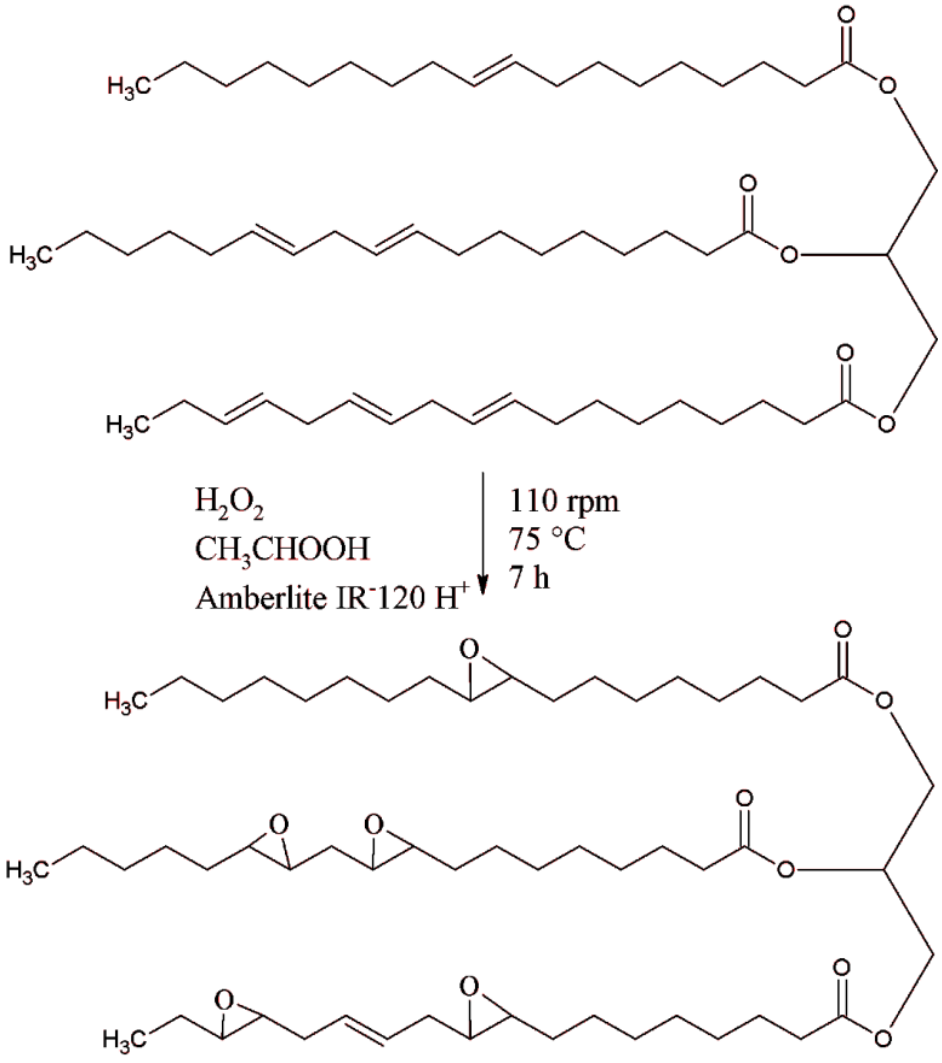

Figure 3.1. *In situ* epoxidation of hemp oil.

Figure 3.2. Epoxidation reaction in a Mettler Toledo LabMax reactor.

3.4 Synthesis of acrylated epoxidized hemp oil

AEHO was obtained via the acrylation of the EHO. A solution of EHO, hydroquinone inhibitor (0.0033 g /ml of EHO + acrylic acid) and AMC-2 catalyst (1.75% by weight of EHO + acrylic acid) were added to a Mettler Toledo LabMax automatic reactor, Figure 3.3. The reactor comprised of a 4 L four-necked reaction vessel equipped with a mechanical 'ship anchor' stirrer and

thermometer. Stirring was initiated and the reactor temperature was increased until the mixture reached 50 °C. The mixture was maintained at that temperature for 30 minutes after which the acrylic acid (ACROS Organics) was added in a molar ratio of 1.1 moles per mol of EHO. The exothermic reaction increased the temperature of the mixture rapidly, thus the reactor was set to maintain a constant temperature of 90 °C. Furthermore the reaction conditions were maintained for a period of 12 h. The reaction evolution was monitored by periodic titrations of the AEHO/acrylic acid mixture using sodium hydroxide and phenolphthalein as an acid-base indicator. The reaction was considered to be completed when no further changes in the amount of sodium hydroxide used to neutralize the resin were observed. Figure 3.4 shows schematically the *in situ* acrylation of the epoxidized hemp oil.

Figure 3.3. Acrylation reaction in a Mettler Toledo LabMax reactor.

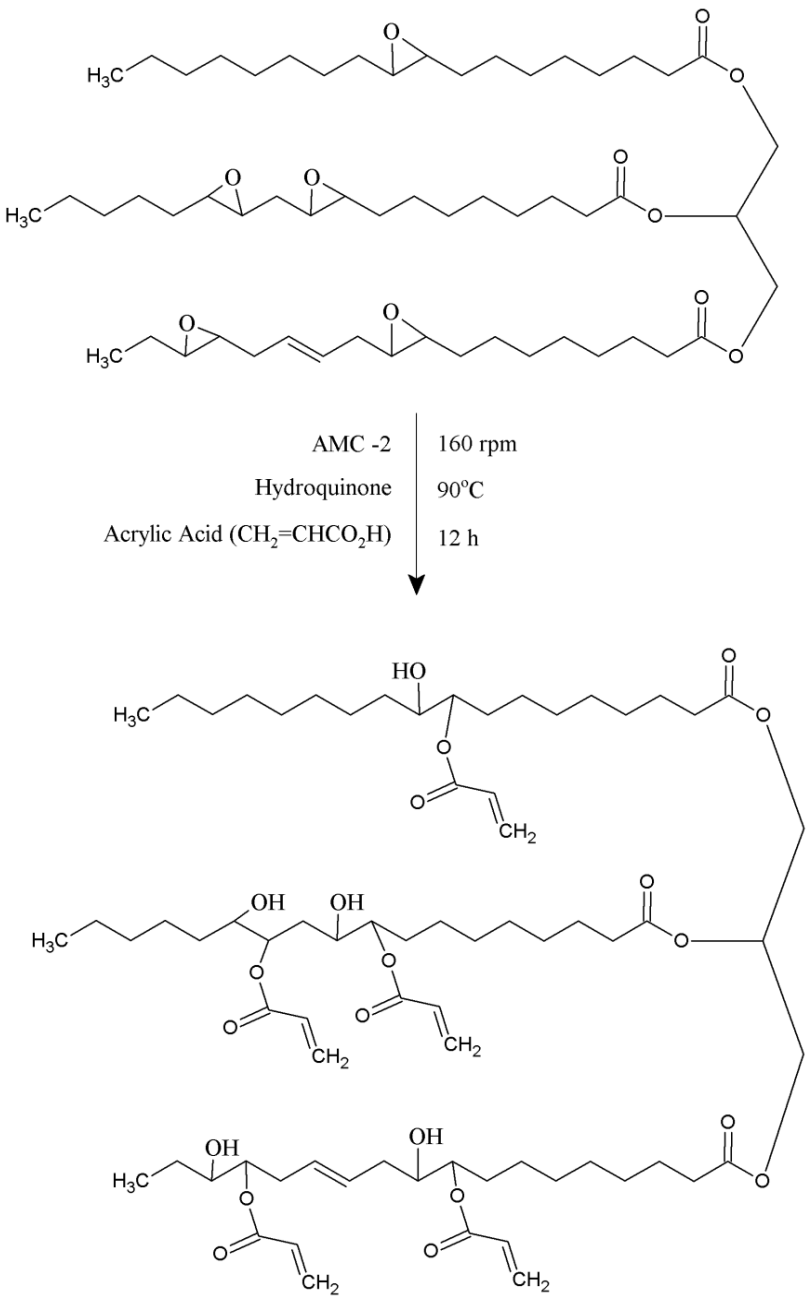

Figure 3.4. Synthesis of AEHO.

3.5 Characterisation of hemp oil bioresins

The synthesis and characterisation of EVO and AEVO bioresins is widely studied and understood, for example (Cai et al. 2008; Dinda et al. 2008; Espinoza-Pérez, Haagenson, et al. 2009; Espinoza-Pérez et al. 2008; Espinoza-Pérez,

Wiesenborn, Kristi, et al. 2007; Espinoza-Pérez, Wiesenborn, et al. 2009; Goud, V et al. 2007; Goud, V, Patwardhan, A & Pradhan, N 2006; Goud, V, Pradhan & Patwardhan 2006; Goud, VV et al. 2010; Goud, VV et al. 2007; Goud, VV, Patwardhan, AV & Pradhan, NC 2006; Khot et al. 2001; La Scala, J & Wool 2002; La Scala, J & Wool 2005; Li, Y et al. 2010; Lu, J, Khot & Wool 2005; Lu, J & Wool 2006; Miyagawa et al. 2007; Mungroo et al. 2008; Petrovic et al. 2002; Scala, J & Wool 2002; Wool, R. & Khot 2001; Wool, Richard. et al. 2000; Wool, R. & Sun 2005). Therefore the focus of the characterisation in this work utilises these reliable, well established methods and principles to characterise novel hemp oil based bioresins. The quality of EVO bioresins is largely dependent on the degree of epoxidation, measured by oxirane oxygen content and the number and consumption of carbon-carbon double bonds (C=C) measured by the iodine value (Espinoza-Pérez et al. 2008; Espinoza-Pérez, Wiesenborn, Kristi, et al. 2007). With regards to the characterisation of the AEHO synthesis and final product quality, several commonly used characterisation techniques are employed. To monitor the progress of the acrylation reaction, consumption of acrylic acid is determined through titrating with sodium hydroxide and an indicator. Both Fourier transform infrared (FTIR) and proton nuclear magnetic resonance (^{1}H-NMR) spectroscopy are also used to monitor the reaction and characterise the final product. Viscosity measurements are also performed.

3.5.1 Moles of ethylenic unsaturation of hemp oil

The moles of C=C in 100 g of hemp oil and the molar mass of the triglyceride (TAG) were determined based on the method described by Cooney (2009). Table 3.1 gives the composition of the studied hemp oil in conjunction with fatty acid properties.

Table 3.1. Properties of fatty acids associated with the studied hemp oil.

Fatty acid (FA)	FA (%)	Molar mass (g/mol)	No. of C=C	Moles of C=C per 100 g of HO	Moles of FA per 100 g of HO
Palmitic (16:0)	6.0	256.42	0	0.000	0.023
Stearic (18:0)	2.0	284.48	0	0.000	0.007
Oleic(18:1)	12.0	282.46	1	0.042	0.042
Linoleic (18:2)	57.0	280.45	2	0.406	0.203
α-Linolenic (18:3)	19.0	278.43	3	0.205	0.068
γ-Linolenic (18:3)	1.7	278.42	3	0.018	0.006
Other	2.3	292.00	0	0.000	0.008
Total	**100.0**			**0.672**	**0.358**

N.B. Hemp Oil (HO).

From the values calculated in Table 3.1 the molar mass for each triglyceride of hemp oil was calculated using Equation 3.1.

$$MM_{FFA} = \frac{100g\ of\ HO}{0.358\left(\frac{Mol\ FA}{100g\ of\ HO}\right)} = 279.33\frac{g}{mol} \tag{3.1}$$

The molar mass per triglyceride of hemp oil was determined from Equation 3.2, whereby the molar masses of glycerol and water are 92.09 and 18 g/mol respectively.

$$\left(3 \times 279.33\ \frac{g}{mol}\right) + \left(92.06\ \frac{g}{mol} - \left(3 \times 18\ \frac{g}{mol}\right)\right) = 876.05\ \frac{g}{mol} \tag{3.2}$$

The number of C=C per triglyceride was determined from Equation 3.3;

$$\frac{0.672\ mol\ C{=}C}{100\ g\ of\ HO} \times \frac{100g\ of\ HO}{0.358\ mol\ FA} \times \frac{3\ mol\ FA}{1\ mol\ TAG} = 5.63\ \frac{C{=}C}{TAG} \tag{3.3}$$

Finally the moles of C=C per 100 g of hemp oil was calculated from Equation 3.4;

$$5.63\ \frac{mol\ C{=}C}{mol\ TAG} \times \frac{mol\ TAG}{876.05\ g} \times 100\ g\ of\ HO = 0.64\ mol\ C{=}C \tag{3.4}$$

3.5.2 Iodine value

The iodine value is used to quantify the degree of C=C present in a plant oil and is used to monitor the epoxidation reaction. As such it is defined as the mass in grams of iodine that is consumed by 100 g of plant oil. That is, the higher the iodine value, the more C=C that is present in a plant oil. In terms of producing a

high quality EVO, the plant oil should contain a large percentage of C=C. Furthermore a successful epoxidation reaction will see a high proportion of those C=C converted into epoxides. In this study the iodine value of hemp oil was theoretically determined from the following Equations as per (ASTM 2011) with the results present below in Table 3.2 whereby C_{FFA} is the free fatty acid coefficient.

$$IV_{FFA} = (\%\ \text{palmitic acid} \times C_{FFA}) + (\%\ \text{oleic acid} \times C_{FFA}) + (\%\ \text{linoleic acid} \times C_{FFA}) + (\%\ \text{linolenic acid} \times C_{FFA}) + (\%\ \text{gadoleic acid} \times C_{FFA}) + (\%\ \text{eruic acid} \times C_{FFA}) \quad (3.5)$$

$$IV_{TAG} = (\%\ \text{palmitic acid} \times C_{TAG}) + (\%\ \text{oleic acid} \times C_{TAG}) + (\%\ \text{linoleic acid} \times C_{TAG}) + (\%\ \text{linolenic acid} \times C_{TAG}) + (\%\ \text{gadoleic acid} \times C_{TAG}) + (\%\ \text{eruic acid} \times C_{TAG}) \quad (3.6)$$

$$C_{FFA} = \frac{253.81 \times \text{mass of DB}}{\text{molar mass of fatty acid}} \quad (3.7)$$

$$C_{TAG} = \frac{253.81 \times \text{mass of DB}}{\text{molar mass of fatty acid} + 12.68} \quad (3.8)$$

Table 3.2. Iodine value and coefficients for hemp oil.

Fatty acid (FA)	FA (%)	Molar mass (g/mol)	No. of DB	C_{FFA}	C_{TAG}	IV_{FFA}	IV_{TAG}
Palmitic (16:0)	6.0	256.42	0	0.000	0.000	0.000	0.000
Stearic (18:0)	2.0	284.48	0	0.000	0.000	0.000	0.000
Oleic(18:1)	12.0	282.46	1	0.899	0.860	10.783	10.320
Linoleic (18:2)	57.0	280.45	2	1.810	1.732	103.171	98.708
α-Linolenic (18:3)	19.0	278.43	3	2.735	2.616	51.960	49.697
γ-Linolenic (18:3)	1.7	278.42	3	2.735	2.616	4.649	4.447
Other	2.3	292.00	0	0.000	0.000	0.000	0.000
Total	**100.0**					**170.563**	**163.171**

Experimental iodine values were obtained using Wij's method (Cooney, T 2009; Dinda et al. 2008; Goud, V et al. 2007; Goud, V, Patwardhan, A & Pradhan, N 2006; Goud, VV et al. 2007; Goud, VV, Patwardhan, AV & Pradhan, NC 2006; Mungroo et al. 2008) which involved titrations using Wij's iodine solution as per (ASTM 2011). After mixing Wij's solution with the hemp oil sample, the degree

of ethylenic unsaturation was calculated by examining the amount of iodine that reacted with the C=C present in the oil. An experimental iodine value of approximately 159 was obtained from the titrations. This value is slightly higher than that obtained from Cooney (2009) who found an iodine value of 122 for hemp oil. For comparative purposes typical iodine values for soybean and canola oils as per the literature are approximately 140 and 112 respectively (Espinoza-Pérez, Haagenson, et al. 2009). Following the completion of the epoxidation reaction the iodine value was determined to be approximately 21 and by using Equation 3.9 where IV_o and IV_f are the iodine values of the epoxidized and raw hemp oil samples respectively. The conversion relative to the iodine value was calculated as 87.1%.

$$IV_0 = \frac{IV_0 - IV_f}{IV_0} \times 100 \qquad (3.9)$$

3.5.3 Oxirane oxygen content

An oxirane ring, Figure 3.5 is a highly reactive and highly strained cyclic ether with bond angles of approximately 60° (Mungroo et al. 2008). Formation of crosslinking occurs throughout the epoxy resin when cured due to the presence of these highly reactive oxirane rings. According to Mungroo et al. (2008), and Goud et al. (2007) higher quality polymers are correlated with high level crosslinking due to higher conversion of double bonds to oxirane rings (epoxides).

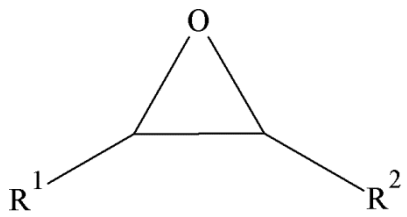

Figure 3.5. Structure of an epoxide, whereby R^1 and R^2 represent the continuation of the fatty acid chains either side of the epoxide.

Oxirane oxygen content is a measure of the amount of C=C which has been transformed into epoxides through the epoxidation process. In this work the

oxirane oxygen content of each sample was determined analytically by the direct titration method with hydrobromic acid solution in acetic acid as per the literature (Cooney, T 2009; Dinda et al. 2008; Goud, V et al. 2007; Goud, V, Patwardhan, A & Pradhan, N 2006; Goud, VV et al. 2007; Mungroo et al. 2008). The maximum theoretical oxirane oxygen content (OO_t) was determined from Equation 3.10. Whereby IV_0 is the triglyceride iodine value of the plant oil, A_i (126.9) is the atomic mass of iodine and A_0 (16.0) is the atomic mass of oxygen.

$$OO_t = \left[\frac{\left(\frac{IV_O}{2A_i}\right)}{100+\left(\frac{IV_O}{2A_i}\right)A_O}\right] \times 100A_O \tag{3.10}$$

$$\text{Conversion relative to } OO = \frac{OO_e}{OO_t} \times 100 \tag{3.11}$$

The hydrobromic acid serves to open the epoxide through the process of bromination, subsequently forming a hydroxyl group. A colour change of the solution typically from violet to yellow to clear indicates the reaction is complete. From the titration, the oxirane oxygen content of EHO was determined to be 8.3%. This represents a relative conversion of C=C to oxirane of 89.4% based on the theoretical oxirane oxygen content of 9.3% calculated from Equations 3.10 and 3.11. In comparison typical oxirane oxygen content values for commercial ESO and ELO are approximately 7.0% and up to 9.6% respectively (Hallstar 2011a, 2011b).

3.5.4 Acid value

As per La Scala et al. (2004) acid number titration was used to determine the extent of the acrylation reaction of EHO by measuring the amount of unreacted acrylic acid in the AEHO mixture. 5 g of acetone was added to 1 g of the AEHO reaction mixture and then mixed using a magnetic stirrer until the AEHO was dissolved in the acetone. Three drops of 0.5 wt% solution phenolphthalein in 50% ethanol pH indicator were added to the mixture to establish the neutralisation point. The solution was then titrated with 0.5 N NaOH until the

end point. The reaction was deemed to be complete when the acid number was equal to or less than approximately 10 (mg NaOH/ g AEHO). If the acid number was found to be greater than 10 the reaction was continued until the subsequent acid number was equal to or 10.

3.5.5 Viscosity

Viscosity measurements were performed at room temperature (25 °C) with a Brookfield DV–II+ viscometer using a plate spindle. Viscosity measurements were taken for hemp oil, EHO, AEHO, AEHO mixed with styrene, commercial ESO, commercial synthetic epoxy and commercial vinylester, Table 3.3. Hemp oil exhibited a viscosity of approximately 60 cP while EHO, AEHO and AEHO mixed with styrene displayed viscosities of 845, 20550 and 360 cP respectively. It can be observed that the viscosity of AEHO alone is too high for most composite processing techniques therefore, 33% by weight of styrene was added to the AEHO bioresin in order to decrease viscosity and improve processability for manufacturing composite parts by traditional composite processing techniques. For comparative purposes the viscosities of Plasthall ESO, R246TX epoxy and SPV6036 vinylester were also measured at 340, 1490 and 425 cP respectively.

Table 3.3. Measured viscosities of bioresins and comparative synthetic resins.

Resin	Viscosity (cP)
Hemp oil	60
EHO	845
Plasthall ESO	340
Synthetic epoxy (R246TX)	1490
AEHO	20550
AEHO + styrene (33%)	360
Vinylester (SPV6036)	425

3.5.6 Spectroscopic analysis

FTIR Spectroscopy

The premise behind the use of FTIR spectroscopy is the ability to identify and analyse the structure of the plant oil before and after epoxidation or acrylation. Specifically FTIR spectroscopy is used to quantify the development of epoxy groups and the percentage consumption of C=C in the EVO (Espinoza-Pérez et al. 2008; Mungroo et al. 2008).

Fundamentally, FTIR spectroscopy operates by measuring the absorption of light in the infrared region, which is specific for each molecular group present in the chemical structure of the material under investigation. Different molecules absorb specific frequencies distinctive of their structure which in turn is dependent on the mass of the atoms and the varying strength of the bonds between the atoms. Therefore particular frequencies can be accurately associated with different bond types enabling identification of the structure of the sample. When a particular molecule within the structure of the sample absorbs IR radiation of a certain wavelength it is displayed in the spectrum as a peak at that particular wave number (Ebbing & Gammon 2005).

In this study a Nicolet 6700 FTIR spectrometer (Thermo Fisher Scientific) was used to characterise the epoxidation reaction. Samples were analysed at a resolution of 4 cm^{-1} and 64 scans. Analysis was performed using OMNIC software version 6.2. All tests were performed on room temperature (25 °C) samples.

Figure 3.6 presents the spectra obtained from the hemp oil (top) and EHO (middle) samples. On the spectra significant areas at specific wave numbers are documented and outlined below. Peak (a) indicated at wavenumber 3010 cm^{-1} corresponds to the consumption of C=C in the epoxidation reaction (Chen, J et al. 2002; Cooney, T 2009; Espinoza-Pérez, Haagenson, et al. 2009). From Figure 3.6 it can be noted that the peak is reduced in size between the hemp oil and the EHO. Upon successful completion of the epoxidation reaction this peak is

completely removed. The main peak of interest occurs at 823 cm^{-1}, (b) and is associated with epoxide formation (Cooney, T 2009; Espinoza-Pérez, Haagenson, et al. 2009; Vlček & Petrović 2006). By examining Figure 3.6 it can be observed that there is a noticeable peak present in the EHO spectra compared with the hemp oil spectra indicating the formation of epoxy groups.

Similarly Figure 3.6 also presents the FTIR spectra associated with the acrylation reaction of the EHO (bottom). The peak visible at 3500 cm^{-1}, (c) is attributed to hydroxyl groups which indicate opening of the epoxides (Kahraman et al. 2006; La Scala, JJ et al. 2004). Furthermore the peak visible at 1630 cm^{-1}, (d) is attributed to the stretching vibration of the C=C. The peaks of the most importance regarding the acrylation reaction are visible at 1400, 985 and 810 cm^{-1} (e). Accordingly these peaks are attributed to the formation of acrylic functional groups in the AEHO (Fu et al. 2010).

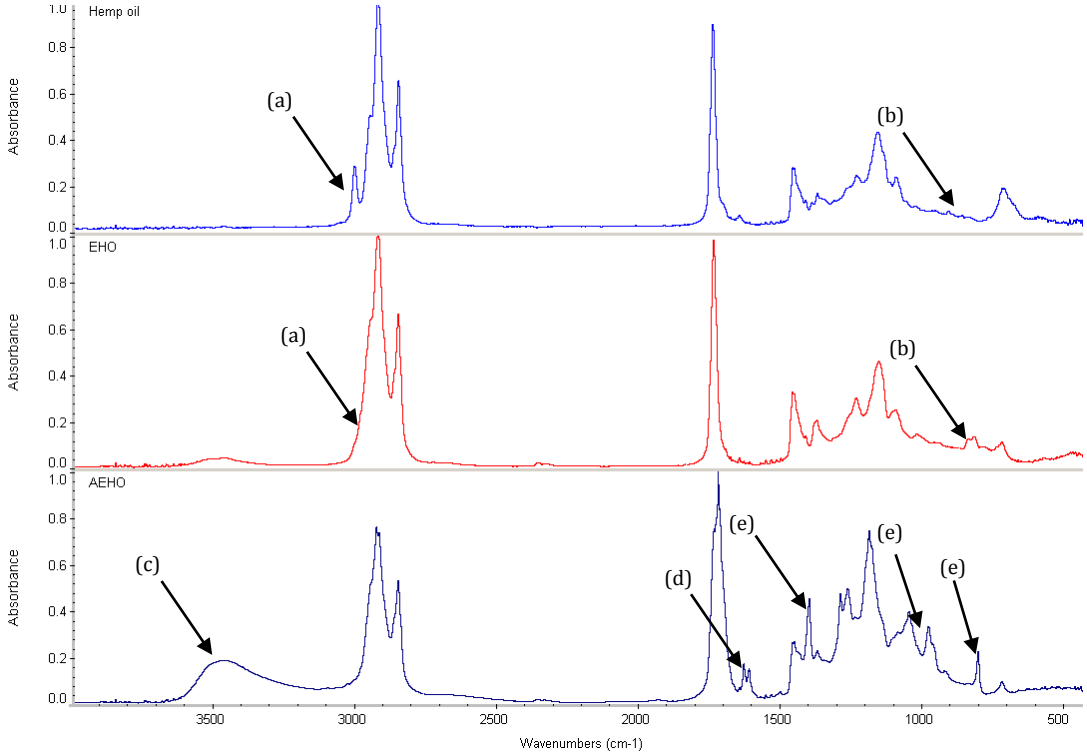

Figure 3.6. FTIR spectra of hemp oil (top), EHO (middle) and AEHO (bottom).

^{1}H-NMR Spectroscopy

^{1}H-NMR is an established method used in the characterisation and analysis of plant oil based bioresins (Kahraman et al. 2006; La Scala, J & Wool 2002; Lu, J,

Khot & Wool 2005; Lu, J & Wool 2006). Also ^{1}H-NMR does not require the use of standards per se and is able to be used in determining both the type of functional groups and the level of functionality (La Scala, JJ 2002). Specifically in this study ^{1}H-NMR was used to analyse the degree of unsaturation in hemp oil and the degrees of epoxidation and acrylation of hemp oil based bioresin samples.

Approximately 100 mg of sample was dissolved in 1 ml of deuterated chloroform containing tetramethylsilane (TMS) (Sigma Aldrich). The samples were then transferred to clean NMR sample tubes (Wilmad LabGlass 5 mm Thin Wall, 528-PP-7) and a Bruker AV400 NMR spectrometer (Queensland University of Technology) was used to collect the spectrums, Figure 3.7. All samples were analysed at ~25 °C with sixteen scans being performed for each sample. MesReNova v8.0.0-10524 software was used to process all spectra. The TMS peak was referenced at 0 ppm and the applicable peaks were integrated as discussed in La Scala (2002).

Figure 3.7 depicts the ^{1}H-NMR spectra of hemp oil, EHO and AEHO. The main peaks of interests occur at; epoxide (2.8-3.3 ppm) and C=C (5.2-5.5 ppm). According to the ^{1}H-NMR spectrum for hemp oil and EHO there are approximately 5.1 epoxy groups per triglyceride which represents a relative conversion to oxirane of approximately 92%. Indeed this result is similar in agreement with that found by the direct titration method (89.4%) as discussed in section 1.7.3. In comparison epoxidized canola oil (ECO) and ESO synthesised by Espinoza-Pérez, et al. (2009) contained 3.8 and 4.0 with epoxy groups per triglyceride and relative conversion to oxirane of 98.5 and 91.0% respectively. Additionally Meyer et al. (2008) epoxidized soybean and jatropha oils with 3.8 and 3.0 epoxy groups per triglyceride and relative conversion to oxirane of 83.3 and 87.4% respectively. Lu et al. (2006) synthesised acrylated epoxidized linseed oil (AELO) from commercial epoxidized linseed oil (ELO) with a reported 6.2 epoxy groups per triglyceride. Although no information was given regarding the relative conversion to oxirane, it is not unreasonable to assume that the conversion is greater than 90% as it is a commercial product.

As discussed previously in section 1.6 AEHO is synthesised from EHO. Therefore it is expected that the epoxide peaks (2.8-3.3 ppm) would reduce throughout the reaction. In this case the epoxide peak was completely diminished and the reaction was deemed to be complete. Furthermore the formation of acrylate groups is expected to appear in the ^{1}H-NMR spectra. Indeed these acrylate peaks are apparent and form peaks situated at 5.8-6.7 ppm. These peaks represent the three protons attached to the C=C of the acrylate esters (Campanella, La Scala & Wool 2009; La Scala, JJ 2002; Lu, J, Khot & Wool 2005; Lu, J & Wool 2006; Scala, J & Wool 2002).

According to the ^{1}H-NMR spectra of AEHO, there are approximately 4.1 acrylates per triglyceride. Similar results were found by other researchers in the studies of AESO and AELO whereby the number of acrylates per triglyceride determined was 3.4 and 5.7-5.8 respectively (Campanella, La Scala & Wool 2009; Lu, J & Wool 2006). As presented in La Scala (2002) it is assumed that for each acrylate group attached to a triglyceride a hydroxyl group should be present. Therefore it is reasonable concluded that there are also 4.1 hydroxyl groups per triglyceride. Due to the nature of the synthesis mechanism there is some propensity for epoxide homopolymerisation throughout the acrylation reaction. Accordingly in this case some epoxide homopolymerisation was evident as represented by peaks 3.26-4.2 ppm. As a result of this epoxide homopolymerisation, conversion to AEHO was limited to approximately 81%.

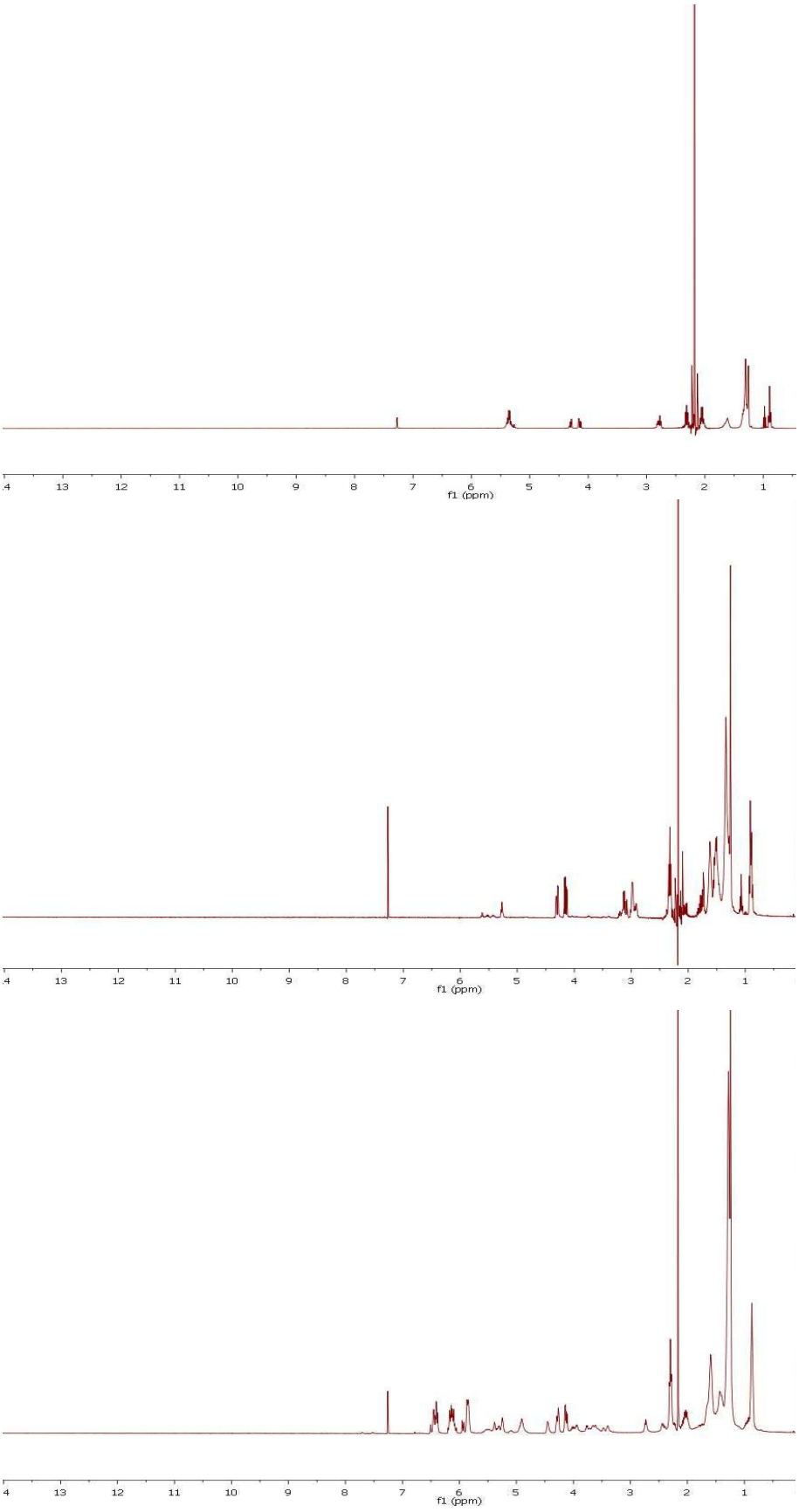

Figure 3.7. ^{1}H-NMR of hemp oil (top), EHO (middle) and AEHO (bottom).

3.6 Conclusions

EHO was successfully synthesised through the *in situ* epoxidation of hemp oil. Process parameters were used as per Cooney (2009) and resulted in an EHO bioresin yield of approximately 75% by volume. AEHO was also synthesised from the EHO via *in situ* acrylation. Viscosities of hemp oil, EHO and AEHO were determined and compared with commercial ESO, synthetic epoxy and vinylester. Characterisation was performed on both EHO and AEHO to determine the number of C=C, the degree of epoxidation and the degree of acrylation. Techniques were employed to achieve these specific objectives such as titrations, FTIR and ^{1}H-NMR.

The degree of C=C in the hemp oil and EHO was quantified by determining the iodine values, which respectively were 122 and 21 for hemp oil and EHO. Due to these values the conversion relative to iodine value was calculated as approximately 89.4%. FTIR was used to monitor the epoxidation and acrylation reactions by analysing the peaks pertinent to C=C consumption and epoxide and acrylate formation.

To determine the degree of epoxidation and the number of epoxy groups per triglyceride, titrations and ^{1}H-NMR were employed. EHO exhibited an oxirane oxygen content of approximately 8.3% and a relative conversion to oxirane of 89.4%. Similarly from ^{1}H-NMR spectroscopy analysis the oxirane oxygen content was calculated as approximately 8.6% and a relative to conversion to oxirane of 92%. Furthermore according to the ^{1}H-NMR spectrum for hemp oil and EHO there are approximately 5.1 epoxy groups per triglyceride which compares favourably to those found for other oils.

According to the ^{1}H-NMR analysis of AEHO, acrylate peaks were apparent and were of the magnitude of approximately 4.1 acrylates per triglyceride. As per the literature AESO and AELO were found to contain 3.4 and 5.7-5.8 acrylates per triglyceride respectively. Some epoxide homopolymerisation was found to occur in the synthesis of AEHO as represented by peaks 3.26-4.2 ppm. As a

result of this epoxide homopolymerisation, conversion to AEHO was limited to approximately 81%. Overall this chapter has demonstrated that EHO and AEHO can be successfully synthesised and are in turn, comparable to other plant oil based bioresins such as ECO, ESO, AESO, ELO and AELO.

Following on from the synthesis and characterisation, Chapter 4 investigates the curing behaviour and develops curing kinetic parameters and models for the synthesised hemp oil based bioresins.

Chapter 4

CURE KINETICS OF HEMP OIL BASED BIORESINS

4.1 Introduction

Chemical kinetics, by definition, is the study of rates of chemical processes during chemical reactions. Kinetic studies includes the investigation of how different experimental conditions can influence the speed of a chemical reaction and yield information about the reaction's mechanism that can describe the characteristics of a chemical reaction. This chapter presents the investigation of the kinetics of the curing process of each one of the thermoset bioresins covered in this study. Numerous complex physical and chemical changes occur during the curing cycle of a thermosetting resin. The physical properties and the processability of thermosetting resins are largely dependent on the reaction rate and degree of cure. These in turn are heavily dependent on the curing conditions, specifically the time and temperature of the cure cycle. It is therefore important to perform cure kinetic studies to establish the optimum processing conditions for thermosetting resins that will provide the required structural performance for specific applications.

While extensive cure kinetic studies have been conducted on numerous, different synthetic thermoset systems (Chen, W-Y, Wang & Chang 2004; Du et al. 2004; Ghaemy, M., Barghamadi & Behmadi 2004; Ghaemy, M, Rostami & Omrani 2006; Kenny 1994; Kenny & Trivisano 1991; Kissinger 1957; Mathew et al. 1999; Ramírez et al. 2007; Ramos et al. 2005; Rosu, Mititelu & Cascaval 2004;

Vyazovkin & Sbirrazzuoli 1996, 1999; Wisanrakkit & Gillham 1990), cure kinetic studies of vegetable oil (VO) based resins, particularly EVO are somewhat limited. Several studies have been conducted by Liang & Chandrashekhara (Liang & Chandrashekhara 2006), Liang et al. (Liang et al. 2005) and Zhu et al. (Zhu, Jiang et al. 2004) that involve the cure behaviour, cure kinetics and rheology analysis of ESO, epoxidized methyl soyate (EMS) and epoxidized allyl soyate (EAS). Badrinarayanan et al. (Badrinarayanan et al. 2009) studied the cure kinetics of soybean oil-styrene-DVB thermosetting copolymers. Park et al. (2004) performed limited cure characterisation of ESO and epoxidized castor oil (ECO) that involved examining the degree of cure as a function of temperature. A detailed investigation into the thermal decomposition of epoxidized soybean oil acrylate (ESOA) was performed by Behera and Banthia (2008) using related kinetic techniques. Dynamic kinetic analysis was performed on linseed oil (LO) based thermosetting resins by Haman et al. (2009) while Tellez et al. (2008) conducted thermal analysis and rheological characterisation on partially-aminated epoxidized linseed oil (ELO). Martini et al. (2009) conducted a study regarding the curing of ELO methyl esters with different dicarboxylic anhydrides. Souza et al. (2004) evaluated the kinetic and thermoanalytic parameters of sunflower oils (SFO) using Differential Scanning Calorimetry (DSC).

From the literature it is apparent that the curing characteristics vary for different resin systems. Consequently a variety of kinetic models have been implemented for each different resin system. Due to the gap in the literature regarding cure kinetic studies of hemp oil based bioresins, the aim of this research is to study the cure kinetics and model the cure behaviour of epoxidized hemp oil (EHO) and acrylated epoxidized hemp oil (AEHO) based bioresin systems. Specifically the objectives of this chapter are to:

- Study the cure kinetics and model the curing behaviour of EHO based bioresin cured with triethylenetetramine (TETA).

- Study the cure kinetics of EHO based bioresin cured with a combination of isophorone diamine (IPD) and TETA and compare this with the cure kinetics and curing behaviour of EHO based bioresin cured with TETA.

- Study the cure kinetics and model the curing behaviour of AEHO based bioresin.

4.2 Materials

EHO and AEHO bioresins were synthesised as discussed in chapter 3, and they were used in this study as the base bioresin systems. For the EHO, the hardener used were Isophorone diamine (IPD with amine hydrogen equivalent weight (AHEW) ≈ 42.6) supplied from ATL composites (Southport, Queensland, Australia) and Triethylenetetramine (TETA with AHEW ≈ 24) from Huntsman, and they were used as received, Figure 4.1 the chemical structure of the hardeners). In the case of the AEHO acrylic bioresin, the added styrene monomer was supplied by Fischer Scientific (United Kingdom), the Promoter N2-51P was sourced from Axon Nobel Ltd and a 40% MEKP based catalyst was used for the curing and received from FGI Australia Ltd Company. The Styrene monomer, the Promoter and the Catalyst were used as received.

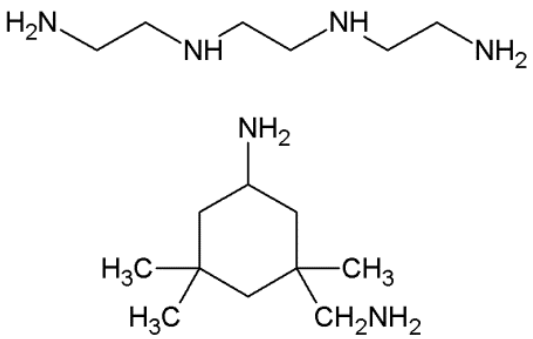

Figure 4.1. Molecular structures of TETA (top) and IPD (bottom).

4.3 Experimental investigation

4.3.1 Theoretical analysis

Both, dynamic and isothermal methods can be used to analyse the cure kinetics of thermosetting polymers. Dynamic kinetic methods use a constant heating rate and are not quantitatively applicable to autocatalytic systems. Isothermal kinetic methods use a constant temperature and are able to be applied to both autocatalytic and n^{th} order systems.

DSC measures the heat generated by reactions. The main assumption used to study the cure kinetics by this technique is that the heat flow, dH/dt, is proportional to the reaction rate, dα/dt. The degree of cure, α, is proportional to the heat generated during the exothermic cure reaction and can be calculated by Equation 4.1 where, ΔH_t is the accumulative heat of reaction given from DSC scans up to a certain time, t, and ΔH_{total} is the total reaction heat. The accumulative heat of reaction is obtained by integrating the exothermic peak of the DSC curve. In the same way, the residual heat of reaction is obtained by integrating the whole peak shown in the DSC runs performed at the reheating stage. The total reaction heat is the sum of the isothermal heat of reaction plus the residual heat of reactions (Lem & Han 1984; Vilas et al. 2001). For modelling purposes it is adequate to consider the total heat of reaction values obtained from dynamic runs to be of the same order as the isothermal heat of reactions plus residual heat of reactions (Kenny & Trivisano 1991). The reaction rate can be calculated from Equation 4.2.

$$\alpha = \frac{\Delta H_t}{\Delta H_{total}} \tag{4.1}$$

$$\frac{d\alpha}{dt} = \frac{(dH/dt)}{\Delta H_{total}} \tag{4.2}$$

Isothermal cure kinetics

From Equations 4.1 and 4.2, kinetic models capable of predicting the curing behaviour of thermosetting polymers can be developed. Except for the models derived by Horie et al. (1970) and Sourour and Kamal, (1976) phenomenological models employed by many investigators are purely empirical (Lem & Han 1984). The general form of the rate Equation, in absence of diffusion control, that is used in all the kinetic models is shown in Equation 4.3, where *k(T)* is the reaction rate constant, and *f(α)* is the function that is dependent on *α*. The reaction rate constant is an Arrhenius function of temperature, as shown in Equation 4.4, where *A* is the pre-exponential factor, E_a is the activation energy (the difference in enthalpies of the transition state and the initial state), *R* is the universal gas constant, and *T* is the absolute temperature.

$$\frac{d\alpha}{dt} = k(T)f(\alpha) \tag{4.3}$$

$$k(T)_i = A_i e^{-\frac{E_a}{RT}} \tag{4.4}$$

Numerous different expressions have been proposed for the function *f(α)*, with the being simplest the nth order Equation, Equation 4.5, where k is the reaction rate constant and n is the order of reaction.

$$\frac{d\alpha}{dt} = k(1-\alpha)^n \tag{4.5}$$

Typically, the form of *f(α)* used for autocatalytic reactions is that shown in Equation 4.6 if the initial reaction rate is zero, or that shown in Equation 4.7 if the initial reaction rate is not zero:

$$\frac{d\alpha}{dt} = k\alpha^m(1-\alpha)^n \tag{4.6}$$

$$\frac{d\alpha}{dt} = (k_1 + k_2\alpha^m)(1-\alpha)^n \tag{4.7}$$

where k_1 and k_2 are the reaction rate constants and m and n are orders of reaction.

In autocatalytic reactions, one of the reaction products is also a catalyst for further reactions. The expression shown in Equation 4.7 corresponds to Kamal's model which has been successfully applied to many autocatalytic reactions of a diversity of resin systems (Kamal 1974).

Vitrification usually occurs during the isothermal curing of thermosetting resins. This phenomenon involves a transformation from a semi-liquid or rubbery state to a glassy state as a result of an increase in the molecular weight caused by the high degree of polymerization. Near vitrification, the reaction rate decreases drastically and the kinetics are affected by the local viscosity, which in turn is dependent on the temperature and extent of the reaction. As a consequence, the reaction 'freezes' and the degree of reaction reaches a maximum value, $\alpha_{max}<1$, for a given cure temperature. Therefore, the previously mentioned phenomenological models can be modified to account for vitrification, by adding a new term that is a function of α_{max}, Equation 4.8 (Stevenson 1986; Vilas et al. 2001).

$$\frac{d\alpha}{dt} = k(T)g(\alpha_{max})f(\alpha) \tag{4.8}$$

Different expressions have been proposed for the function $g(\alpha_{max})$. Some examples are shown in Equation 4.9 (Lee & Lee 1994; Stevenson 1986) and Equation 4.10 (Chern & Poehlein 1987; Cole 1991), where x and C are new adjustable parameters.

$$g(\alpha_{max}) = \left(\frac{\alpha_{max}-\alpha}{\alpha_{max}}\right)^x \tag{4.9}$$

$$g(\alpha_{max}) = \frac{1}{1+e^{C(\alpha-\alpha_{max})}} \tag{4.10}$$

In addition, Kamal's model can be modified to account for the vitrification phenomenon, incorporating an α_{max} term to prevent the conversion exceeding the degree of cure associated with the vitrification Equation 4.11:

$$\frac{d\alpha}{dt} = (k_1 + k_2\alpha^m)(\alpha_{max} - \alpha)^n \quad (4.11)$$

Dynamic analysis

Dynamic DSC measurements overcome some of the drawbacks of isothermal DSC analysis, such as being time-consuming (Yousefi, Lafleur & Gauvin 1997) inaccuracy of the initial cure data caused when the sample must be heated quickly to the chosen cure temperature (Peyser & Bascom 1977) and data errors caused by the premature reaction start during the initial heating ramp up to the cure temperature. Some authors have found the kinetic parameters estimated from non-isothermal DSC measurements to be different from those obtained through isothermal DSC measurements (Han & Lee 1987; Prime, Michalski & Neag 2005). However, other authors have found similar values for the kinetic parameters evaluated by both techniques (González-Romero & Casillas 1989; Patel, Shah & Patel 1986).

Two dynamic kinetic models based on multiple heating rates that are useful in determining the activation energy of the curing reaction have been proposed by Kissinger (1957) and Ozawa-Flynn-Wall (Flynn & Wall 1966; Ozawa 1965). Both methods are independent of the reaction order and therefore simplify the complexity of the curing reaction. The activation energy can be estimated using the former method from the gradient of the plot $\ln(q/T_m^2)$ vs. $1/T_m$, Equation 4.12, or with the Ozawa-Flynn-Wall method from the slope of the curve $\log q$ vs. $1/T_m$, Equation 4.13, where q is the heating rate and T_m is the peak temperature.

$$\frac{d\left[ln\left(\frac{q}{T_m{}^2}\right)\right]}{d\left(\frac{1}{T_m}\right)} = -\frac{E_a}{R} \quad (4.12)$$

$$logq = log\left(\frac{AE_a}{g(\alpha)}\right) - 2.315 - \frac{0.4567E_a}{RT_m} \quad (4.13)$$

4.3.2 Sample preparation

For EHO/TETA and EHO/TETA/IPD samples, molar ratios of 1:1 (EHO:TETA) and 1:0.5:0.5 (EHO:TETA:IPD) were used, respectively. Samples for DSC analysis were prepared by thoroughly mixing 10 g of EHO bioresin with the hardener at room temperature. This process was repeated to prepare 'fresh' samples for each DSC scan. After the EHO was acrylated to form AEHO, 33% by weight of styrene was added in order to decrease viscosity and improve processability for manufacturing composite parts by traditional composite processing techniques. Afterwards, the promoter was incorporated to 10 g of the AEHO/styrene mixture (0.25% by weight) and thoroughly mixed. Subsequent to this the catalyst was added (4% by weight) and stirred thoroughly for several minutes before every DSC run.

4.3.3 Cure kinetics using DSC

Dynamic and isothermal analysis was performed with a TA Instruments DSC Q100 Differential Scanning Calorimeter, Figure 4.2. Dry nitrogen gas at 60mL/min was used during the experiments to purge the DSC cell. Samples between 10-15 mg were enclosed in hermetic aluminium DSC sample pans. Dynamic scans were performed at four different heating rates: 5, 10, 15 and 20 °C/min from 15 °C to a maximum of 300 °C. The cured samples were then cooled to 15 °C at a rate of 10 °C/min. To complete the heat-cool-heat cycle, the samples were reheated to 300 °C to confirm the nonexistence of any residual curing. Isothermal scans determined from the dynamic DSC data were performed at four different temperatures, Table 4.1. The isothermal scans were deemed to be complete when the thermograms levelled off to a predetermined baseline.

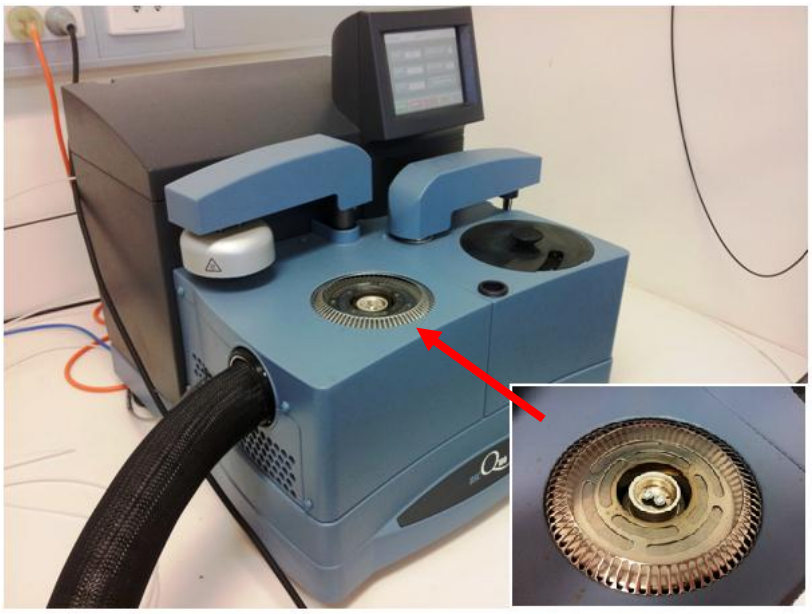

Figure 4.2. TA Instruments DSC Q100 showing sample placement.

Table 4.1. Isothermal temperatures used for the different bioresin systems

Bioresin system	Isothermal temperatures (°C)
EHO/TETA	110, 115, 117.5, 120
EHO/TETA/IPD	110, 115, 117.5, 120
AEHO	50, 60, 70, 75, 80

4.4 Results and discussion

4.4.1 Cure kinetics of epoxidized hemp oil

Dynamic kinetic analysis

Both the Kissinger and Ozawa-Flynn-Wall methods were used in the dynamic kinetic analysis. Total reaction heat ΔH_{total} was determined as the area under the dynamic thermograms up to full conversion, Figures 4.3 and 4.4. The average total reaction heat was taken as the average of ΔH_{total} at each heating rate. The results in conjunction with the peak temperatures, T_m of the thermograms are summarised in Table 4.2. T_m was determined from the peak of the exotherms at each heating rate using Universal Analysis 2000 version 3.9A software supplied with the DSC Q100 Instrument.

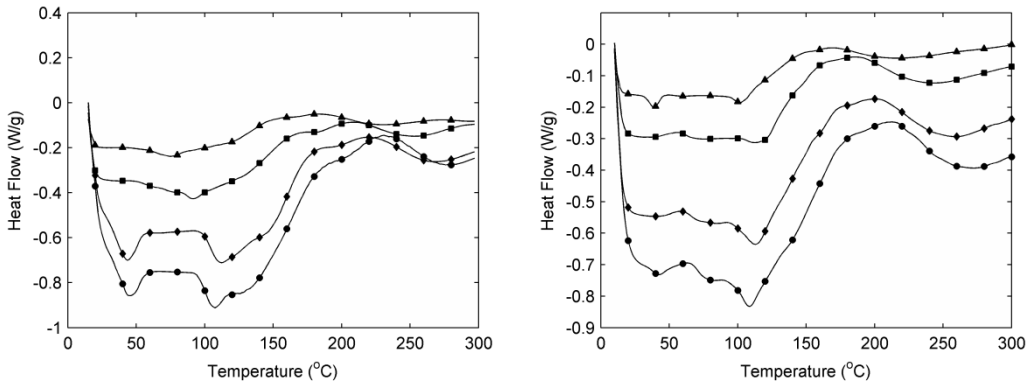

Figure 4.3. Dynamic DSC thermograms for EHO/TETA (left) and EHO/TETA/IPD (right) with 5 °C/min (▲), 10 °C/min (■), 15 °C/min (♦) and 20 °C/min (●).

Table 4.2. Total reaction heats and peak temperatures for both EHO based bioresin systems at different heating rates.

q (°C/min)	ΔH_{total} (J/g)		T_m (°C)	
	TETA	TETA/IPD	TETA	TETA/IPD
5	87.4	93.2	157.2	144.9
10	94.6	94.3	168.4	159.9
15	106.6	96.2	182.9	173.8
20	120.8	104.0	195.3	185.7
Avg. ΔH_{total}	102.4	96.9		

IPD was found to influence the total reaction heat, average total reaction heat and peak temperature. The total reaction heat was lower for EHO/TETA/IPD samples compared with EHO/TETA with the exception of 5°C/min with EHO/TETA samples displaying a higher variation of total reaction heat over the heating rate range than EHO/TETA/IPD samples. Slightly lower values of average total reaction heat were observed for samples containing TETA/IPD compared with TETA samples indicating an influence by IPD. Overall the TETA system displayed a wider range of total reaction heat than the IPD system. Values of peak temperature showed a similar range for both sample types with TETA/IPD samples displaying lower values throughout the range. Similar findings in terms of the influence of IPD on total reaction heat and peak temperature were also reported by Czub (2006a, 2006b).

For both bioresin systems, peak temperatures and total heat of reactions were found to increase with increased heating rates as shown in Table 4.2. Through application of Kissinger and Ozawa-Flynn-Wall methods, the activation energies were determined from the gradients of Figure 4.4 for both bioresin systems.

Due to the observed linearity of the plots, validity of both models is suggested. Activation energies for both Kissinger and Ozawa-Flynn-Wall models proved to be similar for both systems.

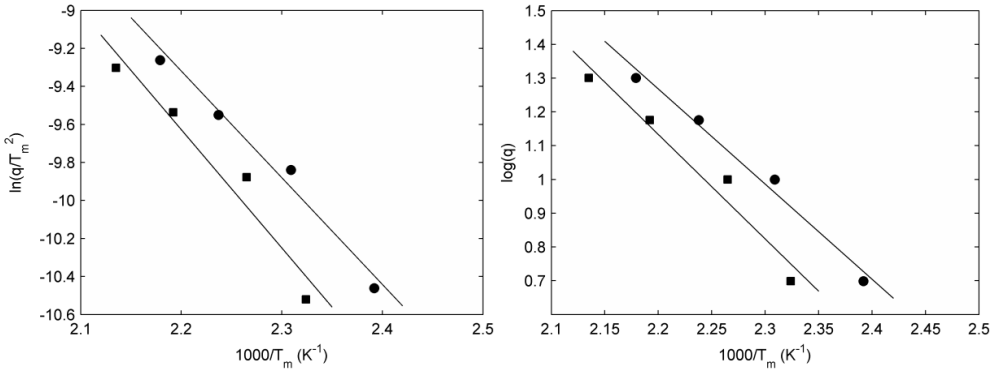

Figure 4.4. Activation energies obtained from Kissinger's (left) and Ozawa-Flynn-Wall (right) method's for EHO/TETA, (■) and EHO/TETA/IPD (●).

Using the Kissinger model, values of 51.8 and 46.6 kJ/mol were obtained for EHO/TETA and EHO/TETA/IPD systems respectively. From the Ozawa-Flynn-Wall model values of 56.3 and 51.3 kJ/mol were obtained for EHO/TETA and EHO/TETA/IPD systems, respectively. These results are consistent with the findings of other researchers (Barral et al. 2000; Chen, W-Y, Wang & Chang 2004; Islam, M S, Pickering & Foreman 2009; Martini, Braga & Samios 2009) who also found activation energies from the Ozawa-Flynn-Wall model to be marginally higher than the values determined by the Kissinger model. These results show that the system containing IPD displays activation energies approximately 10% lower than the TETA/IPD system. Furthermore this suggests that the addition of IPD enhances the curing reaction of the EHO bioresin system.

Isothermal kinetic analysis

Kamal's autocatalytic model modified to account for diffusion was used in this study, Equations 4.7 and 4.8. The kinetic parameter, k_1 was determined by extrapolating the isothermal reaction rate curves to α = 0. The values of the activation energies and the pre-exponential factors were determined by plotting $\ln k_{1,2}$ versus $1000/T$. The activation energies and pre-exponential were determined from the gradients and y-intercepts respectively. The data exhibited

a linear form thereby indicating behaviour predicted by Equation 4.4. Table 4.3 summarises the activation energies and pre-exponential factors for both bioresin systems.

Table 4.3. Activation energies (kJ/mol) and pre-exponential factors for both bioresin systems.

Bioresin system	E_{a1}	E_{a2}	A_1	A_2
EHO/TETA	139.5	-80.5	$e^{34.64}$	$e^{-31.69}$
EHO/TETA/IPD	114.7	-39.2	$e^{27.62}$	$e^{-20.15}$

The bioresin system containing IPD exhibits lower activation energy for E_{a1} than the system without IPD. Values of E_{a2} for both systems display anti-Arrhenius behaviour as k_2 was found to decrease with temperature therefore implying a negative activation energy. This phenomenon is associated with curing of 100% EHO bioresin and not synthetic resins or blends. The nature and cause of this behaviour was not identified although it is thought to be due to an unidentified competitive reaction that gives rise to the appearance of k_2 decreasing with increasing temperature (Helfferich 2004). Further investigation regarding this is required.

From Table 4.4 it can be seen that as the temperature increased the values of k_1 increased and k_2 decreased for both systems. The higher magnitude of values for k_1 compared with k_2 for the TETA/IPD system indicates that the reaction mechanism is more n^{th} order dominant than autocataltyic. This can also be observed from Figure 4.5 whereby it is evident that the maximum reaction rate occurs closer to the beginning rather than in the intermediate conversion stage. Total heat of reaction was found to increase with increasing isothermal temperature. Samples containing IPD displayed higher total heat of reaction than samples without, indicating enhanced curing with IPD.

Table 4.4. Autocatalytic model parameters for both bioresin systems.

Sample	T (°C)	ΔH_{total}	k_1	k_2	m	n	m+n	C	α_c
EHO/TETA	110.0	60.4	0.00010	0.00166	0.80	4.37	5.17	100	0.59
	115.0	69.6	0.00020	0.00116	0.75	3.51	4.26	140	0.68
	117.5	80.9	0.00025	0.00101	0.74	2.30	3.04	170	0.79
	120.0	92.2	0.00030	0.00087	0.71	1.64	2.35	200	0.90
EHO/TETA/IPD	110.0	66.6	0.00021	0.00053	1.02	2.87	3.89	80	0.65
	115.0	76.8	0.00031	0.00046	0.92	2.65	3.57	105	0.75
	117.5	90.1	0.00040	0.00043	0.86	1.70	2.56	120	0.88
	120.0	96.3	0.00053	0.00038	0.71	1.38	2.09	130	0.94

Figure 4.5 display plots of experimental data and model predictions for both bioresin systems at 115 °C. Similar results were obtained throughout this study at all temperatures. Acceptable agreement of fit between experimental data and the autocatalytic model is observed throughout the entire temperature range for both systems.

Values of *m* and *n* were found to decrease when the temperature increased for both systems. Subsequently the overall reaction order was found to decrease with an increase in temperature. Average total reaction orders ($m + n$) were found to be equal to 3.7 and 3.0 for the EHO/TETA and EHO/TETA/IPD systems, respectively. Throughout the entire temperature range TETA/IPD based samples displayed higher conversions than TETA samples which can be seen in Figure 4.6.

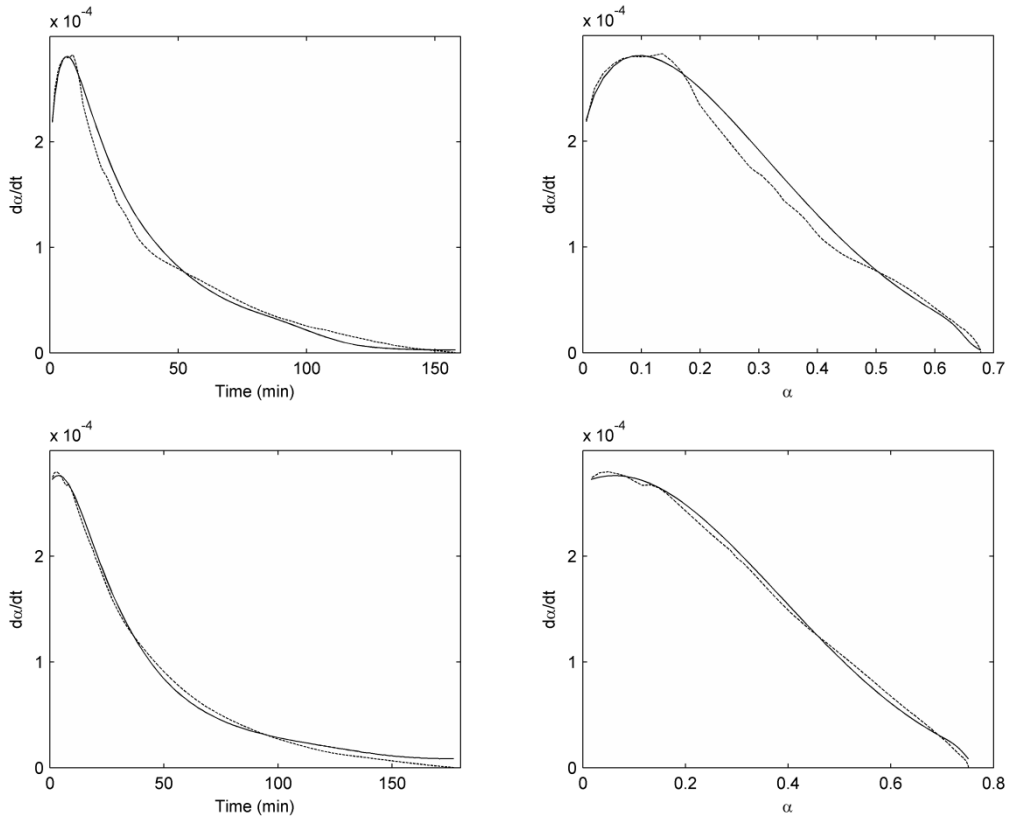

Figure 4.5. Comparison of experimental data (dashed line) with model predictions (solid line) at 115 °C for EHO/TETA (top row) EHO/TETA/IPD (bottom row).

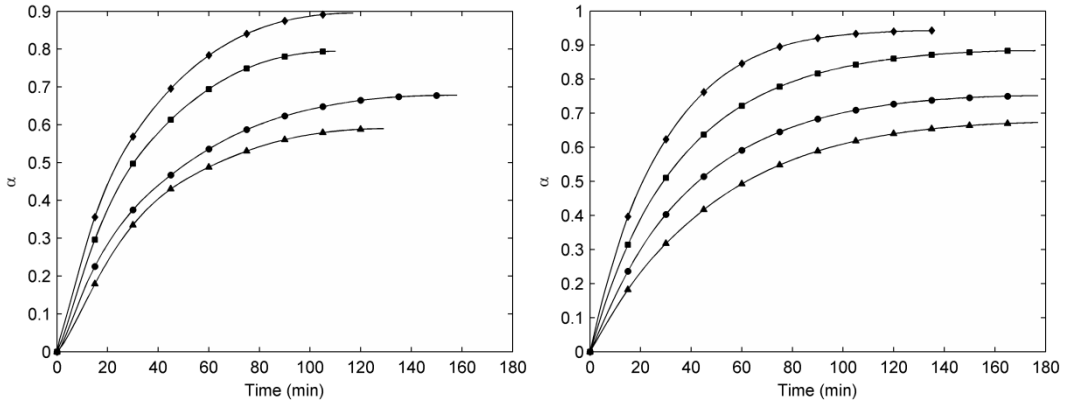

Figure 4.6. Degree of cure (α) as a function of time for EHO/TETA (left) and EHO/TETA/IPD (right) at 110 °C (▲), 115 °C (●), 117.5 °C (■) and 120 °C (♦).

4.4.2 Cure kinetics of acrylated epoxidized hemp oil

Dynamic kinetic analysis

The curves obtained from the dynamic DSC runs at different heating rates are shown in Figure 4.7. It can be seen that both peak temperature and heat of reaction increased with increased heating rates, showing the same trend observed previously for the EHO/TETA, EHO/TETA/IPD and epoxy(Dupuy, Leroy & Maazouz 2000; Islam, M S, Pickering & Foreman 2009; Omrani et al. 2008) systems. In contrast to this, many authors did not find a clear trend regarding epoxy (Barral et al. 2000; Karkanas & Partridge 2000), polyester and vinylester (Lem & Han 1984; Lu, M, Shim & Kim 1999) systems. Therefore, considering the results of this study in conjunction with the aforementioned cases the difference between the heat of reaction values was less than 5%, it can be concluded that the dispersion of the data is in the order of the experimental and data processing error. Accordingly no correlation can be established between the heat of reaction and the heating rate, as suggested by Kenny and Trivisano (1991). Table 4.5 presents the values of peak temperatures and heat of reactions calculated from the dynamic DSC curves.

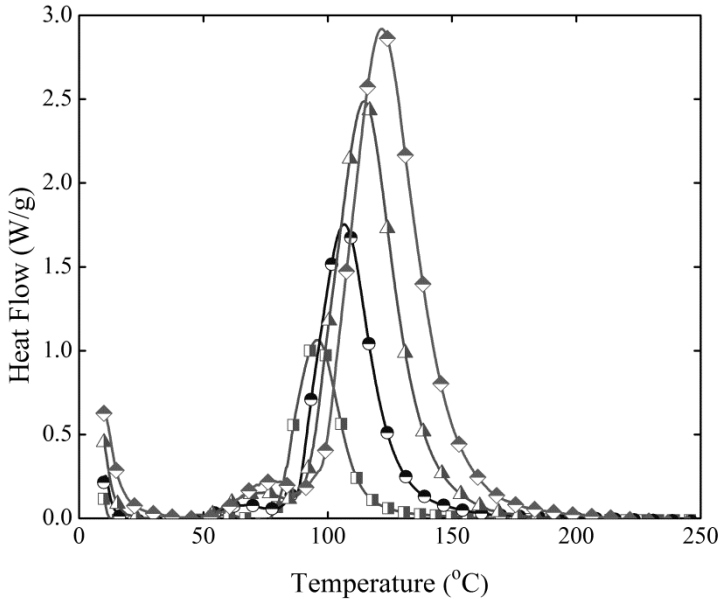

Figure 4.7. Dynamic DSC curves of AEHO based bioresin at 5 (—▯—), 10 (—●—), 15 (—▲—) and 20 °C/min (—◇—).

Table 4.5. Heats of reaction and peak temperatures at different heating rates.

q (°C/min)	ΔH_{total} (J/g)	T_m (°C)
5	317.0	96.1
10	317.1	106.5
15	320.2	114.8
20	334.9	121.9
Avg. ΔH_{total} (J/g)	322.3	

Plots of $\ln(q/T_m^2)$ vs. $1000/T_m$, and $\log q$ vs. $1000/T_m$ corresponding to the Kissinger and Ozawa-Flynn-Wall methods respectively, are shown in Figure 4.8. Both models appear to be valid given that the degree of linearity found in the plots is high. The activation energy found by applying the Kissinger model was 58.87 kJ/mol, while the Ozawa-Flynn-Wall model gave slightly higher activation energy, of 62.02 kJ/mol. These results are consistent with other researchers' findings for epoxy (Barral et al. 2000; Chern & Poehlein 1987; Islam, M S, Pickering & Foreman 2009), ELO (Martini, Braga & Samios 2009) and EHO, who also found activation energies from the Ozawa-Flynn-Wall model to be marginally higher than values determined by the Kissinger model.

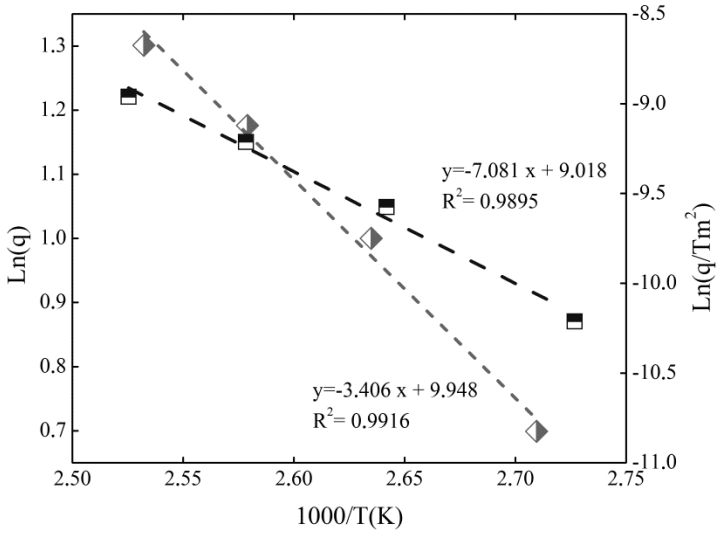

Figure 4.8. Plot to determine Kissinger (⬒) and Ozawa-Flynn-Wall (⬗) activation energies.

Isothermal kinetics analysis

Isothermal reaction rate profiles obtained for the different applied cure temperatures are shown in Figure 4.9. A significant induction time (the period of time which there is no reaction) can be seen for the 50 °C isothermal curing

condition. As expected, the higher the temperature, the faster the overall reaction. In addition, the onset of reaction and the maximum reaction rate occur earlier as the cure temperature is increased.

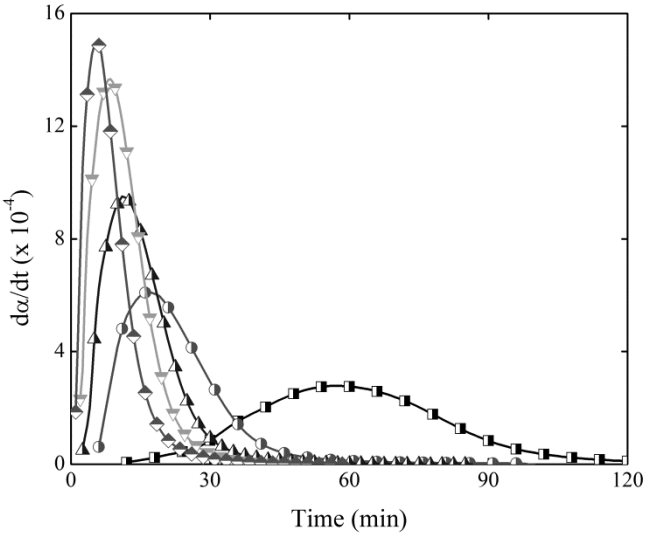

Figure 4.9. Reaction rate versus time at 50 (–■–), 65 (–◑–), 70 (–◭–), 75 (—▽—) and 80 ˚C (—◈—).

Values of the reaction rate *dα/dt* plotted in Figure 4.9 were calculated by dividing the original DSC signal, *dH/dt*, by the averaged total heat of reaction obtained from the dynamic DSC runs, Table 4.5, as stated in Equation 4.2. The total heat of reaction developed in each isothermal experiment, ΔH_{total}, was obtained by the integral of the peaks of the original DSC plots, *dH/dt* vs. *time*. The values ΔH_{total} obtained in the isothermal runs are presented in Table 4.6. The value of ΔH_{total} was not expected to change with the curing temperature, since it comprises of both the total and residual heat of reaction developed in each isothermal experiment. However, an increasing trend was observed with increasing curing temperature in accordance with the findings of Omrani et al. (2008) and Kenny and Trivisano (1991). These authors suggested that the inconsistencies found were caused by some inaccuracies associated with the ΔH_{total} values as they may be affected by the sum of the integration errors of two different peaks and the superposition of the glass transition signal upon the residual reactivity peak.

Table 4.6. Total heat of reaction developed in each isothermal experiment

Cure Temperature (°C)	ΔH_{total} **(W/g)**
50	273.38
65	274.14
70	282.43
75	292.56
80	301.80

H_{total} was higher when it was calculated from dynamic runs Table 4.5. In addition, its value changed as the curing conditions (both isothermal and non-isothermal) were modified. Therefore, for modelling purposes, the averaged value of H_{total} obtained from the dynamic runs (322.3 J/g, shown in Table 4.5) was considered as the total heat of reaction, as suggested by Kenny and Trivisano (1994).

The evolution of the degree of cure with time at the curing temperatures used in this study can be seen in Figure 4.10. As expected, the maximum conversion increased and was reached faster at higher isothermal temperatures. For instance α_{max} was reached in 25 minutes at 80 °C compared with approximately 110 minutes at 50 °C. The induction time mentioned previously is also visible in these plots. After this time, the degree of cure increased rapidly within the initial stage of reaction at all temperatures because in this stage the reaction is chemically controlled. At higher α values, diffusion-controlled mechanisms related to the vitrification phenomenon cause the degree of cure to slow down and finally level off to a maximum value, α_{max}, when vitrification is reached.

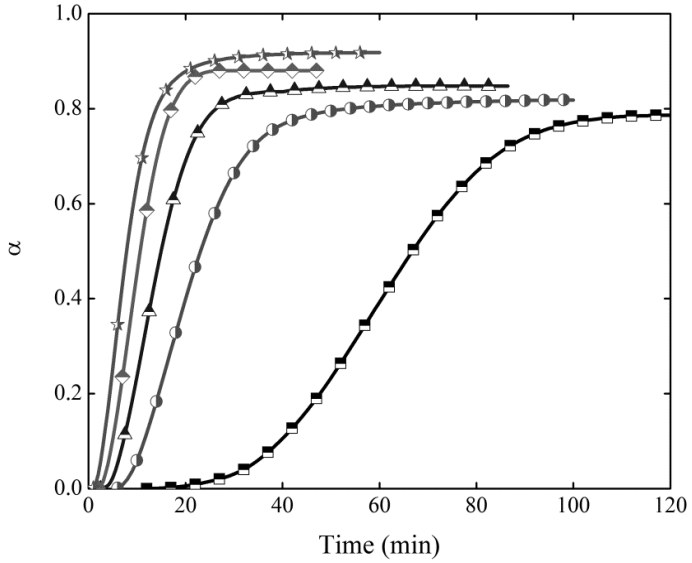

Figure 4.10. Degree of cure as a function of time for AEHO based resin at 50 ˚C (—■—), 65 ˚C (—◑—), 70 ˚C (—▲—), 75 ˚C (—◆—), and 80 ˚C (—★—).

Figure 4.11 shows plots of $d\alpha/dt$ as a function of α for the isothermal temperatures. It can be seen that the reaction rate at any given value of α increased as the temperature of cure increased. In addition, the value of $d\alpha/dt$ becomes zero at conversions lower than 1, showing once again that vitrification took place at all the temperatures studied. The behaviour of the reaction rate curves suggest an autocatalytic reaction as opposed to simple *n*th order kinetics, because the reaction rate reached a maximum value after the beginning of the cure cycle.

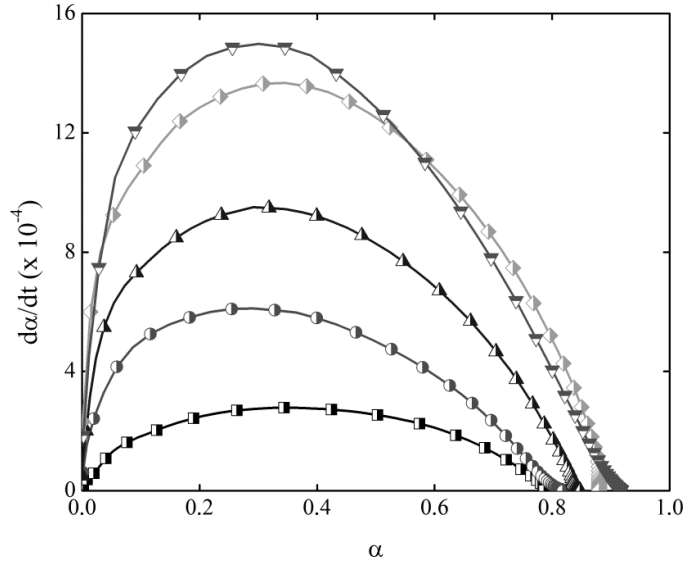

Figure 4.11. Reaction rate versus degree of cure at 50 °C (—■—), 65 °C (—◑—), 70 °C (—▲—), 75 °C (—◈—), and 80 °C (—▽—).

Therefore, Kamal's autocatalytic model, Equation 4.7, was initially used to model the cure kinetics of the AEHO based resin. Figure 4.12 shows the fitting of the experimental data with this model for the resin cured at 65 °C. It can be seen that the model could not properly fit the experimental data, because it does not account for the vitrification phenomenon that was observed to occur at all the cure temperatures. It should be noted that the same unsatisfactory results were obtained for the other temperatures studied. In order to improve the model accuracy by considering vitrification, a modified form of Kamal's model, Equation 4.11, was used.

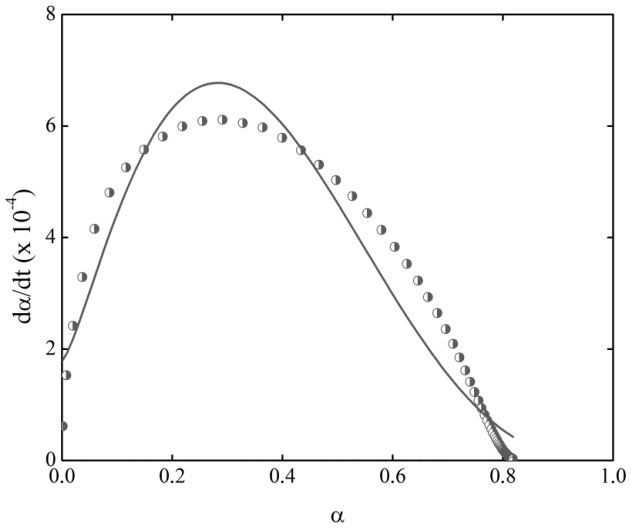

Figure 4.12. Experimental data (◑) fitted with Kamal's model (———).

The results of experimental data and model predictions for reaction rate as a function of degree of cure and as a function of time for all the temperatures are shown in Figures 4.13 and 4.14 respectively. The agreement of fit is very good for all the temperatures, suggesting that the modified Kamal's autocatalytic model accounting for vitrification can be used to predict the curing behaviour of AEHO based bioresin. The values of the model parameters obtained from the fitting of the experimental curves are presented in Table 4.7.

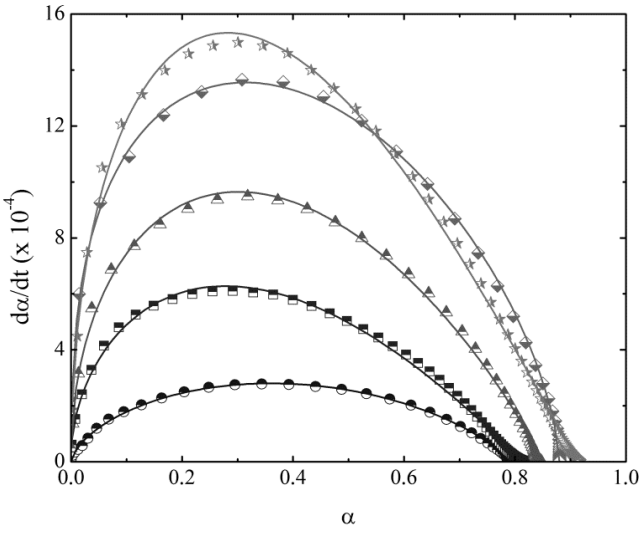

Figure 4.13. Experimental isothermal DSC data at 50 °C ( ), 65 °C ( ), 70 °C ( ), 75 °C ( ), and 80 °C ( ), fitted with the modified Kamal's model accounting for vitrification (solid line).

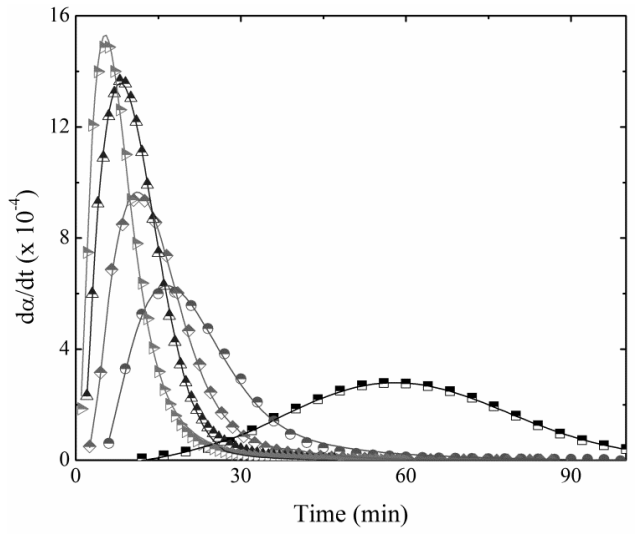

Figure 4.14. Comparison of experimental data with model predictions (solid line) for reaction rate versus time at 50 °C ( ),65 °C ( ), 70 °C ( ), 75 °C ( ) and 80 °C ( ).

The values of both k_1 and k_2 increased as the temperature increased, and the values of k_2 were higher compared with the values of k_1, suggesting that the reaction may be more influenced by autocatalytic mechanisms rather than by n^{th} order mechanisms. With the exception of the test performed at 80 ˚C, values of *m* were found to decrease when the temperature increased, in accordance to previous findings on the EHO bioresin systems. Moreover, values of *n* did not show a clear trend, as found by other authors, (Lem & Han 1984; Vilas et al. 2001) although they seem to decrease with the increase of temperature between 65 and 75 °C. In a study involving unsaturated polyester resin, it is

interesting to note that Vilas et al. (2001) found a decreasing trend for *m* and *n* values when experimental data was fitted with traditional autocatalytic models, while they could not obtain any clear trend when an autocatalytic model modified to account for vitrification was used to fit the same data.

Table 4.7. Autocatalytic model parameters.

T (°C)	k_1	k_2	m	n	$m+n$	α_{max}
50	8.20E-06	0.00103	0.658	0.756	1.414	0.811
65	1.50E-05	0.00233	0.536	1.034	1.570	0.822
70	2.94E-05	0.00296	0.500	0.889	1.390	0.844
75	3.80E-05	0.00301	0.380	0.661	1.041	0.896
80	5.00E-05	0.00471	0.508	1.107	1.615	0.918

Both reaction rate constants, k_1 and k_2, displayed Arrhenius behaviour, as shown in Figure 4.15. The activation energies and pre-exponential factors were determined from the gradients and y-intercepts of the curves, respectively. The results, summarized in Table 4.8, showed that the activation energies obtained from the isothermal DSC experiments were very similar to the values calculated with the Kissinger and Ozawa-Flynn-Wall models applied to the dynamic DSC experimental data.

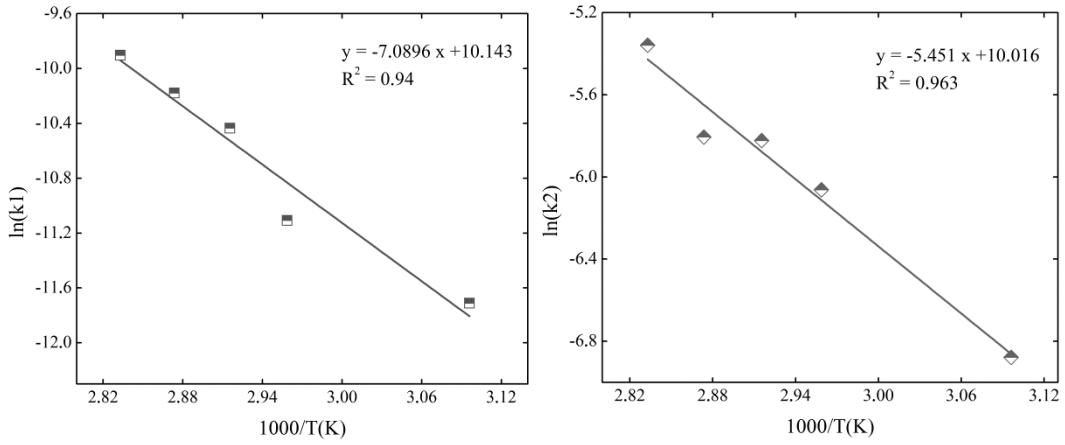

Figure 4.15. Arrhenius-type plot for reaction constant k_1 and k_2.

Table 4.8. k_1 and k_2 activation energies and pre-exponential factors for AEHO based resin.

E_{a1} (kJ/mol)	E_{a2} (kJ/mol)	A_1	A_2
58.94	45.32	$e^{10.14}$	$e^{10.02}$

4.5 Conclusions

An EHO based bioresin system cured with two different systems; TETA and TETA/IPD was studied and compared. Cure kinetic analysis was performed using two dynamic models; Kissinger and Ozawa-Flynn-Wall and one autocatalytic model developed by Kamal modified to account for diffusion post-vitrification. It was found that the total heats of reaction were slightly influenced by the addition of IPD. From the observed dynamic activation energies the bioresin system containing IPD exhibited activation energies approximately 10% lower than the TETA system.

Both bioresin systems displayed autocatalytic mechanisms with the system containing IPD being characterised as heavily influenced by n^{th} order mechanicsms. Maximum conversions of the TETA/IPD system were consistantly higher than those of the TETA system throughout the entire temperature range. Cure kinetic parameters where obtained for both systems with k_1 and k_2 increasing and decreasing respectively as temperature increased. The observed decrease in k_2 is thought to be due to an unidentified competive reaction. The total order of the reaction was found to decrease with an increase in temperature for both systems. An autocatalytic model developed by Kamal, modified to account for diffusion post-vitrification was found to satisfactorily describe the cure behaviour of both bioresin/hardener systems. It was found that IPD increased the curing rate of the EHO bioresin systems.

The cure behaviour of AEHO based bioresins was investigated by dynamic and isothermal DSC. As expected, the maximum degree of cure increased as the cure temperature increased. The conversion was found to be 0.81 at the lowest temperature used in the DSC tests (50 °C) while the highest conversion was 0.92 at the highest cure temperature used (80 °C). The AEHO showed an autocatalytic behaviour and the vitrification phenomenon prevented the conversion reaching full conversion. Therefore, a modified expression of the autocatalytic Kamal's model that takes into account vitrification was used for the kinetic model. This model accurately fitted the experimental kinetic values

for all temperatures, enabling it to be used in further numerical modelling of the curing of AEHO bioresins and biocomposites containing AEHO.

The activation energies estimated from dynamic and isothermal measurements were found to be similar. They were calculated from dynamic DSC data using the Kissinger (58.87 kJ/mol) and Ozawa-Flynn-Wall (62.02 kJ/mol) models, and from isothermal DSC data using the Arrhenius-type dependence of the reaction rate constants, k_1 and k_2, with temperature (58.94 kJ/mol and 45.32 kJ/mol respectively). The value of k_2 was found to be higher than the value of k_1 for all temperatures, suggesting that the curing behaviour of this bioresin is more influenced by autocatalytic mechanisms than by *n*th order mechanisms.

Using the curing parameters determined in this chapter, Chapter 5 investigates the thermo-mechanical properties of hemp oil based bioresins and biocomposites.

Chapter 5

THERMO-MECHANICAL PROPERTIES OF HEMP OIL BASED BIORESINS AND BIOCOMPOSITES

5.1 Introduction

In the search for high performance construction materials, fibre composites are now being more widely utilized than in the past. Fibre composites generally use petro-chemically derived polymer resins for example; epoxy, unsaturated polyester and vinylester. However, these resins also have serious shortcomings in terms of biodegradability, initial processing cost, recyclability, energy consumption and processing health hazards. Increasing environmental awareness throughout society and now within the civil engineering and construction industries is driving the research, development and utilization of more 'green' building materials, specifically the development of bioresins and biocomposites based on renewable natural materials.

Plant-oil based bioresins are an emerging 'green' thermoset material and due to their biological origin they represent a sustainable, low environmental impact option to existing petrochemically derived resins. These plant-oil based bioresins may be reinforced with natural or synthetic fibres thereby creating a class of materials termed, natural fibre composites or biocomposites. Currently

a high proportion of biocomposites are being produced using petro-chemical based matrices reinforced with natural fibres (Dash et al. 1999; Datta, Basu & Banerjee 2002; Gassan & Bledzki 1999; Jústiz-Smith, Virgo & Buchanan 2008; Mishra et al. 2000; Mohanty & Misra 1995; Ray, Sarkar & Bose 2002; Tripathy et al. 2000). However, these composites may more aptly be termed hybrid composites as they contain both natural and synthetic constituents.

In terms of an environmental perspective it is imperative to produce composites in which both the matrix and fibre reinforcement are derived from natural resources thereby fostering sustainability. Natural materials such as plant based bioresin and fibres have low environmental impact given that they are natural in origin and are therefore a suitable renewable resource from which to produce biocomposites. In this chapter, two different types of thermosetting hemp oil based bioresins are applied to jute reinforced biocomposites.

Firstly, the effect of EHO concentration on the thermo-mechanical behaviour (glass transition temperature, storage modulus and crosslink density), flexural properties and moisture absorption (saturation moisture level and diffusion coefficient) of EHO based bioresin epoxy blends is reported. Comparisons with commercial epoxidized soybean oil (ESO) based bioresin epoxy blends and a control synthetic epoxy resin were also performed. EHO based bioresin epoxy blends applied to jute fibre based biocomposites are also presented and compared in terms of mechanical properties thermo-mechanical behaviour (glass transition temperature, storage modulus and crosslink density), and moisture absorption (saturation moisture level and diffusion coefficient) with biocomposite samples prepared using commercially available ESO based bioresins.

The second part of this study involves the production and characterisation of AEHO based bioresins and jute fibre reinforced biocomposites. Comparisons with commercial VE based resin and 50/50 (VE/AEHO) blended bioresin systems both in neat resin form and applied to biocomposites was performed.

Neat bioresin samples containing AEHO, 50/50 (VE/AEHO) and VE were investigated and reported in terms of thermo-mechanical properties (glass transition temperature, storage modulus and crosslink density), flexural properties and moisture absorption (saturation moisture level and diffusion coefficient). In terms of biocomposite production and characterisation, novel 100% biocomposites made of AEHO based bioresin reinforced with woven jute fibre mat were manufactured by the hand lay-up technique. Mechanical properties (tensile, flexural, Charpy impact and interlaminar shear), thermo-mechanical properties (glass transition temperature, storage modulus and crosslink density) and water absorption properties (saturation moisture level and diffusion coefficient) were investigated and compared with samples manufactured under the same conditions but using 50/50 (VE/AEHO) and VE resins as the polymeric matrix.

5.2 Materials

Plasthall ESO, oxirane oxygen content 7.0% (Hallstar) and EHO as synthesised according to Chapter 3 were used as the bioresin components for the epoxy blends. EHO was previously characterised to contain 8.3% oxirane oxygen content with approximately 5.1 epoxy groups per triglyceride. Kinetix R246TX epoxy resin, EEW ≈ 195, isophorone diamine (IPD), AHEW ≈ 42.6, supplied by ATL composites (Southport, Queensland, Australia) and triethylenetetramine (TETA), AHEW ≈ 24, was used as supplied.

AEHO as synthesised according to Chapter 3 and containing 4.1 acrylate and hydroxyl groups per triglyceride was used as the base bioresin. FG vinylester SPV6003 (FGI Australia) was used as received for the control samples. In the case of the AEHO bioresin, the added styrene comonomer was supplied by Fischer Scientific (United Kingdom), the Promoter N2-51P was sourced from Axon Nobel Ltd and a 40% MEKP based catalyst was used for the curing and sourced from FGI Australia. The Styrene comonomer, the promoter and the

catalyst were all used as received. Bidirectional woven jute fabric, 90°/0°, 550 g/m^2 was used as natural fibre reinforcement.

5.3 Experimental investigation

5.3.1 Sample preparation and production

EHO based samples

EHO and ESO based bioresin epoxy blends were prepared by mixing EHO or ESO with a base synthetic epoxy resin, R246TX. The bioresin blends chosen for this study were 0/100%, 10/90%, 20/80%, 30/70% and 40/60% (EHO/R246TX and ESO/R246TX). To produce the bioresin samples, the bioresin blend and hardener were thoroughly mixed, degassed, poured into a waxed mould, cured as outlined below and finally cut to size.

Flat composite panels were manufactured using the hand lay-up process. The lay-up consisted of 4 layers of woven jute mat reinforcement. The fibre was washed with warm water to remove any dust particles and other such contaminants dried for 12 h at 110 °C and finally cut to size, No chemical treatments were performed on the fibre. The manufacture of the composite panels was performed immediately upon removing the fibre from the oven to prevent atmospheric moisture absorption which could impinge upon the final composite's mechanical properties. Control samples (100/0%) were prepared using synthetic epoxy, R246TX and jute fibres. Manufactured panels were 300×300×5 mm with a fibre weight percentage of approximately 20%. A flat metal plate was placed on top of the composite sample to improve the surface finish and to ensure a consistent thickness.

Curing temperatures and programs were used as determined from the results found in chapter 4 so as to ensure sample curing. Initial curing for both bioresin and biocomposite samples was performed at room temperature (~25 °C) for 4 h

followed by post curing at 120 °C for a further 4 h. Following this the samples were then removed from the mould, cut to size, dried at 80 °C for 4 h to ensure the removal of any induced moisture and then cooled in a desiccator ready for testing. An exception to this process was that the water absorption samples were further dried at 110 °C for 1 h and cooled in a desiccator as per ASTM D570.

AEHO based samples

To prepare the AEHO bioresin, 33 wt% of styrene was added in order to decrease viscosity and improve processability for manufacturing composite parts by traditional composite processing techniques. Afterwards, the promoter was incorporated to the AEHO/styrene mixture (0.25 wt%) and thoroughly mixed. Subsequent to this the catalyst was added (4 wt%) and stirred thoroughly for several minutes. The resin was degassed under vacuum. Both VE and 50/50 (VE/AEHO) were prepared in following a similar method. However for the VE resin system no styrene was added as the system already contains 33 wt% of styrene. Regarding the VE system, 0.25% and 2% promoter and catalyst were used respectively. For the 50/50 (VE/AEHO) system 0.25% and 3% promoter and catalyst were used respectively. Neat bioresin and resin samples were also produced by pouring into a waxed glass mould. Biocomposite panels were manufactured following the same process as the EHO based samples as outlined above.

Initial curing for both bioresin and biocomposite samples was performed at room temperature (~25 °C) for 4 h followed a 4 h post curing stage performed at 80 ˚C for the vinyl ester and at 120 ˚C for the bioresin composites respectively to achieve maximum conversion. Following this the samples were removed from the moulds, cut to size, dried at 80 °C for 4 h to ensure the removal of any induced moisture and then cooled in a desiccator ready for testing. An exception to this process was that the water absorption samples were further dried at 110 °C for 1 h and cooled in a desiccator as per ASTM D570. Thickness of the

specimens was approximately 5 mm. Fibre wt% was determined as approximately 25%.

5.3.2 Microscopic analysis

Cross section morphologies of the biocomposite samples were investigated with a JEOL JSM 6460 LV scanning electron microscope (SEM) at National University of Mar Del Plata, Argentina (UNMdP), Figure 5.1. The fractured surfaces were coated with gold and the samples were scanned at room temperature with an accelerating voltage of 15 kV.

Figure 5.1. JEOL JSM 6460 LV scanning electron microscope (SEM).

5.3.3 Mechanical testing

Interlaminar shear strength (ILSS) testing was performed to determine the effects of bioresin concentration on the fibre-matrix interfacial shear strength. Testing was performed using ISO 14130 on a MTS Alliance RT/10 10 kN machine with a crosshead speed of 1 mm/min. Five specimens of each sample type were used in each mechanical test.

Charpy impact tests were conducted to determine the effects of bioresin concentration on the impact properties of the biocomposites. Impact properties

of the samples were determined using ISO 179 on an Instron Dynatup M14-5162, Figure 5.2. Charpy impact strength (kJ/m^2) was calculated from Equation 5.1, whereby a_{cU}, h, b an W_B are the Charpy impact strength, thickness, width and the energy at break of the test specimen. Essentially this corresponds to the energy at break of the specimen divided by the cross sectional area.

Figure 5.2. Instron Dynatup M14-5162 as used for Charpy impact tests.

$$a_{cU} = \frac{W_B}{bh} \times 10^3 \quad (5.1)$$

Flexural testing was conducted to determine the behaviour of both bioresin and biocomposite specimens subjected to 3-point simple beam loading. Bioresin flexural properties were obtained through 3-point bending tests conducted in accordance with ISO 178 using a MTS Alliance RT/10 machine, Figure 5.3. A cross head speed of 2 mm/min and a span/depth ratio of 16:1 were used with specimen dimensions being 80 × 10 × 4 mm. Biocomposite flexural properties were measured in accordance with ISO 14125.

Tensile tests were conducted in accordance with ISO 527. Tests were performed with a cross-head speed of 2 mm/min using a MTS Insight 100 kN machine, Figure 5.3. Specimen dimensions were 250 × 25 × 5mm.

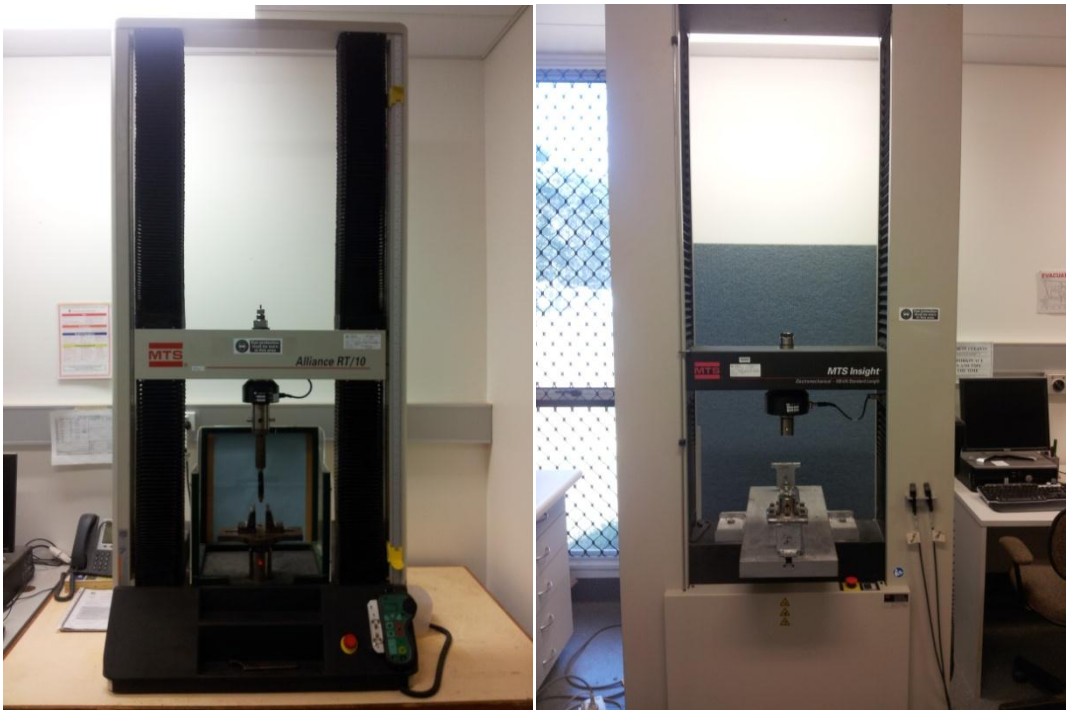

Figure 5.3. MTS Insight 100 (left) and MTS Alliance RT/10 (right) machines as used for tensile, flexural and ILSS tests.

5.3.4 Dynamic mechanical analysis

A calibrated TA Instruments Q800 DMA was used for the dynamic mechanical analysis (DMA). Rectangular specimens with the dimensions 58 × 10 × 5 mm were tested in dual cantilever mode, Figure 5.4. Testing was performed at a temperature ramp of 3 °C/min over a temperature range of approximately 25–180 °C. A frequency of 1.0 Hz with an oscillating displacement of ±10 μm was also used. Storage modulus (E') and tan δ were plotted as a function of temperature by Universal Analysis 2000 version 3.9A software. Glass transition temperature (T_g) was calculated as the peak of the tan δ curve and crosslink density (ν_e) was calculated from the theory of rubber elasticity, Equation 5.2 (Shabeer, Chandrashekhara & Schuman 2007). Where E', ν_e, R and T are the storage modulus in the rubbery plateau region (T_g + 40 °C), crosslink density,

gas constant (8.314 J/(K·mol)) and the absolute temperature in K, respectively (Miyagawa et al. 2004).

$$E' = 3v_e RT \tag{5.2}$$

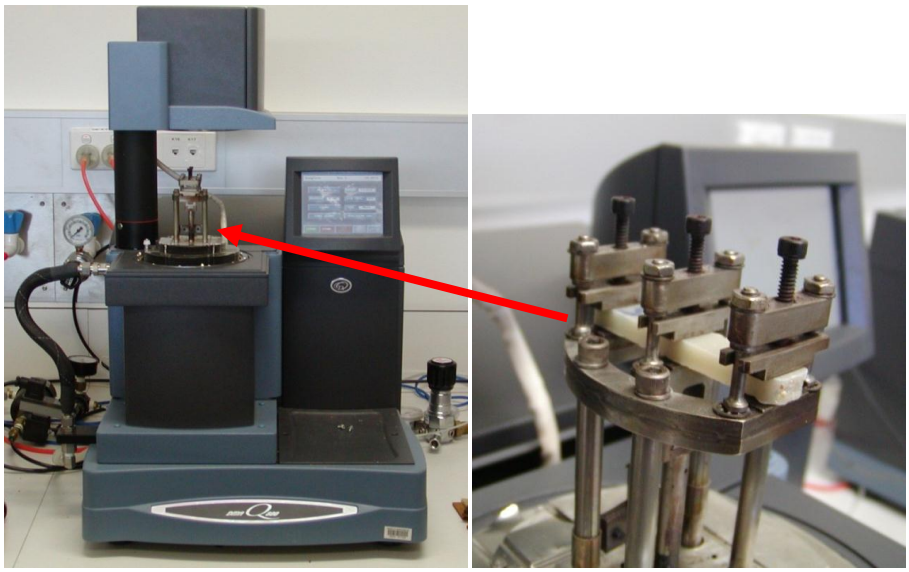

Figure 5.4.TA Instruments Q800 DMA (left) with test specimen positioned in dual cantilever arrangement (right.)

5.3.5 Moisture absorption

Moisture absorption tests were performed in order to ascertain the saturation moisture level and the diffusion coefficient of the bioresin and biocomposite samples. Specifically the effects of bioresin loading on the moisture absorption were of interest. Testing was performed in accordance with ASTM D570. Specimens measured 76.2×25.4×5 mm for both neat resin and jute fibre samples. Three specimens of each sample type were used. The specimens were cut to size and the edges were finished with No. 0 sandpaper. After this the specimens were dried at 110 °C for 1 h, cooled in a desiccator and weighed to the nearest 0.001 g. The specimens were immersed in distilled water at 23±1 °C and removed at regular intervals, wiped free of surface moisture, immediately weighed to the nearest 0.001 g and then replaced in the water. Equation 5.3 was used to calculate the diffusion coefficient, where *D, h,* M_m and *m* are diffusion coefficient, thickness of specimen, saturation moisture level and gradient of the

linear region from the plot of weight gain against square root of time (Morye & Wool 2005).

$$D = \pi \left(\frac{h}{4M_m}\right) m^2 \quad (5.3)$$

5.4 Results and discussion

5.4.1 Microscopic analysis

In fibre composites effective wetting and compatibility between the fibre reinforcement and the polymer matrix is paramount in obtaining satisfactory fibre-matrix adhesion and ultimately acceptable end state composite properties. SEM micrographs of both epoxidized and acrylated samples were taken to investigate the fibre-matrix interfaces.

EHO based samples

The fracture surfaces of the synthetic epoxy, EHO and ESO based jute fibre reinforced samples were examined by SEM to evaluate the degree of fibre-matrix adhesion. 300× magnification was used to give a representative image of the overall fibre-matrix behaviour whereas 1000× magnification was used to more closely examine individual fibre-matrix behaviour. Figures 5.5–5.10 display the typical fibre-matrix interface of all three different sample types. It can be seen that fibre pullout is apparent for all sample types and is visible at 300× magnification. Also apparent is the fibre-matrix interface and the presence of some gaps between the fibre and the matrix. Indeed this fibre-matrix interface condition was anticipated to a certain degree as no chemical treatment was performed on the jute fibre reinforcement. Figure 5.11 presents an SEM micrograph of a synthetic epoxy/EHO (60/40) jute reinforced biocomposite sample. From the Figure it is apparent that fibre-matrix interfacial adhesion is significantly poor. Similar images were observed from a synthetic epoxy/ESO

(60/40) samples. Consequently the conclusions drawn as a result of these findings are reduced fibre-matrix interfacial adhesion with increased EVO content and indicated incompatibility between natural fibre and high concentration EVO/epoxy blends.

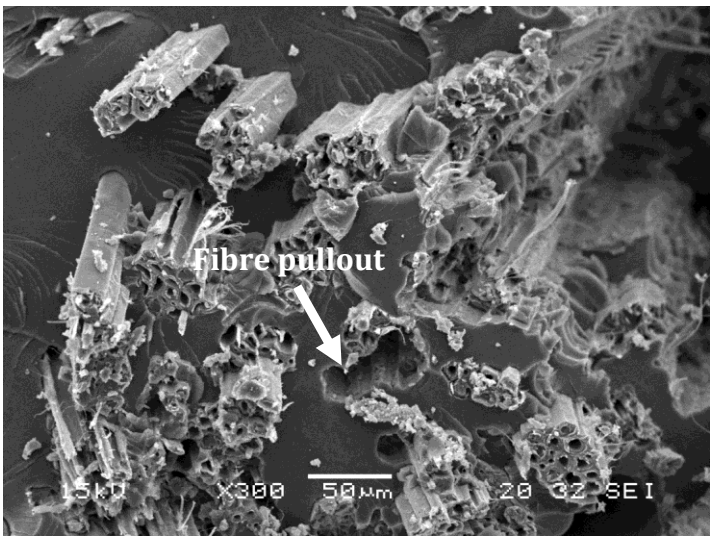

Figure 5.5. SEM micrograph of synthetic epoxy reinforced jute fibre biocomposite.

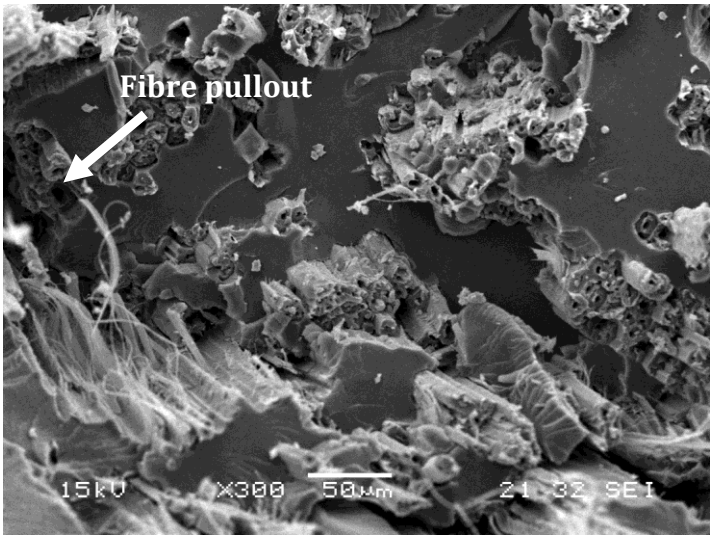

Figure 5.6. SEM micrograph of synthetic epoxy EHO 80/20 reinforced jute fibre biocomposite.

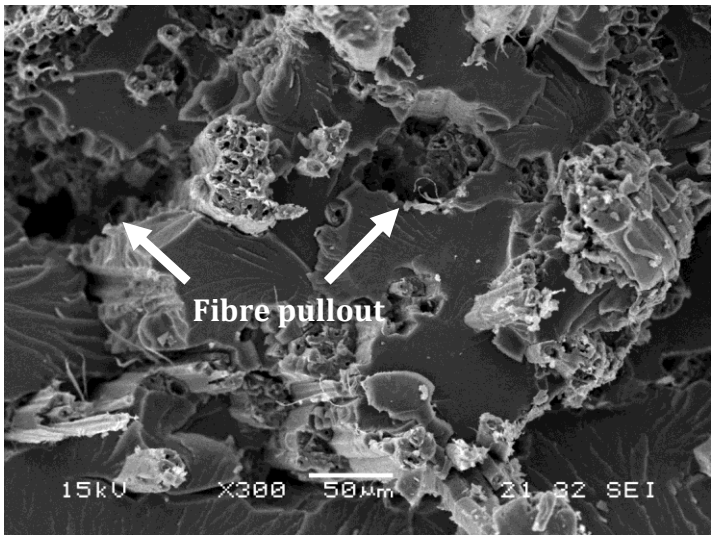

Figure 5.7. SEM micrograph of synthetic ESO 80/20 reinforced jute fibre biocomposite.

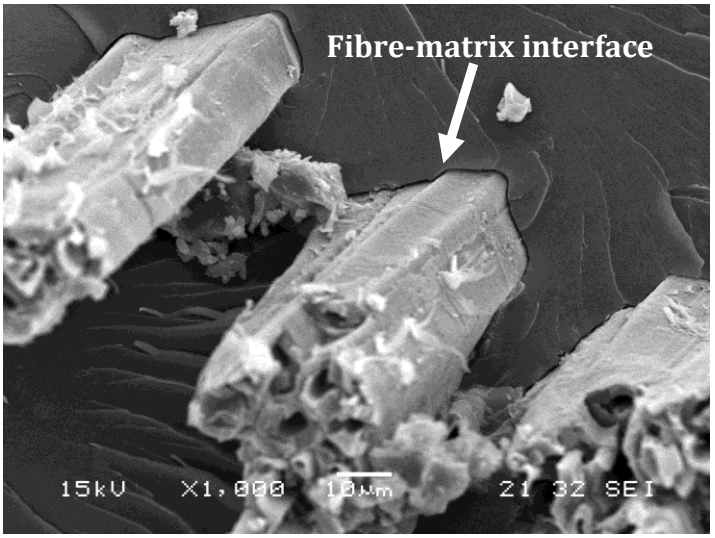

Figure 5.8. SEM micrograph of synthetic epoxy reinforced jute fibre biocomposite.

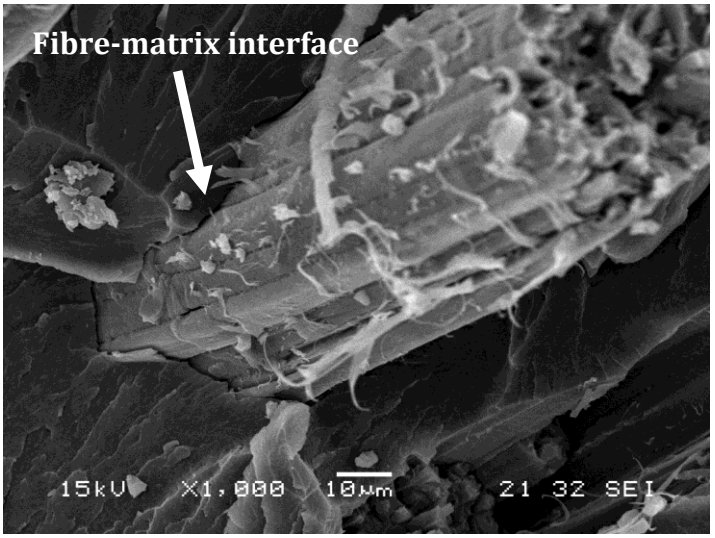

Figure 5.9. SEM micrograph of synthetic epoxy EHO 80/20 reinforced jute fibre biocomposite.

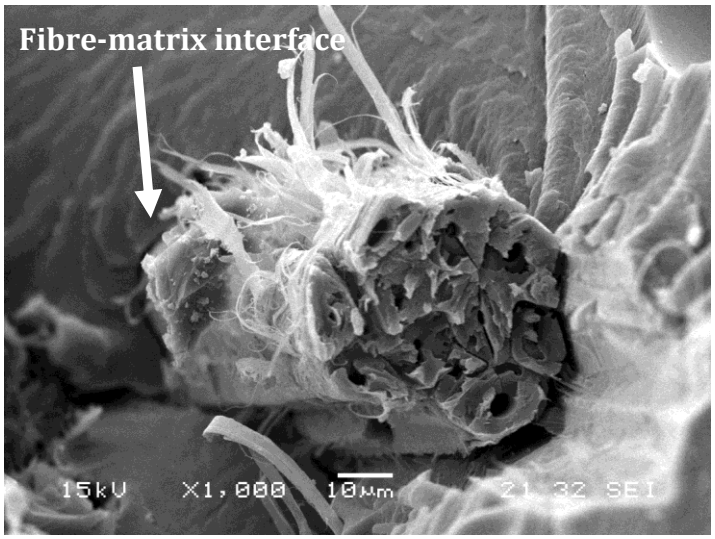

Figure 5.10. SEM micrograph of synthetic ESO 80/20 reinforced jute fibre biocomposite.

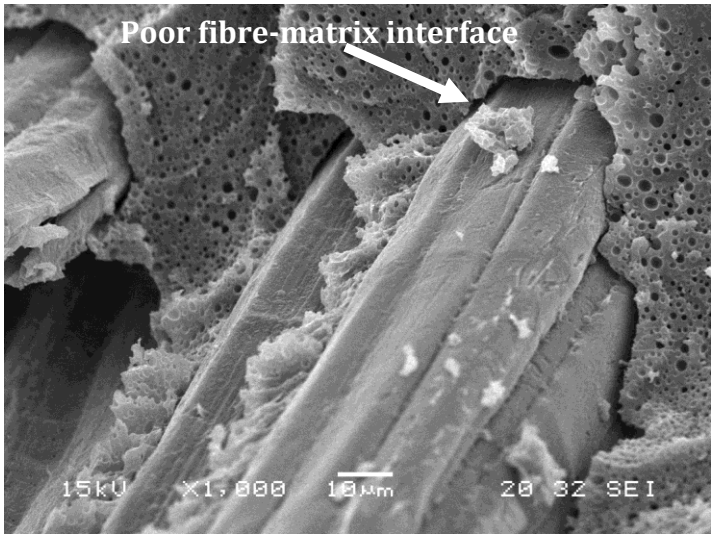

Figure 5.11. SEM micrograph of synthetic EHO 60/40 reinforced jute fibre biocomposite.

AEHO based samples

The fracture surfaces of the VE, 50/50 (VE/AEHO) and AEHO based jute fibre reinforced samples were examined by SEM to evaluate the degree of fibre-matrix adhesion. Using the same premise as the EHO samples 300× magnification was used to give a representative image of the overall fibre-matrix behaviour whereas 1000× magnification was used to more closely examine individual fibre-matrix behaviour.

Figures 5.12–5.17 display the typical fibre-matrix interface of all three different sample types. Fibre pullout is evident for all sample types and is visible at 300×

magnification. Also apparent is the fibre-matrix interface and the presence of some gaps between the fibre and the matrix. Indeed this fibre-matrix interface condition was anticipated as no chemical treatment was performed on the jute fibre reinforcement. Samples containing 100% VE were observed to have the poorest fibre-matrix interface, with the 100% AEHO samples displaying improved fibre-matrix adhesion. It is proposed that the improved fibre-matrix interfacial adhesion of the 100% AEHO based samples is due to surface chemical compatibility between the natural fibres and the bioresin. Moreover Kabir et al. (2012) reasons that the presence of hemicelluloses and lignin present on the untreated fibre surface causes a reduction in composite performance through reduced stress transfer efficiency. Specifically the interaction of the reactive hydroxyl groups on the fibre surface with the matrix is impeded. It is likely that the greater quantity of hydroxyl groups present in the AEHO bioresin compared with the VE contributes to enhanced fibre-matrix adhesion. These hydroxyl functional groups present in the AEHO serve to interact with the hydroxyl groups present in the cellulose of the natural fibres to form strong hydrogen bonds thereby improving adhesion and ultimately flexural and ILSS performance. Therefore as a result of these findings it is expected that ILSS will be higher for samples containing AEHO compared with those based on VE. By utilising chemical treatments on the natural fibres improvements in fibre-matrix interfacial adhesion would be expected (George, Sreekala & Thomas 2001; Kabir et al. 2012; Le Troedec et al. 2008; Li, X, Tabil & Panigrahi 2007; Mehta et al. 2006; Rong et al. 2001; Thomsen et al. 2006; Tripathy et al. 2000; Valadez-Gonzalez et al. 1999).

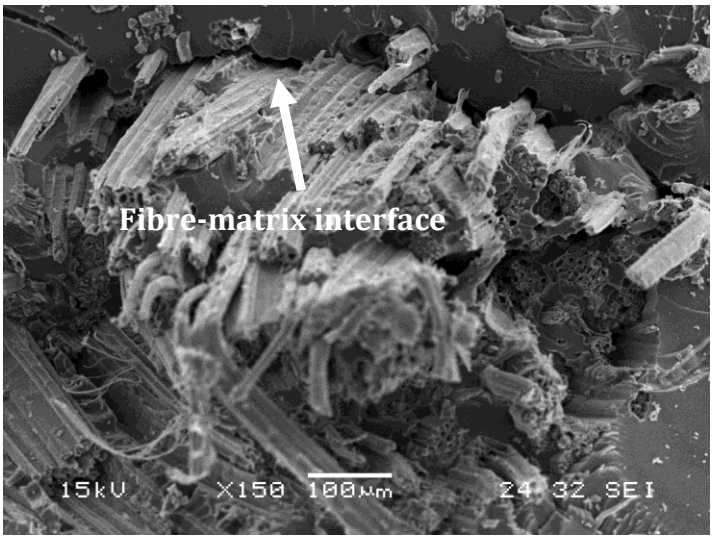

Figure 5.12. SEM micrograph of synthetic vinylester reinforced jute fibre biocomposite.

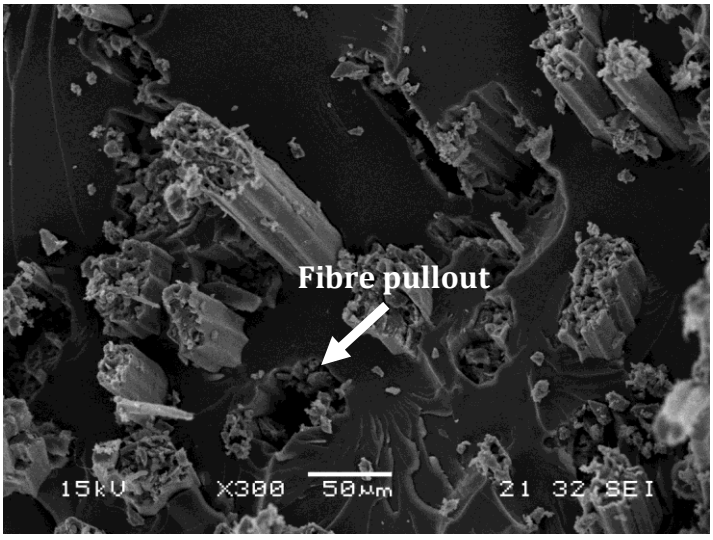

Figure 5.13. SEM micrograph of 50/50 VE/AEHO reinforced jute fibre biocomposite.

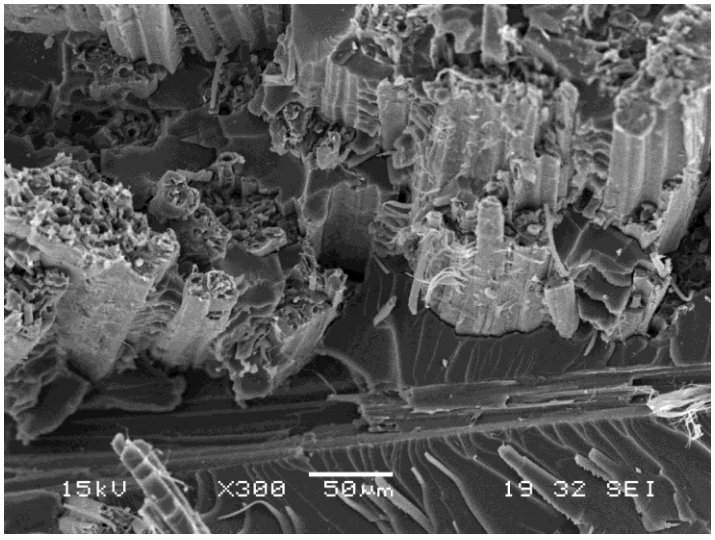

Figure 5.14. SEM micrograph of AEHO reinforced jute fibre biocomposite.

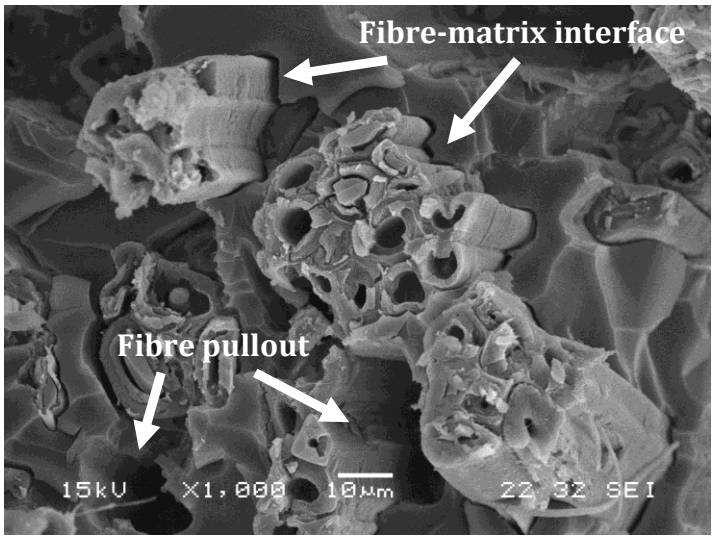

Figure 5.15. SEM micrograph of synthetic vinylester reinforced jute fibre biocomposite.

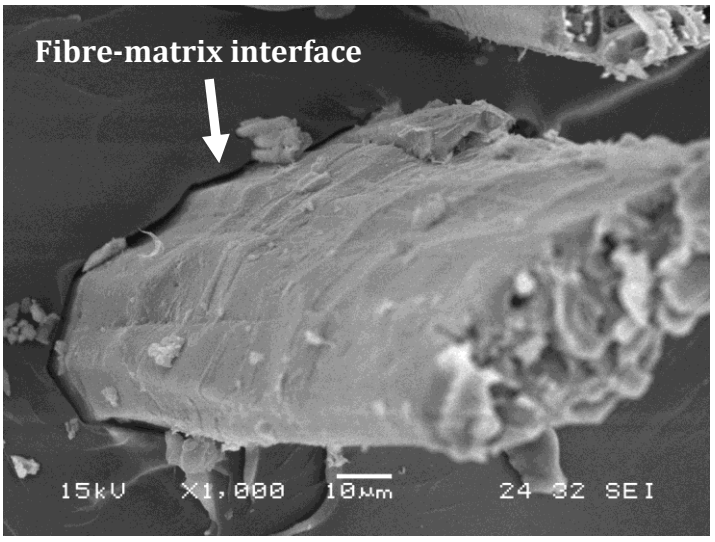

Figure 5.16. SEM micrograph of 50/50 VE/AEHO reinforced jute fibre biocomposite.

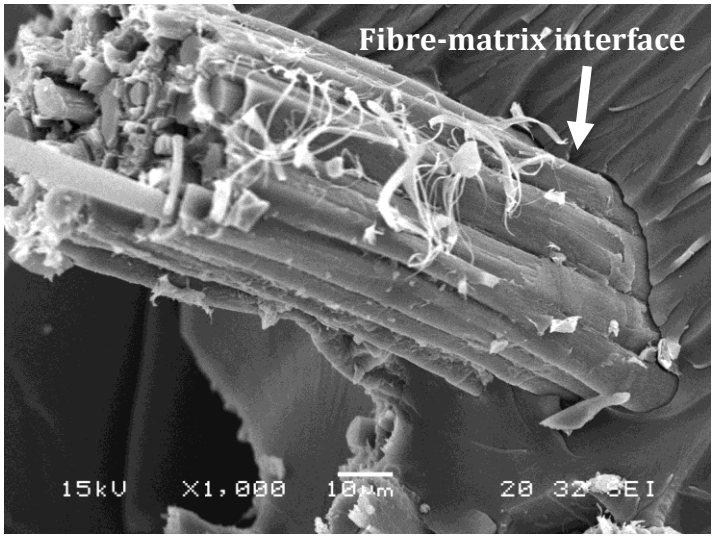

Figure 5.17. SEM micrograph of AEHO reinforced jute fibre biocomposite.

EHO/ESO vs. AEHO fibre-matrix adhesion

Examining the SEM images it is apparent that the fibre-matrix interfacial adhesion is similar. However it is worth remembering that the viewed EHO/ESO samples contain a maximum of 20% bioresin content opposed to 100% AEHO based samples. In fact as can be seen in Figure 5.11 once the EHO/ESO content increases fibre-matrix interfacial adhesion deteriorates. Therefore it can be concluded that in terms of fibre-matrix interfacial adhesion is superior for AEHO samples compared with those utilising EHO/ESO based polymeric matrices.

5.4.2 Interlaminar shear strength

EHO based samples

Samples containing EHO and ESO with jute fibres showed a reduction in ILLS with increasing bioresin content, Figure 5.18. Maximum ILSS occurred with the synthetic epoxy with EHO samples displaying higher ILSS than ESO samples throughout the data range. Due to poor ILSS and therefore compromised results, samples after 20% bioresin concentration were not included in the results. The addition of EVO based bioresin appears to have negative effects on ILSS indicating reduced fibre-matrix adhesion. A discernible reduction in performance was apparent subsequent to 20% bioresin concentration for both bioresins. These findings indicate that increasing bioresin concentration, especially concentrations above 20% has negative effects on ILLS.

The fibre-matrix adhesion was found to be lower when the bioresin content was increased, as shown by the ILLS results and reinforced by the SEM images in section 5.4.1. It is well known that the properties of composite materials are dependent upon the properties of the reinforcement, the properties of the matrix and the characteristics of the matrix/reinforcement interface. Usually, stronger interfaces lead to higher tensile and flexural strengths but reduced impact strength, because energy-consuming mechanisms during composite

fracture such as fibre pull out are inhibited. Therefore, ILLS results suggest that in addition to the lower strength and higher flexibility of the bioresins, the poor adhesion to the fibres could also have influenced the tensile strength (negatively) and the impact strength (positively).

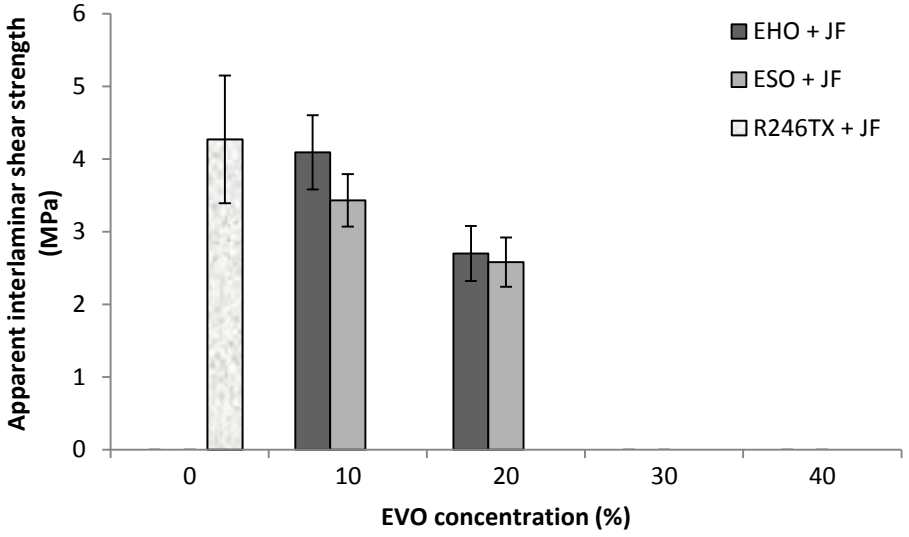

Figure 5.18. Interlaminar shear strength properties of synthetic epoxy, EHO and ESO based biocomposite samples.

AEHO based samples

Figure 5.19 shows the ILSS of the AEHO based biocomposite samples. It was found that AEHO and 50/50 samples displayed higher ILSS than VE based samples with 100% AEHO based samples displaying the highest ILSS. As the flexural properties of the VE neat resin is superior to those of the AEHO systems as presented below in section 5.4.4 these results suggest that the fibre-matrix interfacial adhesion is stronger for the AEHO based samples compared with the VE based samples. This was confirmed in section 5.4.1 whereby it was apparent that AEHO based samples exhibited improved fibre-matrix interfacial adhesion compared with VE based samples. Accordingly, as previously mentioned the surface chemical compatibility between the natural fibres and the bioresin, specifically the greater quantity of hydroxyl groups present in the AEHO bioresin compared with the VE is proposed as the reason for enhanced fibre-matrix adhesion.

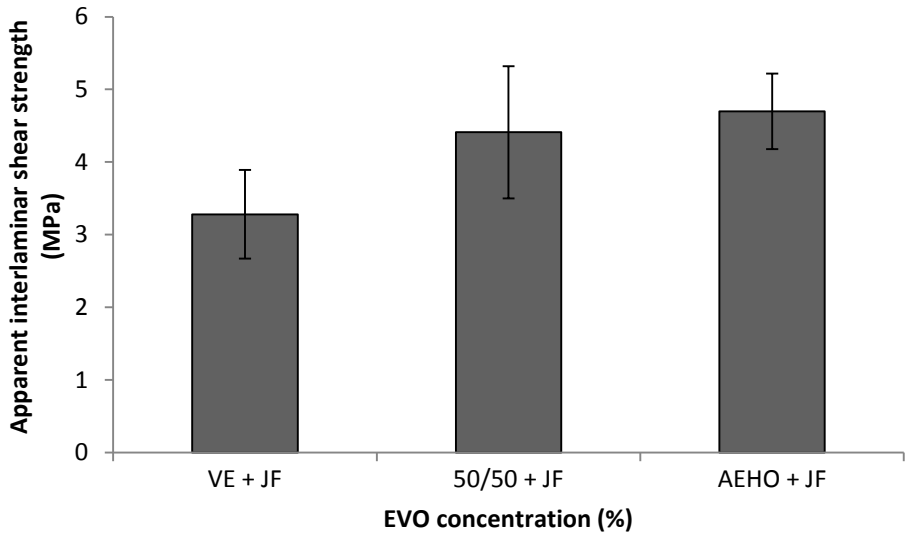

Figure 5.19. Interlaminar shear strength properties of AEHO based biocomposite samples.

5.4.3 Flexural properties

EHO based samples

Flexural properties for the bioresin and biocomposite samples are shown in Figures 5.20 and 5.21. The highest recorded peak flexural stress and flexural modulus were observed for the synthetic epoxy control sample. At a concentration of 10% the EHO sample displayed comparable performance to the synthetic epoxy control. Moreover for both EHO and ESO based samples at concentrations greater than 10%, EHO based samples generally displayed higher flexural properties than ESO based samples. However it was also noted that there was a marked reduction in flexural properties for both EHO and ESO subsequent to 30% concentration. A trend of decreasing flexural properties and subsequently increasing ductility for both EHO and ESO based samples was observed with increasing bioresin concentration resulting in lower flexural performance. This is in agreement with results obtained by Zhu et al (2004) who found similar results for ESO/epoxy blends.

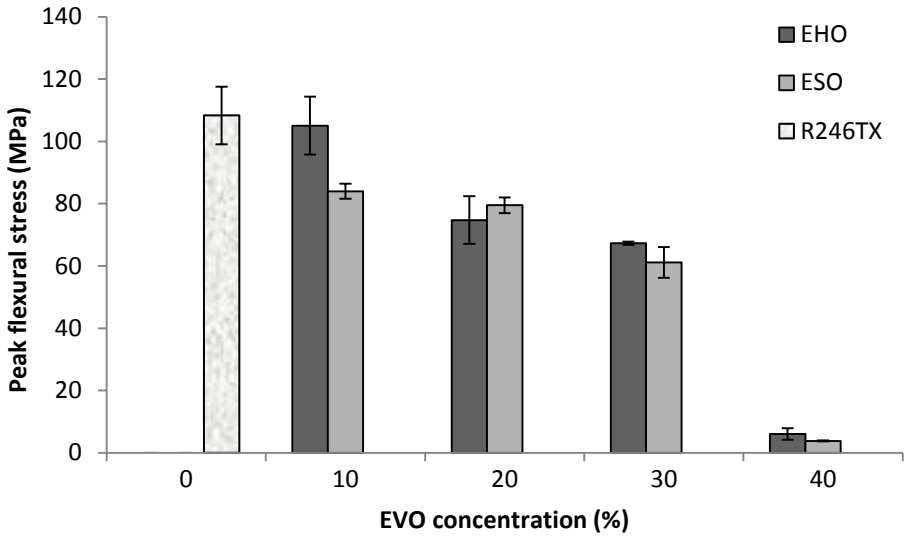

Figure 5.20. Peak flexural strength of synthetic epoxy, EHO and ESO based bioresin samples.

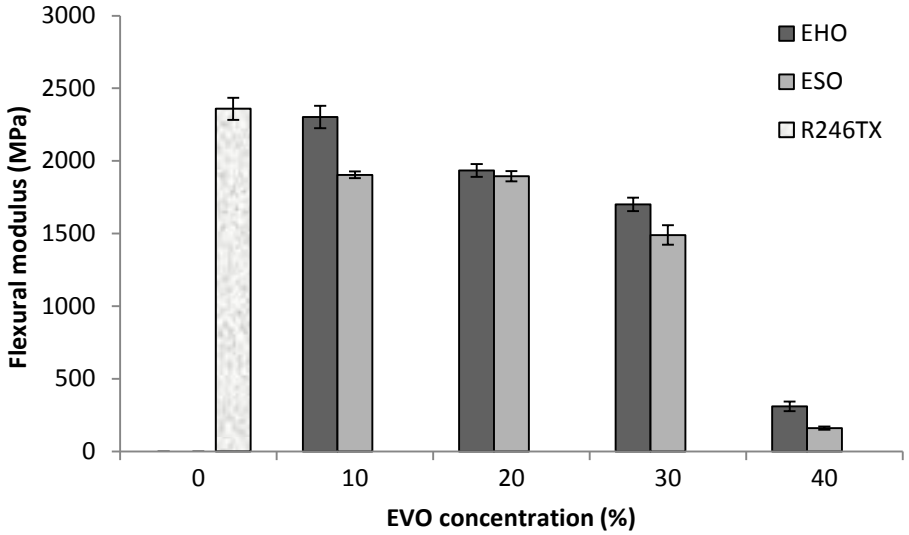

Figure 5.21. Flexural modulus of synthetic epoxy, EHO and ESO based bioresin samples.

EHO based jute fibre samples displayed comparable peak flexural stress and flexural modulus with the synthetic control up to a concentration of 10%, Figures 5.22 and 5.23. Both EHO and ESO samples show evidence of decreasing flexural performance with increasing bioresin concentration. Although there is no literature to the author's knowledge regarding this specific biocomposite, there is also limited literature in general pertaining to bioresins with natural fibres. However, in terms of glass fibre reinforcement these results are in agreement with those found in the literature. For instance, Chandrashekhara et al. (2005) manufactured epoxidized allyl soyate (EAS) based bioresins/epoxy

blends reinforced with glass fibre and found an increase in EAS content resulted in a decrease in flexural properties. Espinoza-Perez et al. (Espinoza-Pérez, Wiesenborn, Tostenson, et al. 2007; Espinoza-Pérez, Wiesenborn, et al. 2009) studied the flexural properties of glass fibre reinforced ESO/epoxy and ECO/epoxy composites and also found that utilisation of the bioresin blends resulted in reductions in both flexural strength and modulus of 15-86% and 13-65% respectively in comparison to the synthetic epoxy control. According to Espinoza-Perez et al. (Espinoza-Pérez, Wiesenborn, Tostenson, et al. 2007; Espinoza-Pérez, Wiesenborn, et al. 2009) similar results were also realised by Tatlari (2008) regarding glass fibre reinforced ESO/epoxy composites.

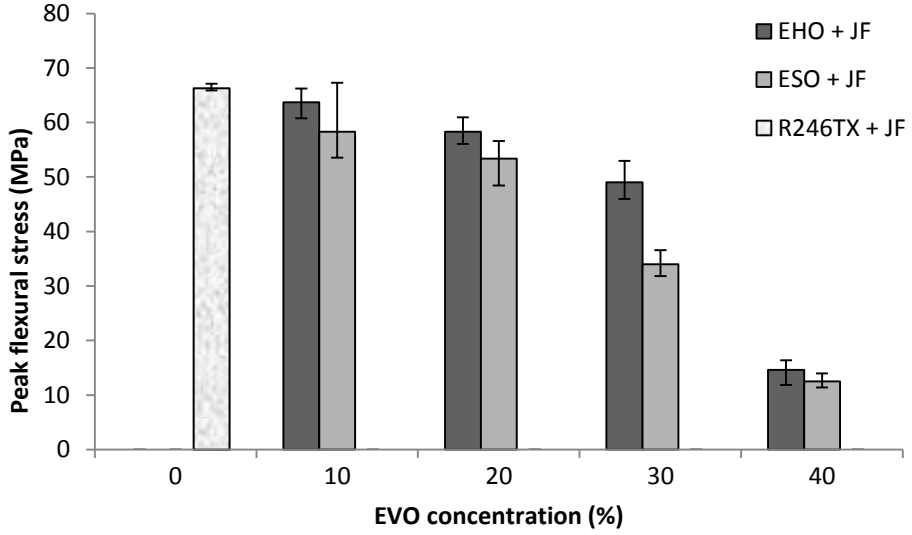

Figure 5.22. Peak flexural strength of synthetic epoxy, EHO and ESO based biocomposite samples.

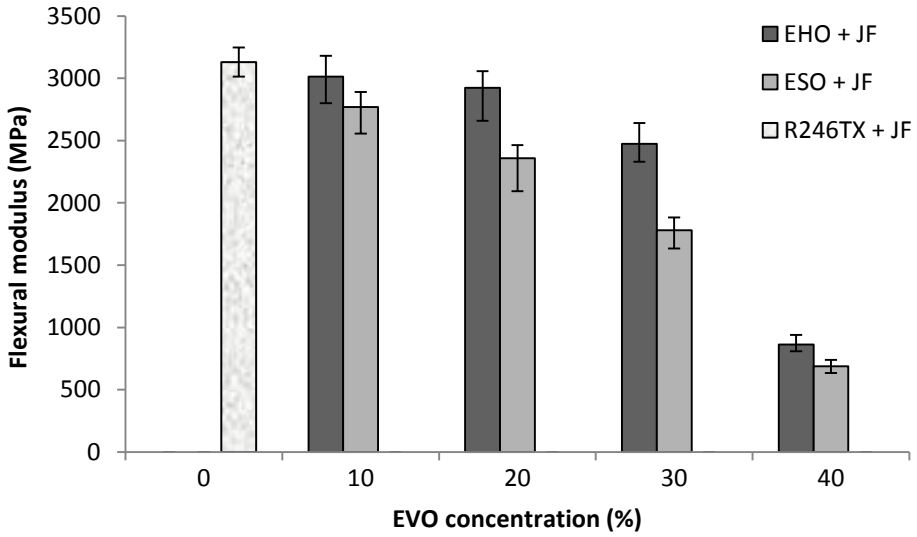

Figure 5.23. Flexural modulus of synthetic epoxy, EHO and ESO based biocomposite samples.

When comparing the flexural properties of the neat resin with those of the biocomposites it was observed that flexural strength was lower in the biocomposites compared with the neat resin. Conversely, the flexural modulus of the biocomposites was found to be higher than the neat resin samples. Given the fact that there is an absence of literature regarding the mechanical properties of EVO based bioresins and their associated natural fibre reinforced biocomposites comparisons are limited. Nonetheless, the addition of the jute fibre reinforcement served to ultimately increase stiffness and consequently brittleness thereby leading to the obtained results. These results may also be attributed to poor fibre-matrix interfacial adhesion which was confirmed in the ILSS section and the associated SEM images in section 5.4.1.

AEHO based samples

A typical flexural sample undergoing 3-point flexural testing is depicted in Figure 5.24. Figure 5.25 depicts the flexural strength of AEHO based bioresins and biocomposites. It was found that the neat VE resin displayed higher flexural stress compared with the AEHO based bioresin samples. Specifically neat VE resin samples exhibited approximately 1.5-3 times the flexural strength of AEHO based samples. This behaviour was anticipated and is attributed to the long fatty acid chains of the AEHO in a similar manner to EHO imparting flexibility to the matrix.

Figure 5.24. MTS Alliance RT/10 machine as used for flexural and ILSS tests.

In terms of biocomposite properties it was observed that the addition of jute fibre reinforcement resulted in an increase in flexural strength for only the 100% AEHO based sample. Both the VE and the 50/50 (VE/AEHO) samples displayed a reduction in flexural strength with the addition of fibre reinforcement. This apparent reduction in flexural strength is attributed to poor fibre-matrix interfacial adhesion for these samples and is supported by the SEM images and ILSS results obtained in sections 5.4.1 and 5.4.2 respectively. As a result of this behaviour the overall flexural strength of all three composite systems is similar in nature and is within 10% difference.

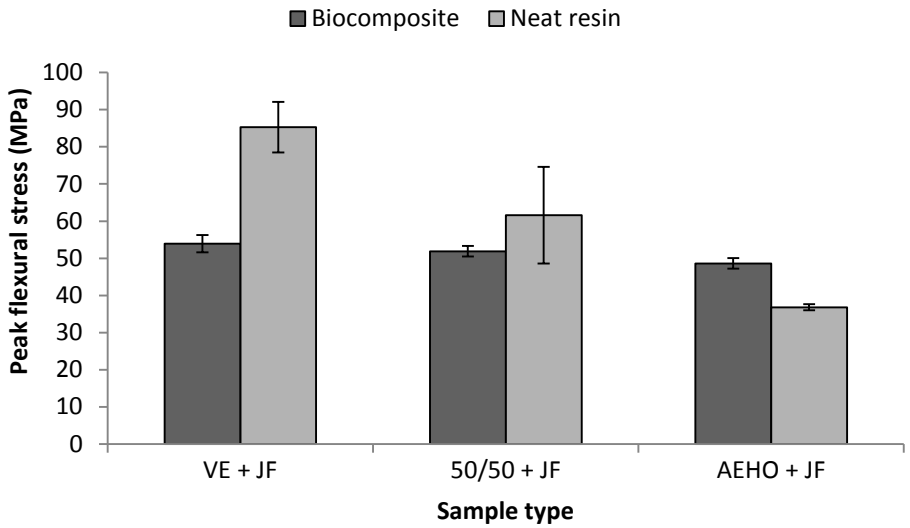

Figure 5.25. Peak flexural strength of AEHO based bioresin and biocomposite samples.

The flexural modulus of AEHO based neat bioresin and biocomposite samples are shown in Figure 5.26. The neat commercial VE resin displayed almost 1.45 and 3.2 times the flexural modulus of the 50/50 and AEHO bioresin samples. The addition of the jute fibre reinforcement to the matrices was found to greatly improve the flexural modulus for all sample types. Improvements in flexural modulus were found to be in the order of 1.43, 1.93 and 3.75 for the VE, 50/50 and AEHO based biocomposite samples respectively. Due to this reinforcement and improvement in flexural modulus, the 50/50 and AEHO based samples displayed flexural moduli that were only approximately 8 and 18% lower than the commercial VE based sample respectively. Flexural properties were found to exhibit a linear trend.

In terms of neat bioresins flexural properties there is limited literature available. However Grishchunk and Karger-Kocis (2010) reported the flexural properties of VE/AESO blends. Daron-XP-45-A2 VE was blended with commercial AESO in concentrations of 100/0, 75/25, 50/50 and 25/75 VE/AESO. The neat VE displayed a flexural modulus and strength of 3212 MPa and 123 MPa. Reductions in flexural properties were observed with increased AESO concentration with the 50/50 displaying a flexural modulus and strength of 1516 MPa and 61 MPa. In comparison the 25/75 sample exhibited a flexural modulus and strength of 234 and 15 MPa. It is worth noting however that in this study styrene was not added to the AESO. In a study conducted by Wool et al. (2000) the flexural modulus of AESO prepared in the ratio 100:45:5 (AESO: styrene: divinyl benzene) was reported as 723 MPa. In comparison the AEHO presented herein is similar with a flexural modulus of 744 MPa. Lu and Wool (2006) produced AELO from a commercially available ELO and obtained a flexural modulus and strength of 2.31 GPa and 78.73 MPa. The high level of epoxides per triglyceride, on average 6.2 resulted in a high number of acrylate groups per triglyceride, approximately 5.7-5.8 thereby resulting in a highly crosslinked, stiff polymer.

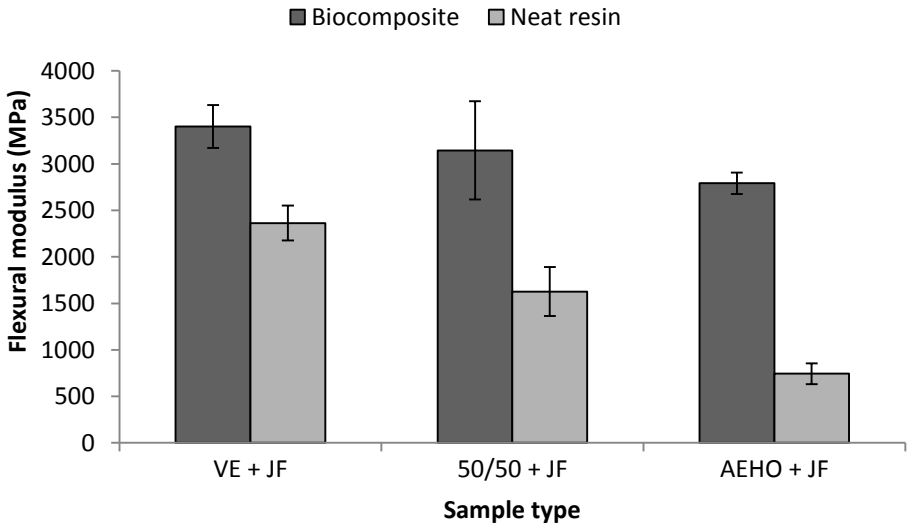

Figure 5.26. Flexural modulus of AEHO based bioresin and biocomposite samples.

Morye and Wool (2005) studied the mechanical properties of glass/flax fibre reinforced AESO based biocomposites. In terms of flexural performance for the

100% flax reinforced samples they obtained flexural modulus and strength of 3.8 GPa and 61 MPa respectively. Fibre wt% was stated as being between 31 to 40%. Williams and Wool (2000) also characterised the mechanical properties of AESO flax fibre reinforced biocomposites in a similar study. Fibre wt% ranged from 20 to 40% with flexural modulus varying from 2.7 GPa to a maximum of 4.2 GPa at 35 wt%. Comparing these results with those obtained for AEHO reinforced jute fibre samples as studied within, it is noted that flexural modulus is comparable for both systems. Similar results were found for the flexural strength whereby at 25 wt% flexural strength was found to be approximately the same as those AEHO reinforced jute fibre samples study herein.

5.4.4 Tensile properties

EHO based samples

In contrast with flexural properties, tensile properties are inherently fibre dependant, although the matrix still must be appropriately able to transfer the loads to the fibre reinforcement. EHO and ESO jute based samples displayed similar tensile behaviour at a concentration of 10% bioresin. Samples containing EHO exhibited higher peak tensile stress and modulus of elasticity than ESO samples throughout the intermediate data range Figures 5.27 and 5.28.

Moreover both EHO and ESO samples showed lower modulus of elasticity throughout the data range than the control. This behaviour is expected due to the lower modulus of elasticity of EVO based bioresins and EVO/Epoxy blends. Peak tensile stress for both EHO and ESO samples up to a concentration of 10% was greater than the control. Similar results were found by Chandrashekhara et al. (2005) in studying the mechanical properties of EAS based bioresins/epoxy blends reinforced with glass fibre. While no data is presented regarding the tensile strength of said biocomposites, the tensile modulus was found to slightly increase with low levels of bioresin concentration before decreasing with increasing bioresin concentration. It is noted however that

lower concentrations of bioresin were used in this study compared to those used within this chapter.

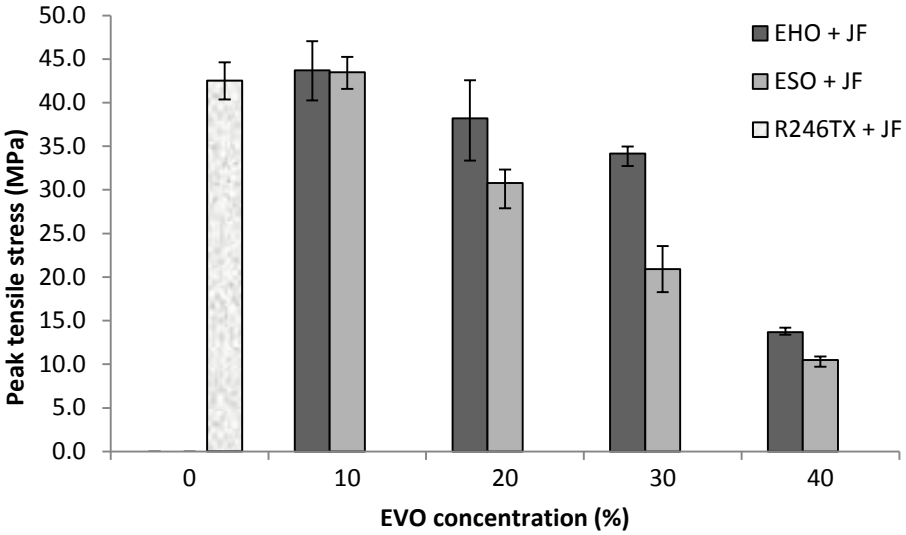

Figure 5.27. Peak tensile strength of synthetic epoxy, EHO and ESO based biocomposite samples.

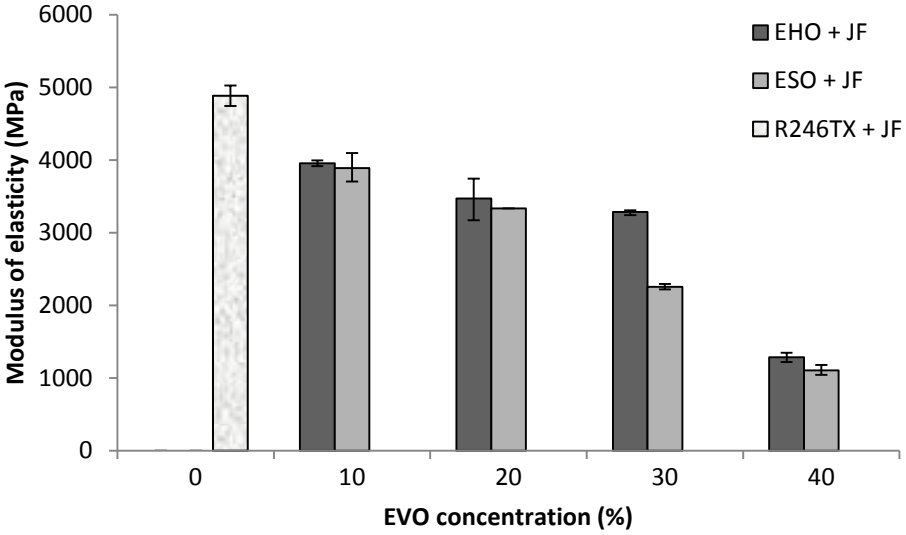

Figure 5.28. Modulus of elasticity of synthetic epoxy, EHO and ESO based biocomposite samples.

AEHO based samples

Figures 5.29 and 5.30 depict the tensile strength and Young's modulus of the AEHO based jute reinforced biocomposites. It can be observed that VE based samples exhibit the highest tensile strength with the addition of AEHO resulting in decreased performance. In terms of Young's modulus all three samples are within 10% of each other. Therefore given the standard deviation (as pictured

from the error bars) it is not unreasonable to state that all three sample types offer similar tensile performance, both in terms of Young's modulus and strength. It is presented that a plausible reason for this similar performance is due to the poor compatibility of the VE with the natural fibre reinforcement. Similarities in performance were also noted in terms of flexural properties as presented in section 5.4.4. Through the addition of natural fibre reinforcement the AEHO based samples exhibit superior fibre-matrix adhesion than VE based samples as shown in the SEM images in section 5.4.1.

As mentioned in section 5.4.4 Morye and Wool (2005) studied the mechanical properties of glass/flax fibre reinforced AESO based biocomposites. In terms of tensile performance for the 100% flax reinforced samples they obtained a Young's modulus and strength of 2 GPa and 31.8 MPa respectively. Fibre wt% was stated as being between 31 to 40%. Williams and Wool (2000) also characterised the mechanical properties of AESO flax fibre reinforced biocomposites in a similar study. Fibre wt% ranged from 20 to 40% with Young's modulus varying from approximately 3.1 GPa to a maximum of 4.7 GPa at 40 wt%. Comparing these results with those obtained for AEHO reinforced jute fibre samples as studied within, it is noted that Young's modulus is comparable for both systems. Similar results were found for the tensile strength whereby at 25 wt% tensile strength was found to be marginally lower than the AEHO reinforced jute fibre samples study herein. Figure 5.31 displays a typical tensile test sample undergoing testing and typical fracture surface.

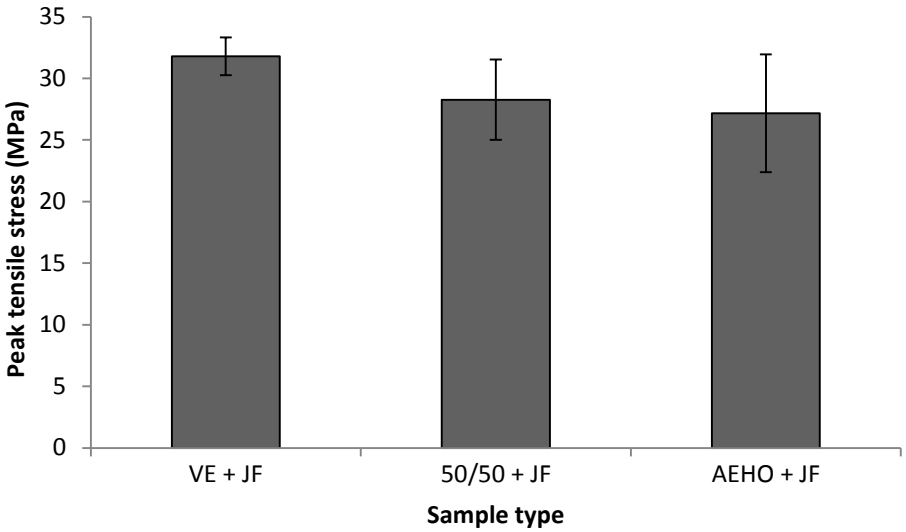

Figure 5.29. Peak tensile strength of AEHO based biocomposite samples.

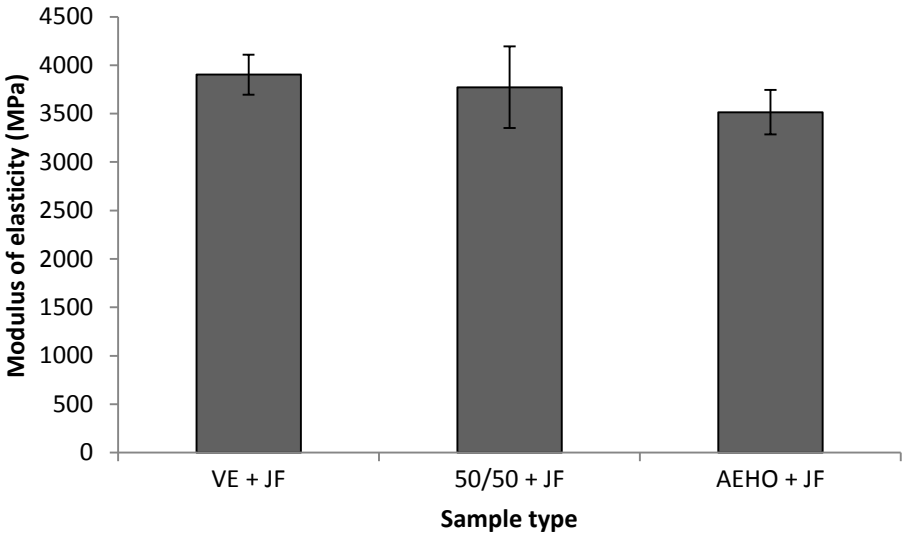

Figure 5.30. Modulus of elasticity of AEHO based biocomposite samples.

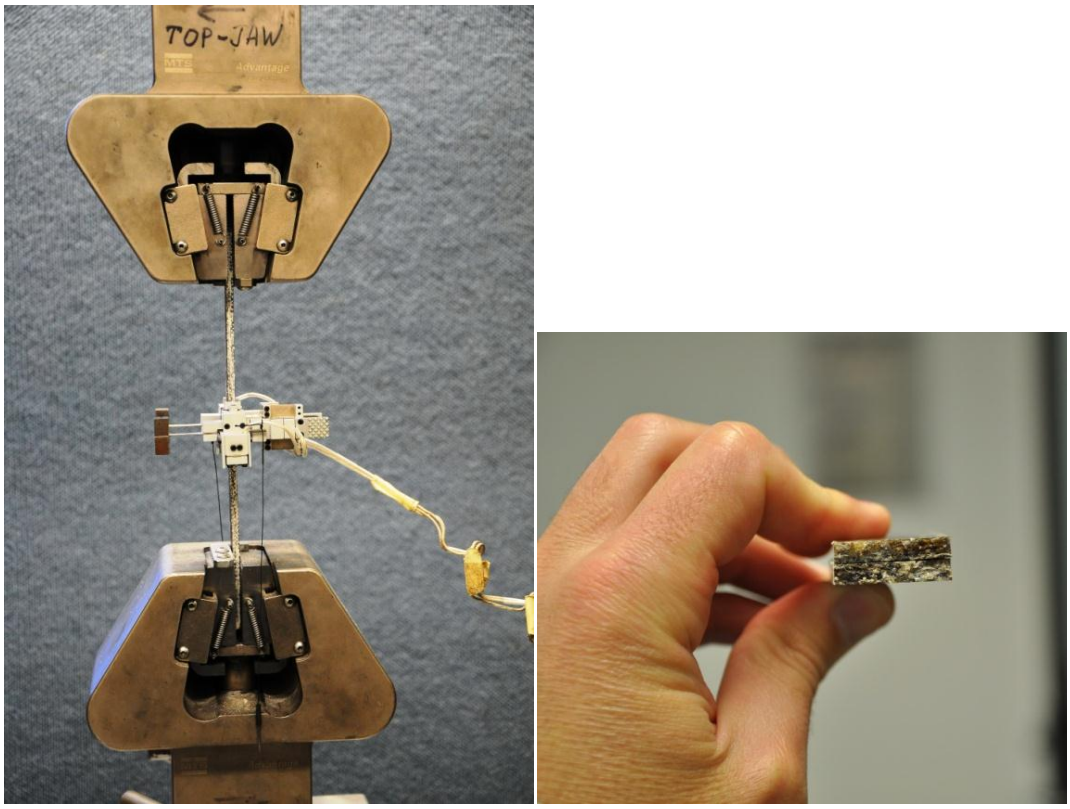

Figure 5.31. Typical tensile test (left) and fracture surface (right) of a biocomposite sample.

5.4.5 Impact properties

EHO based samples

Examining the results from the jute reinforced biocomposites, Figure 5.32 it can be seen that the Charpy impact strength increased for both EHO and ESO samples with increasing bioresin concentration. This behaviour is attributed to the long fatty acid chains of the EVO imparting flexibility to the matrix thereby increasing the energy required to break the biocomposite samples. Throughout the sample range ESO samples displayed higher impact strength compared with EHO samples and the control. This is due to the lower crosslink density of the ESO samples compared with EHO and the synthetic control.

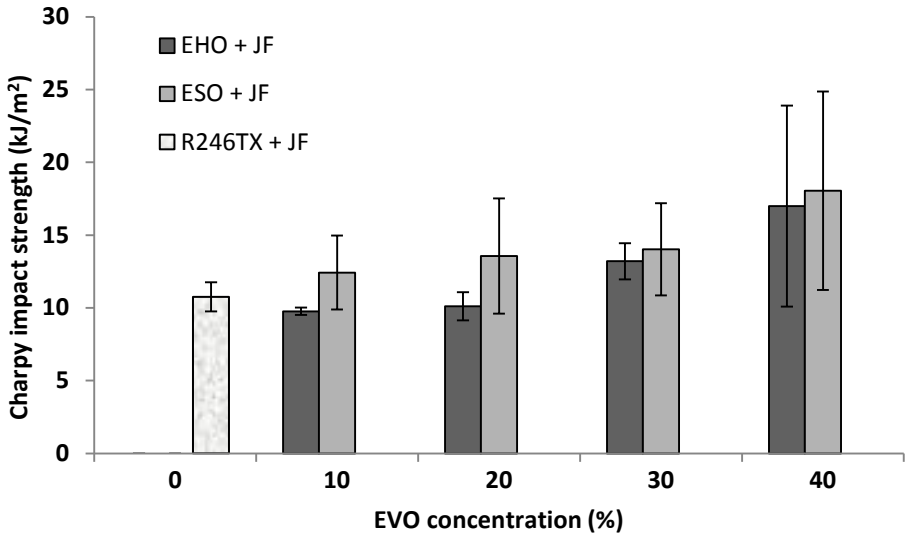

Figure 5.32. Charpy impact strength of synthetic epoxy, EHO and ESO based biocomposite samples.

AEHO based samples

Figure 5.33 displays the Charpy impact strength for the VE and AEHO based biocomposites. It can be observed that the impact properties of all three samples are similar in nature, especially accounting for the standard deviation. In the previous investigation of different synthetic epoxy/bioresin blends the Charpy impact strength was studied. Increases in impact strength associated with increasing bioresin concentration were observed. This behaviour was due to the long fatty acid chains of the epoxidized vegetable oils imparting flexibility to the matrix thereby increasing the energy required to break the biocomposite samples. Therefore for this reason, the impact strength of the VE resin was expected to be lower than that of the acrylated AEHO based bioresins, since the former is much less flexible, as shown in Figure 5.26. However, in section 5.4.1, the fibre-matrix interfacial adhesion of the AEHO based samples was observed to be improved compared with that of the VE sample. Therefore these two seemingly opposite effects could be responsible for the impact properties of all samples having similar performance. Figure 5.34 displays a typical Charpy impact test sample undergoing testing.

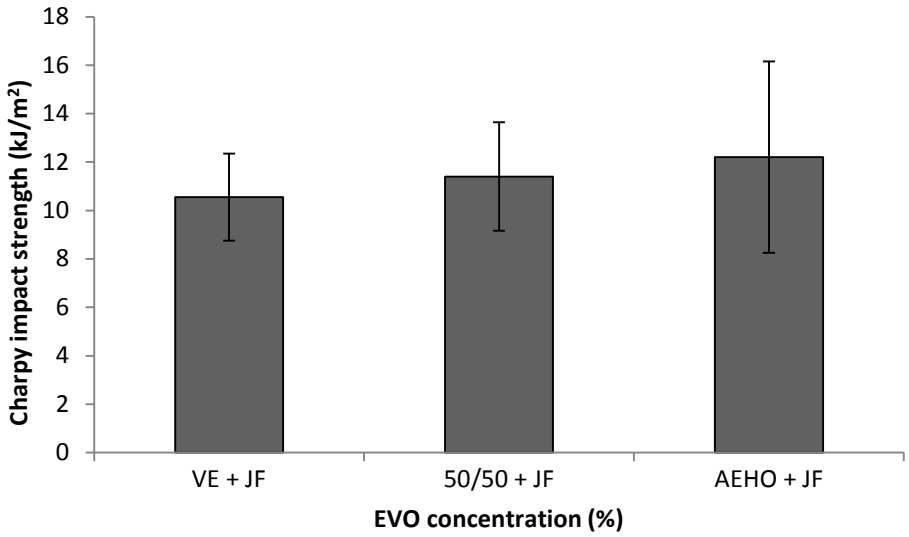

Figure 5.33. Charpy impact strength of AEHO based biocomposite samples.

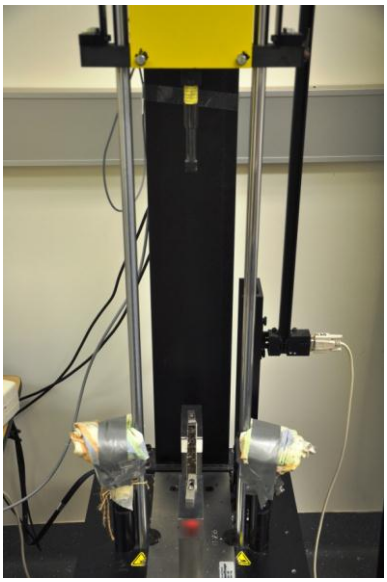

Figure 5.34. Charpy impact strength of AEHO based biocomposite samples.

5.4.6 Dynamic mechanical properties

EHO based samples

DMA was performed on bioresin and biocomposite samples in order to characterize the viscoelastic behaviour of both EHO and ESO based neat bioresins and biocomposites. Figures 5.35 and 5.36 show the storage modulus plotted against temperature for the different bioresin and biocomposite samples. Table 5.1 shows the effects of EHO and ESO concentration on the

storage modulus at 40 °C, T_g and crosslink density. For both bioresin and biocomposite sample types storage modulus was found to decrease with increasing bioresin concentration. Similar behaviour to the flexural properties was observed in that subsequent to 30% bioresin concentration performance was substantially reduced. The highest recorded storage modulus of the bioresin and biocomposite samples was 1820 MPa and 1912 MPa respectively was for the synthetic epoxy control samples. Samples containing EHO displayed higher storage modulus than those containing the same concentration of ESO.

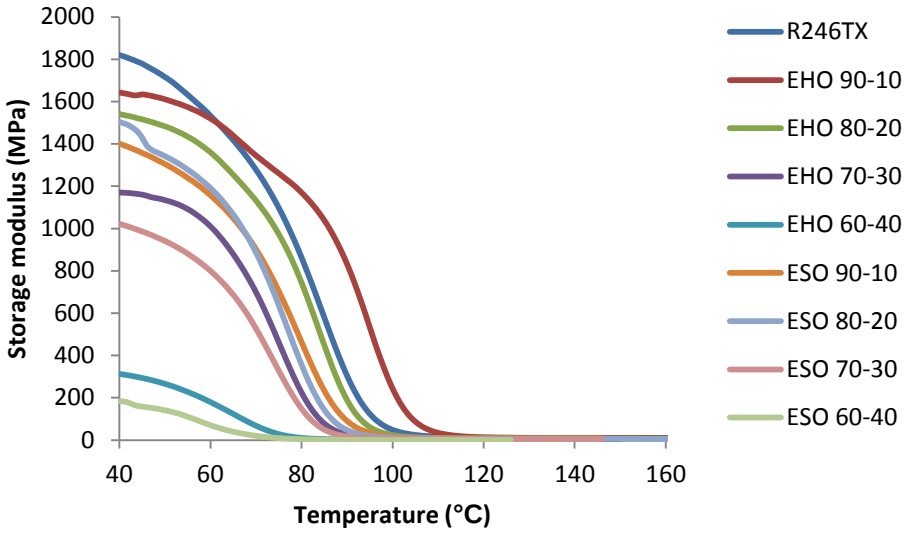

Figure 5.35. Storage modulus of synthetic epoxy, EHO and ESO based neat bioresins.

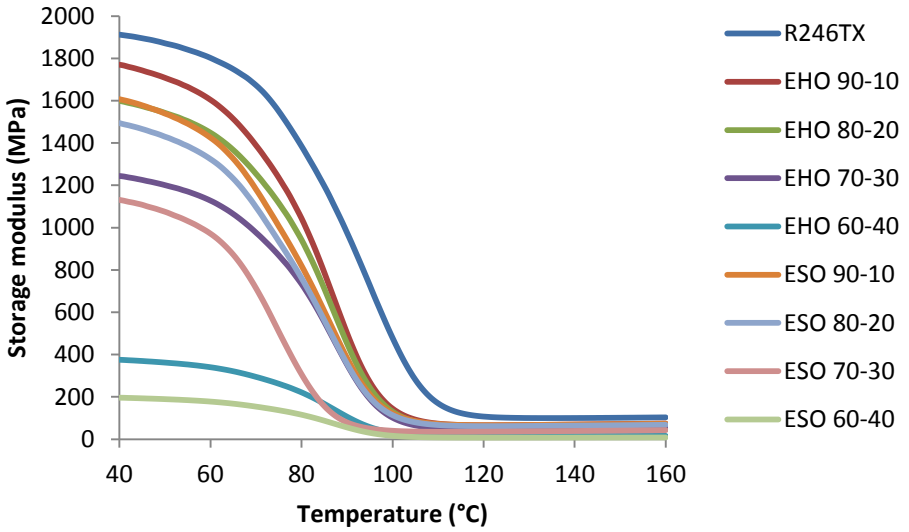

Figure 5.36. Storage modulus of synthetic epoxy, EHO and ESO based biocomposites.

The T_g of EHO and ESO bioresin samples was determined from the peak of the tan δ curve using Universal Analysis 2000 version 3.9A software as shown in Figures 5.37 and 5.38. Commonly a higher T_g is obtained when the bioresin component has a lower epoxide equivalent weight (EEW) and higher epoxy functionality (Miyagawa et al. 2005). This was apparent and expected in this study as EHO has a lower EEW and higher epoxy functionality compared with ESO and consequently displayed higher T_g values than ESO samples throughout the data range. The change in T_g for the bioresin compared to the biocomposite samples was found to be negligible. Of all the different samples the synthetic epoxy control was found to exhibit the highest T_g of 107.4 °C. The relationship between bioresin concentration and T_g was found to be approximately linear thereby supporting the findings of Miyagawa et al. (2004). A reduction in T_g was observed with increasing bioresin content which is also in agreement with results found by Espinoza-Perez et al. (2009) and Miyagawa et al. (2004).

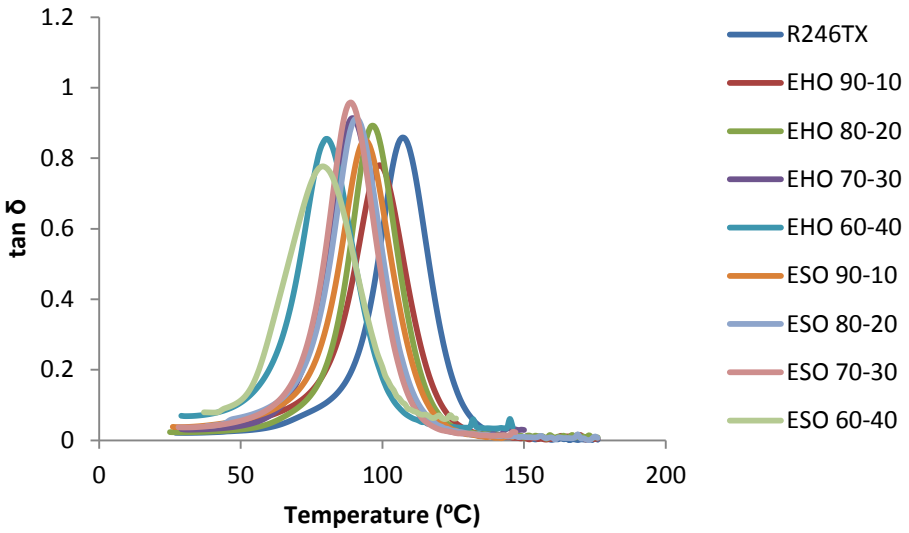

Figure 5.37. Tan δ of synthetic epoxy, EHO and ESO based neat bioresins.

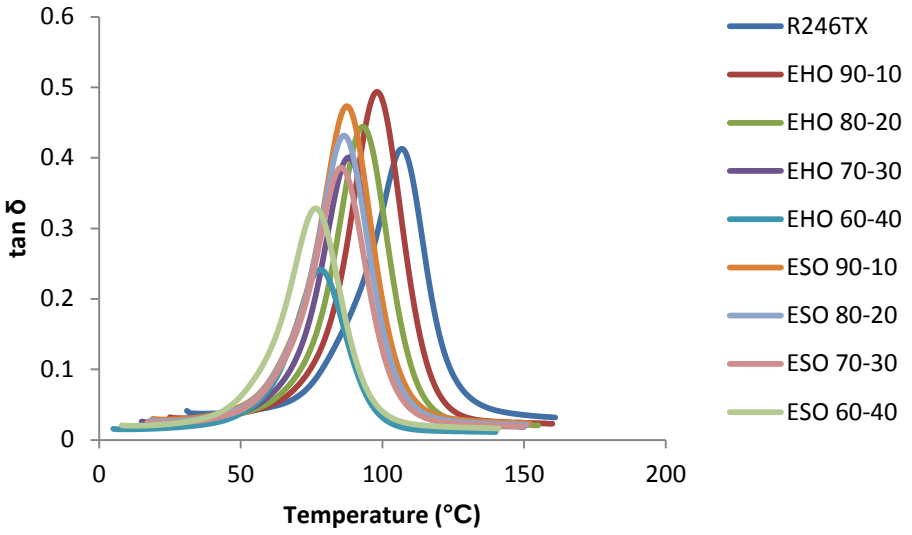

Figure 5.38. Tan δ of synthetic epoxy, EHO and ESO based biocomposites.

Crosslink density is also outlined in Table 5.1. Similar to the storage modulus and the T_g values, the value of the crosslink density was found to decrease with increasing bioresin concentration. These findings are again consistent to those of Miyagawa et al. (2004; 2005). As expected the synthetic epoxy control sample exhibited the highest crosslink density. EHO samples displayed higher crosslink density than ESO samples at the same bioresin concentrations. Subsequent to 30% bioresin concentration the crosslink density markedly decreases suggesting that synthetic epoxy replacement is limited to lower bioresin concentrations. Both EHO and ESO were found to be non-transparent above 30% concentrations which may be due to phase separation (Miyagawa et al. 2004). Crosslink densities were found to be higher for biocomposites samples in comparison to the neat bioresin samples primarily due to improved storage moduli. Similar results were found by Jacob et al. (2006) and Rahman et al. (2012) who found increased crosslink densities of composites in comparison to those of neat resin samples.

Table 5.1. Dynamical mechanical properties of synthetic epoxy, EHO and ESO based bioresins and biocomposites.

Sample type	Storage modulus at 40 °C (MPa)	T_g (°C)	Crosslink density (mol/m^3)
Neat bioresin			
R246TX	1820	107.4	1001
ESO 90-10	1504	93.9	841
ESO 80-20	1401	90.8	623
ESO 70-30	1022	87.7	454
ESO 60-40	185	79.3	62
EHO 90-10	1643	99.1	965
EHO 80-20	1541	96.5	714
EHO 70-30	1170	89.5	418
EHO 60-40	313	80.1	158
Biocomposite			
R246TX	1912	107.1	9936
ESO 90-10	1607	91.4	6599
ESO 80-20	1494	86.1	6252
ESO 70-30	1131	85.2	3601
ESO 60-40	196	76.9	715
EHO 90-10	1770	98.2	6711
EHO 80-20	1599	93.7	5970
EHO 70-30	1244	88.6	4580
EHO 60-40	375	78.6	1427

AEHO based samples

Figures 5.39 and 5.40 depict the thermo-mechanical behaviour of the AEHO based bioresins and biocomposites in terms of the storage modulus and tanδ as a function of temperature. Table 5.2 shows the effects further illustrates the storage modulus at 40 °C, T_g and crosslink density. For all bioresin and biocomposite systems the storage modulus, T_g and crosslink density were found to decrease with the addition of AEHO. As expected VE systems displayed the highest properties of all systems. The addition of jute fibre reinforcement resulted in improved storage modulus ranging from approximately 34% for the VE sample through to a maximum of 215% for the AEHO sample. This behaviour is in agreement with the trends observed in section 5.4.4 for the flexural properties of the biocomposites compared with the neat bioresin samples whereby AEHO samples displayed a larger increase in flexural modulus compared with VE based samples.

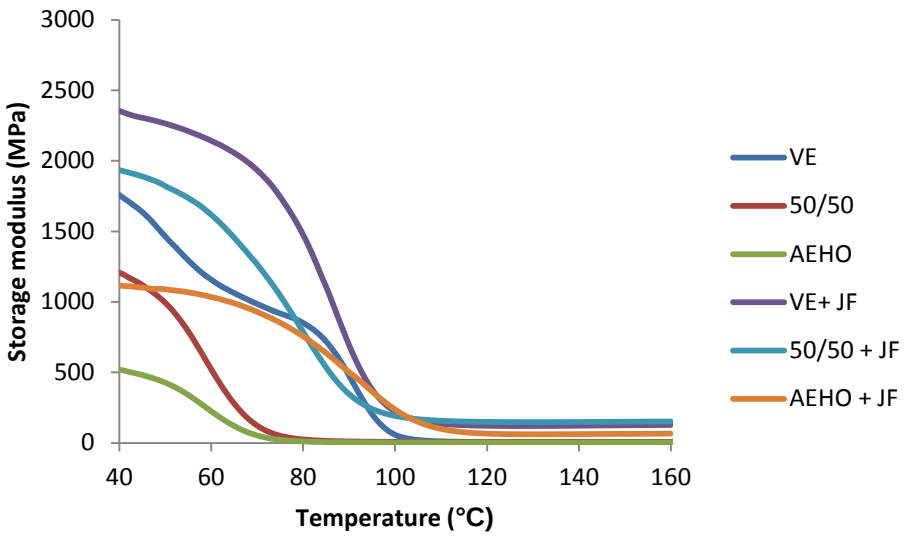

Figure 5.39. Storage modulus of AEHO based bioresins and biocomposites.

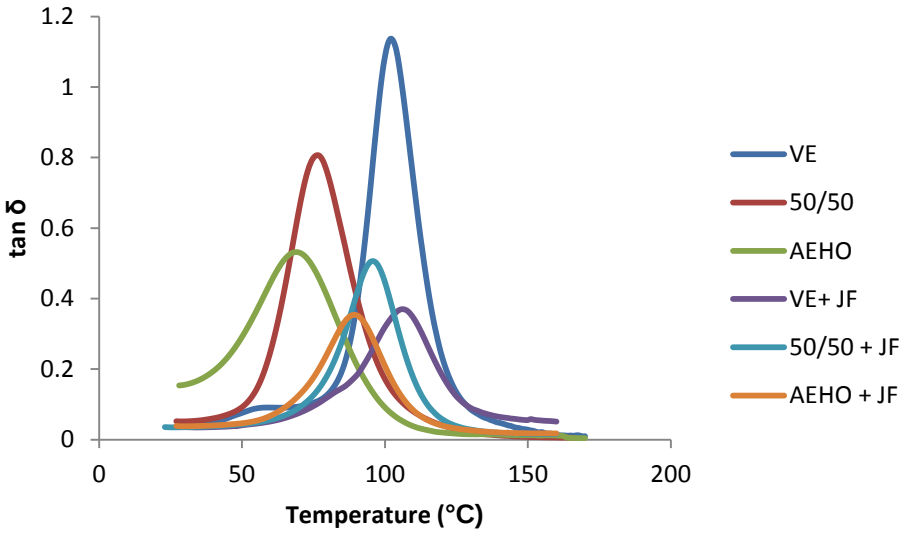

Figure 5.40. Tan δ of AEHO based bioresins and biocomposites.

In terms of T_g the VE systems showed the highest values with reductions being apparent for AEHO based systems. The addition of fibre reinforcement resulted in a marginal increase in T_g for the VE system from 102 to 106 °C. Both AEHO based systems realised an increase in T_g of 25 and 28% from the neat bioresin samples. The tanδ peaks of the AEHO based samples were found to become broader compared with the VE sample. This was also found to be the case for AESO/VE systems as studied by Grishchunk and Karger-Kocis (2010). No peak doubling was found to occur for the 50/50 sample indicating satisfactory compatibility between the VE and AEHO resins. In a study of VE/AESO blends Grishchunk and Karger-Kocis (2010) found T_g also decreased with increased

AESO. Compared to the observed storage modulus of the neat AEHO sample Lu and Wool (2006) and Khot et al. (Khot et al. 2001) found the storage moduli of AESO with 40 wt% styrene and AELO with 33 wt% styrene to be in the order of 1.3 GPa and approximately 2 GPa respectively. Furthermore they also reported T_g values of 79 °C for the AESO and approximately 105 °C for the AELO neat resin samples.

Crosslink densities were also found to decrease with the addition of AEHO. As anticipated the VE based samples displayed the highest crosslink densities out of all the samples. The crosslink density of the neat VE system was found to be almost twice that of the neat AEHO sample. When fibre reinforcement was added the crosslink densities were found to dramatically increase similar to those reported above for the EHO based systems. Accordingly this behaviour is primarily due to the higher storage moduli of the biocomposites compared with the neat bioresins. It is also interesting to note that the biocomposite samples displayed similar crosslink densities with data spread being less than 10%. Given the similarity in crosslink densities for the biocomposites it is reasoned that the greater quantity of hydroxyl groups in the AEHO bioresin compared with the VE are to contribute to the crosslinking of the end biocomposites. Consequently the final result is a greater improvement in crosslink density for the AEHO based samples compared with that obtained from the VE samples.

In comparison to the crosslink densities found in this study, Lu and Wool determined the crosslink density for AELO to be 5050 mol/m^3 (Lu, J & Wool 2006). Indeed it is expected that AEHO would have a lower crosslink density than AELO due to having less acrylates per triglyceride. Campanella et al. (2009) observed that the crosslink density of AESO resins was influenced by the styrene content. Moreover it was observed that crosslink densities ranged from 3700-2100 mol/m^3 for AESO samples containing no styrene through to 35 wt%. In a study to determine properties of an AESO based material intended to be used in the PCB industry Zhan and Wool (2010) determined the crosslink density of AESO polymers containing 30 wt% styrene and 0-15 wt% of DB.

Crosslink densities were found to increase with DB content from 1833 to a maximum of 7133 mol/m^3 at 15 wt% DB.

Table 5.2. Dynamical mechanical properties of AEHO based bioresins and biocomposites.

Sample type	Storage modulus at 40 °C (MPa)	T_g (°C)	Crosslink density (mol/m^3)
Neat bioresin			
VE	1757	102	6654
50/50	1206	76	6542
AEHO	519	68	4301
Biocomposite			
VE + JF	2354	106	13965
50/50 + JF	1934	95	13327
AEHO + JF	1115	87	12861

5.4.7 Moisture absorption

EHO based samples

Akil et al (2009) mentioned three different mechanisms acting in the moisture absorption of fibre reinforced composites. Namely diffusion of water molecules inside the micro gaps between polymer chains, capillary transport into the gaps and flaws of the interfaces between fibre and the matrix and transport through microcracks in the matrix arising from the fibre swelling (particularly in the case of natural fibre composites). Moreover, the hydrophilic nature of natural fibres increases moisture absorption of the final composites.

The moisture absorption results obtained in this work showed that the composites immersed in distilled water at 23.1 °C followed a linear Fickian behaviour, whereby the moisture weight gains gradually reached equilibrium after a rapid initial phase, Figures 5.41 and 5.42. Moisture absorption data, specifically diffusion coefficient and saturation moisture content of the bioresin blends and jute fibre reinforced biocomposites is displayed in Table 5.3. As expected from the crosslink density values obtained with DMA, synthetic control samples exhibited the lowest diffusion coefficient and saturation moisture content of all samples. The moisture absorption of the epoxy bioresin blends and biocomposite samples was found to increase with increased bioresin

loading. This behaviour was also reported by Tan and Chow for epoxidized palm oil (EPO) blends (Tan & Chow 2010).

As previously stated, fibres provide an additional transport mechanism for moisture transport throughout the material and therefore the composite moisture uptake was always higher than the observed on the neat resin samples. As expected, the highest moisture absorption was shown by the jute fibre samples. These fibres dramatically increase both the diffusion coefficient and saturation moisture content of the composites as they absorb moisture as a consequence of their hydrophilic nature given by the hydroxyl groups in the cellulose component of the fibres and swell, allowing the transport of moisture along microcracks in the matrix arising from the swelling of fibres. EHO based samples displayed lower diffusion coefficient and saturation moisture content than ESO based samples, although the difference is insignificant.

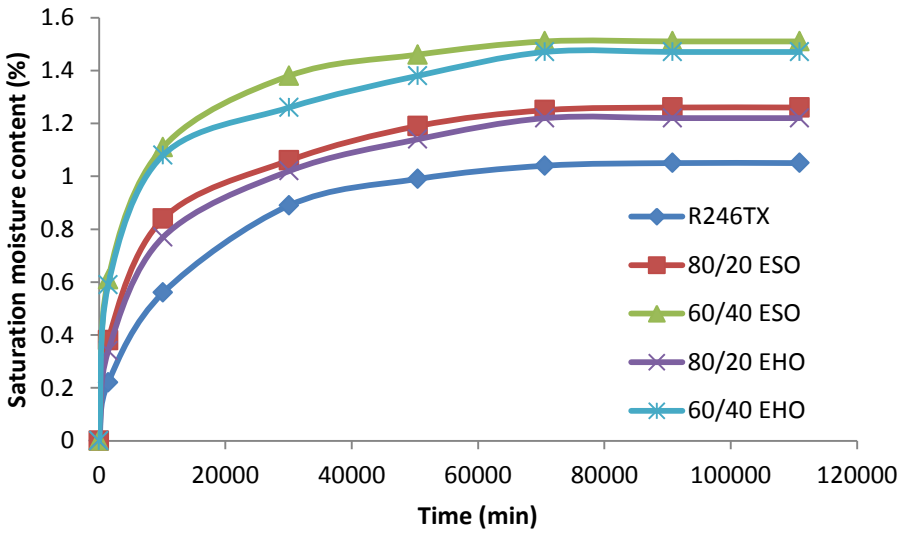

Figure 5.41. Moisture absorption of synthetic epoxy, EHO and ESO based neat bioresins.

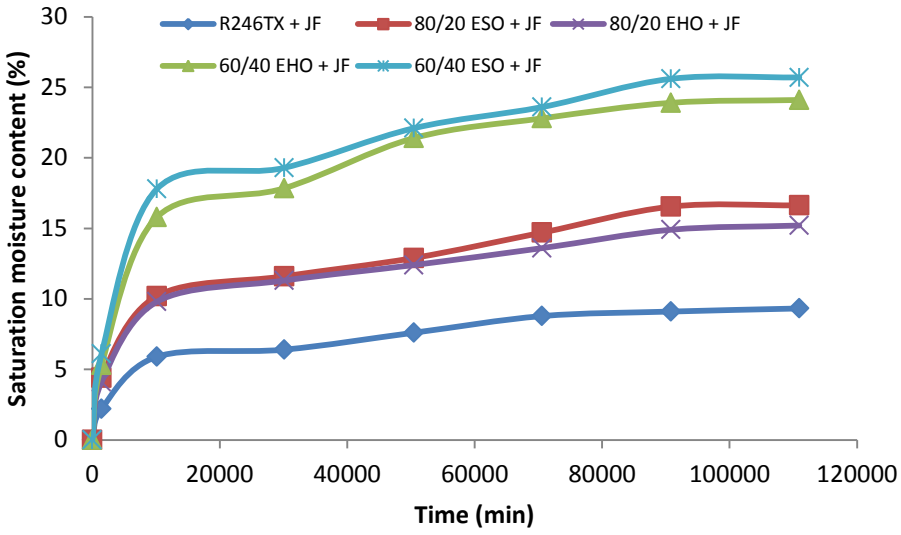

Figure 5.42. Moisture absorption of synthetic epoxy, EHO and ESO based jute reinforced biocomposites.

Table 5.3. Moisture absorption properties of synthetic epoxy, EHO and ESO based bioresin/epoxy blends and biocomposites.

Sample type	Diffusion coefficient $\times 10^{-6}$ (mm^2/s)	Saturation moisture Content (%)
Bioresin samples		
R246TX	1.78	1.05
EHO 20-80	1.85	1.22
ESO 20-80	1.93	1.26
EHO 40-60	1.99	1.47
ESO 40-60	2.03	1.51
Jute fibre samples		
R246TX	4.24	9.32
EHO 20-80	4.60	15.20
ESO 20-80	4.70	16.63
EHO 40-60	5.09	24.13
ESO 40-60	5.46	25.71

AEHO based samples

Figures 5.43 and 5.44 show the moisture absorption behaviour of the AEHO based neat resin and biocomposite samples respectively. This data is further summarised in Table 5.4. From examining the Figures it is apparent that increasing AEHO content results in increasing saturation moisture content and diffusion coefficient. Also as previously found with the EHO based samples overall the moisture absorption is heavily dominated by fibre addition rather than resin type. Through the addition of fibre reinforcement the saturation

moisture content increased approximately by a factor of approximately 6.75-8. Similarly the diffusion coefficients increased by a factor of approximately 11.

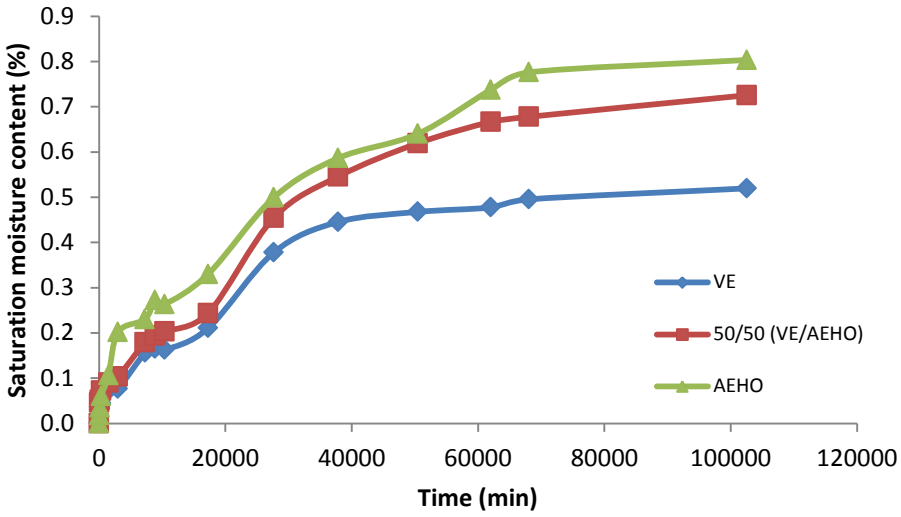

Figure 5.43. Moisture absorption of AEHO based neat bioresins.

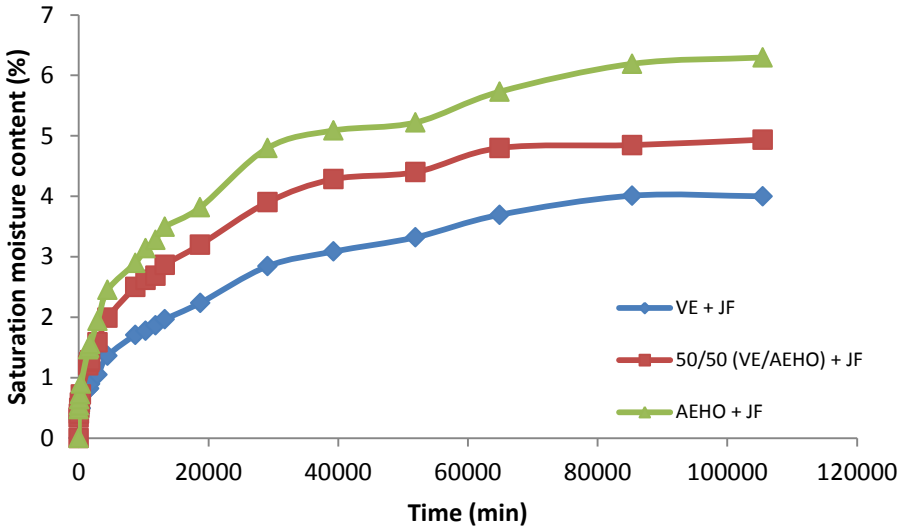

Figure 5.44. Moisture absorption of AEHO based jute reinforced biocomposites.

Table 5.4. Moisture absorption properties of AEHO based bioresins and biocomposites.

Sample type	Diffusion coefficient $\times 10^{-6}$ (mm^2/s)	Saturation moisture Content (%)
Bioresin samples		
VE	0.801	0.52
50/50 (VE/AEHO)	0.847	0.73
AEHO	0.958	0.80
Jute fibre samples		
VE	8.81	4.01
50/50 (VE/AEHO)	9.54	4.94
AEHO	10.90	6.30

5.5 Conclusions

EHO based bioresins and jute fibre reinforced biocomposites were prepared and compared with ESO based samples in terms of SEM, mechanical, dynamic mechanical and moisture absorption properties. EHO based biocomposite samples were found to display higher tensile stress, modulus of elasticity, flexural stress, flexural modulus and interlaminar shear strength than ESO based samples. Mechanical performance decreased for both EHO and ESO bioresins and biocomposites with increased bioresin loading. A significant reduction occurred after 30% bioresin concentration. As expected, synthetic epoxy control samples displayed superior mechanical performance compared with both EHO and ESO samples. From the SEM analysis it was confirmed that fibre-matrix interfacial adhesion was negatively affected with increasing bioresin content.

In terms of DMA, EHO based bioresin and biocomposite samples exhibited higher glass transition temperature (T_g), storage modulus and crosslink density than ESO bioresin and biocomposite samples. Moreover, the addition of EHO/ESO bioresins to the synthetic epoxy resulted in a reduction of the T_g, the storage modulus and the crosslink density values. With an EHO/ESO concentration greater than 30% a significant reduction in properties was observed. The addition of jute fibre reinforcement resulted in higher crosslink densities than the neat resin samples, primarily due to higher storage modulus

values. The change in T_g for the bioresin compared to the biocomposite samples was found to be negligible.

Moisture absorption tests showed that synthetic control samples exhibited the lowest diffusion coefficient and saturation moisture content of all samples. The moisture absorption of the epoxy bioresin blends and biocomposite samples was found to increase with increased bioresin loading. EHO based samples displayed lower diffusion coefficient and saturation moisture content than ESO based samples although the difference is minimal. The type of fibre reinforcement in the biocomposites, in particularly jute fibre, proved to be the dominant moisture absorption factor.

Overall this study has shown that EHO based bioresins when applied to jute fibre reinforced biocomposites can compete with commercially produced ESO in terms of mechanical performance, dynamic mechanical properties and moisture absorption characteristics. However, the general, realistic conclusion is that both EHO and ESO are indeed best suited to a plasticizing role rather than complete bioresin matrices. Although it was shown that EHO can be used in higher concentrations than ESO, thereby resulting in more sustainable biocomposites.

ILSS was found to increase with increasing AEHO content suggesting that the fibre-matrix interfacial adhesion is stronger for the AEHO based samples compared with the VE based samples. In terms of flexural performance the flexural strength of the neat bioresins were found to be higher than those of the biocomposite samples. The VE based neat resin samples showed markedly higher flexural stress than samples containing AEHO. However when jute fibre reinforcement was incorporated, all three systems exhibited similar flexural performance. Flexural modulus was found to increase for all three biocomposite types over the bioresin samples. This was expected due to the addition of the relatively stiff jute fibres. VE samples displayed the highest flexural moduli for both neat bioresin and biocomposite samples however the difference was marginal in the case of the biocomposites. AEHO based jute reinforced

biocomposites were subjected to tensile tests. It was observed that VE based samples exhibited the highest tensile strength with the addition of AEHO resulting in a slight reduction in performance. Young's modulus was found to be similar for all three sample types Charpy impact properties of all three samples were similar in nature, especially accounting for the standard deviation.

DMA was performed in order to characterise the visco-elastic behaviour of the AEHO based bioresins and biocomposites. Specifically VE based samples were found to have higher $T_{g,}$ storage modulus and crosslink density than AEHO based samples. As the AEHO content increased $T_{g,}$ storage modulus and crosslink density were found to decrease. The addition of jute fibre reinforcement resulted in a marginal increase in T_g, for the VE samples however a noticeable increase was observed for AEHO based samples. Similarly to the EHO/ESO samples the crosslink density was found to significantly increase with the addition of jute fibre reinforcement. In studying the moisture absorption of AEHO based bioresins and biocomposites it was found that increasing AEHO content resulted in increasing saturation moisture content and diffusion coefficient. Also as previously found with the EHO based samples overall the moisture absorption was heavily dominated by fibre addition rather than resin type.

In the next chapter owing to the positive results found in this chapter pertaining to the improved fibre-matrix interfacial adhesion of AEHO and jute fibre, it was theorised that perhaps utilising the same fibre and bioresin source in the form of one plant type may have further benefits that negate the need for fibre chemical treatments. Therefore in chapter 6 the production and characterisation in the form of thermo-mechanical properties of 100% hemp based biocomposites is presented.

Chapter 6

PRODUCTION AND CHARACTERISATION OF 100% HEMP BASED BIOCOMPOSITES

6.1 Introduction

As a part of this PhD candidature hemp fibre mat was sourced lead by the interest to investigate the production of 100% hemp based biocomposites. Around this time vacuum infusion facilities also became available thereby presenting the potential to utilise this more commercially favoured composite processing technique and to get closer to industry production processes. Moreover owing to the positive results found in Chapter 5 pertaining to the improved fibre-matrix interfacial adhesion of AEHO and jute fibre it was theorised that perhaps utilising the same fibre and bioresin source in the form of one plant type may have further benefits that negate the need for fibre chemical treatments.

It is understood that the performance of biocomposites is lower than that of traditional composites. Moisture and water absorption can result in swelling of the natural fibres, negatively influence the dimensional stability of the natural fibre composites, and also deteriorate the mechanical properties of the fibres and the composite due to weakening of the matrix-fibre interface. The effect of

water and moisture absorption of natural fibre plastic composites is a serious concern, especially for outdoors applications, and was studied by several authors (Akil et al. 2009; Bledzki & Gassan 1999; Dhakal et al. 2007). Moreover, the adhesion between natural fibres and the polymeric matrix is insufficient, resulting in low mechanical properties of the composites. In addition, plant based natural fibres suffer lignocellulosic degradation at low temperatures (around 200 °C), limiting their use in certain applications and processing temperatures (Francucci, Rodríguez & Vázquez 2012). For this reason many researchers have tried to improve the fibre-matrix interface and decrease fibre moisture uptake. Bledzki and Gassan (1999) made an extensive review on the most used methods for surface modification of natural fibres. They sorted the treatments as chemical or physical methods. Usually, chemical methods bring about an active surface by introducing some reactive groups, and provide the fibres with higher extensibility through partial removal of lignin and hemicelluloses (Rong et al. 2001), while physical methods change structural and surface properties of the fibre and thereby influence the mechanical bonding to polymeric matrices.

Most of the treatments are performed to improve compatibility of natural fibres with petrochemical resins. However, if bioresins are used and in particular bioresins derived from the same plant which the fibres were extracted from, the compatibility may be improved. Therefore, this work studies the performance of 100% hemp based biocomposites, made with an AEHO based bioresin reinforced with untreated hemp fibre random mat and compares it to that of hybrid composites made with VE resin reinforced with the same hemp fibre mat. Mechanical properties (tensile, flexural, Charpy impact and interlaminar shear), dynamic mechanical properties (glass transition temperature, storage modulus and crosslink density) and water absorption properties (saturation moisture level and diffusion coefficient) were investigated.

Liquid composite moulding (LCM) techniques, such as resin transfer moulding (RTM) or vacuum infusion (VI) appear to be a sound choice for processing biocomposites. They make it possible to obtain high quality laminates,

repeatability, high surface finish and dimensional tolerances and because of the low processing temperatures, fibres do not suffer thermo-mechanical degradation as in some thermoplastic processing techniques. In LCM techniques a catalysed resin is forced through a mould which contains the dry reinforcement. In RTM, the preform (a stack of several layers of the fabric used as reinforcement) is compacted between two rigid mould faces. In VI a flexible vacuum bag is used as the upper part of the mould. In this work, VI was used to manufacture the biocomposite panels due to the availability of this technique in the laboratories. VE was chosen as it is analogous to the synthesised AEHO and is the most commercially used resin in industry.

6.2 Materials

AEHO as synthesised according to chapter 3 and containing 4.1 acrylate and hydroxyl groups per triglyceride was used as the base bioresin. FG vinylester SPV6003 (FGI Australia) was used as received for the control samples. In the case of the AEHO bioresin, the added styrene comonomer was supplied by Fischer Scientific (United Kingdom), the Promoter N2-51P was sourced from Axon Nobel Ltd and a 40% MEKP based catalyst was used for the curing and sourced from FGI Australia. The Styrene comonomer, the promoter and the catalyst were all used as received. Short hemp fibre based random mat with a surface density of approximately 730 g/m^2 was used as the natural fibre reinforcement.

6.3 Experimental investigation

6.3.1 Biocomposite specimen production

To prepare the AEHO bioresin, 33 wt% of styrene was added in order to decrease viscosity and improve processability for manufacturing composite parts by traditional composite processing techniques. Afterwards, the promoter was incorporated to the AEHO/styrene mixture (0.25% by weight) and thoroughly mixed. Subsequent to this the catalyst was added (4% by weight) and stirred thoroughly for several minutes. The resin was degassed under vacuum. For the VE resin system no styrene was added as the system already contains 33 wt% of styrene. Regarding the VE system, 0.25% and 2% promoter and catalyst were used respectively. Neat bioresin and resin samples were also produced by pouring into a waxed glass mould.

Flat biocomposite panels were manufactured by the VI technique utilising two layers of hemp mat reinforcement. These mats were washed with a 2% V/V distilled water and detergent solution to remove contaminants, and then dried at 90 °C for 24 h. The manufacture of the composite panels was performed immediately after removing the fibre from the oven in order to prevent moisture absorption and thereby minimise the amount of water present in the natural reinforcement which could lead to void formation and lower mechanical properties of the composites.

Both the catalyst and promoter were added to the resin and mixed thoroughly, the mixed resin was degassed and the resin was infused at a vacuum level of 90 kPa. A glass surface was used as the rigid mould face which was thoroughly waxed before every infusion. The flow front was found to be linear with no race tracking, dry spots or fibre washing observed. After the complete impregnation of the reinforcement, the inlet hose was clamped and the resin pressure distribution along the wetted perform was left to stabilize for two hours. This method helps to remove excess resin and decrease the thickness variations

throughout the composite plate (Govignon, Bickerton & Kelly 2012). Afterwards the outlet hose was clamped and the composite panel was left to cure under vacuum for 24 h at room temperature (~25 °C). A 4 h postcuring stage was performed at 80 °C for the VE and at 120 °C for the bioresin composites respectively to achieve maximum conversion. Figure 6.1 shows a picture of the biocomposite panel during the infusion.

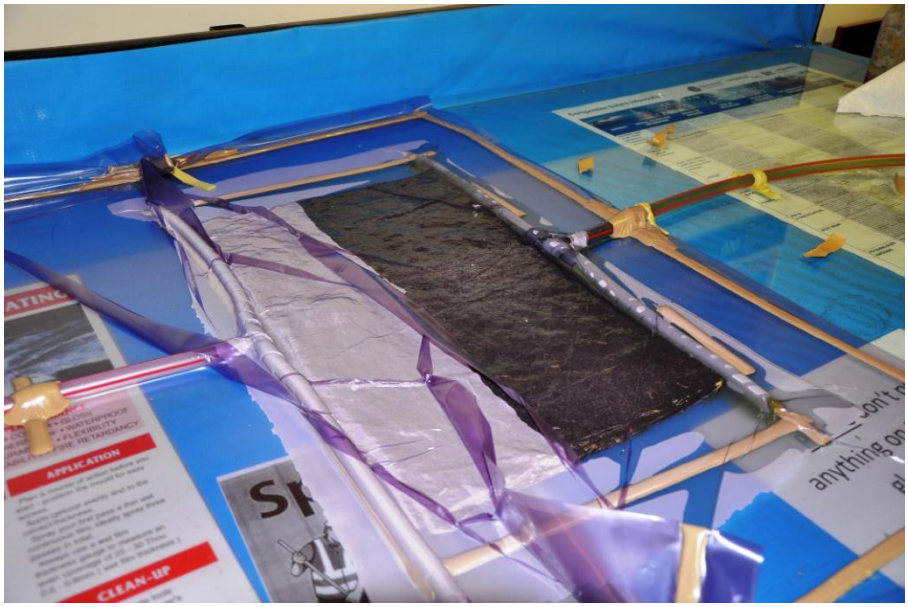

Figure 6.1. AEHO based hemp fibre biocomposite undergoing vacuum infusion.

Although this processing technique does not allow a constant thickness throughout the entire composite plate to be obtained, thickness ranged from 4-5 mm, resulting in a fibre volume fraction distribution between 20-25%, calculated from Equation 6.1, where n is the number of reinforcement layers stacked in the preform, β the surface density (g/cm^2), ρ the fiber density (g/cm^3) and t is the preform thickness (cm). Samples for the mechanical characterization were cut from the manufactured composite plates, dried at 80 °C for 4 h to ensure the removal of any induced moisture and then cooled in a desiccator ready for testing. In addition, neat resin samples were produced by pouring the catalysed resin into a waxed mould, cured as the composite panels and finally cut to size.

$$\text{Fibre volume fraction} = \frac{n \cdot \beta}{\rho \cdot t} \qquad (6.1)$$

6.3.2 Microscopic analysis

Cross section morphologies of the biocomposite samples were investigated with a JEOL JSM 6460 LV scanning electron microscope (SEM) at National University of Mar Del Plata, Argentina (UNMdP). The fractured surfaces were coated with gold and the samples were scanned at room temperature with an accelerating voltage of 15 kV.

6.3.3 Mechanical testing

Interlaminar shear strength (ILSS) testing was performed to determine the fibre-matrix interfacial shear strength. Testing was performed using ISO 14130 on a MTS Alliance RT/10 10 kN machine with a crosshead speed of 1 mm/min. Charpy impact tests were conducted to determine the impact properties of the biocomposite and hybrid composite samples. Impact properties of the samples were determined using ISO 179 on an Instron Dynatup M14-5162. Charpy impact strength (kJ/m^2) was calculated from Equation 6.2, whereby a_{cU}, h, b an W_B are the Charpy impact strength, thickness, width and the energy at break of the test specimen. Essentially Charpy impact strength corresponds to the energy at break of the specimen divided by the cross sectional area.

$$a_{cU} = \frac{W_B}{bh} \times 10^3 \tag{6.2}$$

Flexural testing was conducted to determine the behaviour of both neat resin and composite specimens subjected to 3-point simple beam loading. Bioresin and VE flexural properties were obtained through 3-point bending tests conducted in accordance with ISO 178 using a MTS Alliance RT/10 machine. A cross head speed of 2 mm/min and a span/depth ratio of 16:1 were used with specimen dimensions being 80×10×5 mm. Biocomposite and hybrid composite flexural properties were measured in accordance with ISO 14125. Tensile tests were conducted in accordance with ISO 527. Tests were performed with a cross-head speed of 2 mm/min using a MTS Insight 100 kN machine. Specimen

dimensions were 250×25×5mm. Five specimens of each sample type were used in each mechanical test.

6.3.4 Dynamic mechanical analysis

A calibrated TA Instruments Q800 DMA was used for the dynamic mechanical analysis (DMA). Rectangular specimens with the dimensions 58×10×4 mm were tested in dual cantilever mode. Testing was performed at a temperature ramp of 3 °C/min over a temperature range of approximately 25–180 °C. A frequency of 1.0 Hz with an oscillating displacement of ±10 μm was also used. Storage modulus (E') and tan δ were plotted as a function of temperature by Universal Analysis 2000 version 3.9A software. Glass transition temperature (T_g) was calculated as the peak of the tan δ curve and crosslink density (ν_e) was calculated from the theory of rubber elasticity, Equation 6.3 (Shabeer, Chandrashekhara & Schuman 2007). Where E', ν_e, R and T are the storage modulus in the rubbery plateau region (T_g + 40 °C), crosslink density, gas constant (8.314 J/(K·mol)) and the absolute temperature in K, respectively (Miyagawa et al. 2004).

$$E' = 3\nu_e RT \tag{6.3}$$

6.3.5 Moisture absorption

Moisture absorption tests were performed in order to ascertain the saturation moisture level and the diffusion coefficient of the bioresin and biocomposite samples. Testing was performed in accordance with ASTM D570. Specimens measured 76.2×25.4×5 mm for both neat resin and biocomposite samples. Three specimens of each sample type were used. The specimens were cut to size and the edges were finished with No. 0 sandpaper. After this the specimens were dried at 110 °C for 1 h, cooled in a desiccator and weighed to the nearest 0.001 g. The specimens were immersed in distilled water at 23±1 °C and

removed at regular intervals, wiped free of surface moisture, immediately weighed to the nearest 0.001 g and then replaced in the water. Equation 6.4 was used to calculate the diffusion coefficient. Where D, h, M_m and m are diffusion coefficient, thickness of specimen, saturation moisture level and gradient of the linear region from the plot of weight gain against time (Morye & Wool 2005).

$$D = \pi \left(\frac{h}{4M_m}\right) m^2 \quad (6.4)$$

6.4 Results and discussion

6.4.1 Microscopic analysis

Figures 6.2-6.5 show SEM images of the fracture surface of the samples used in the mechanical tests. 300× magnification was used to give a representative image of the overall fibre-matrix behaviour whereas 1000× magnification was used to more closely examine individual fibre-matrix interface. It can be seen that fibre pullout is evident for all sample types. In addition, the gap between the hemp fibre and the AHEO matrix is significantly smaller than the gap observed between the hemp fibre and the VE matrix. This observation suggests that the samples manufactured with VE have the poorest fibre-matrix interface, with the AEHO samples displaying improved fibre-matrix adhesion. It is proposed that the superior fibre-matrix interfacial adhesion of the 100% AEHO based samples is due to surface chemical compatibility between the natural fibres and the bioresin. It is thought that the greater quantity of hydroxyl groups present in the AEHO bioresin compared with the VE contributes to enhanced fibre-matrix adhesion. These hydroxyl functional groups present in the AEHO serve to interact with the hydroxyl groups present in the cellulose of the natural fibres to form strong hydrogen bonds thereby improving adhesion.

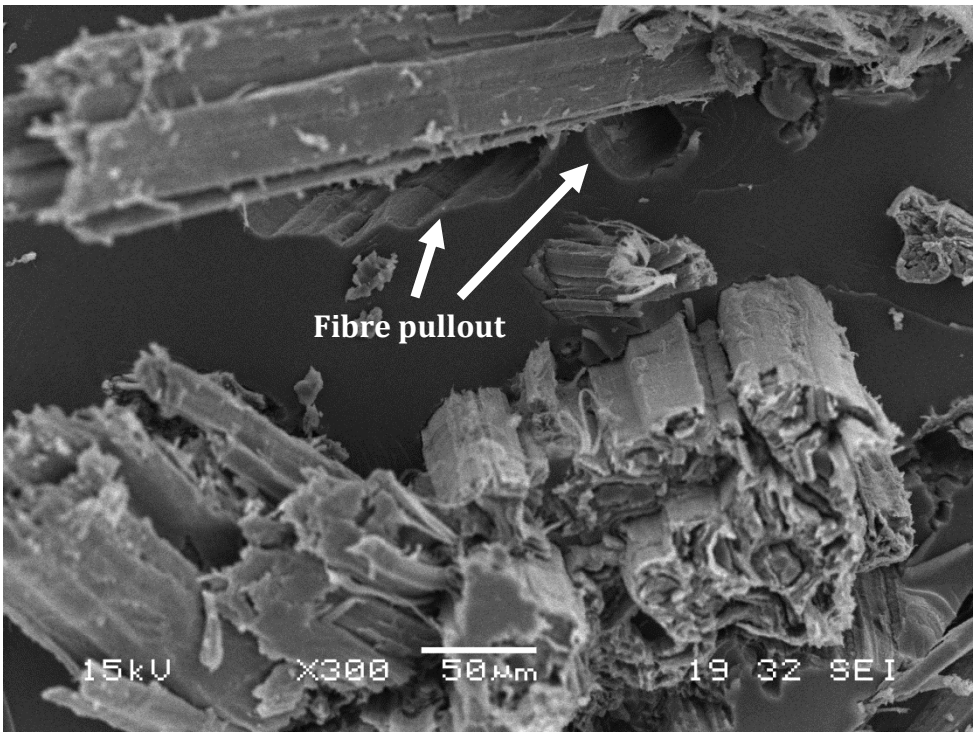

Figure 6.2. 300x SEM image of AEHO/hemp fibre biocomposite.

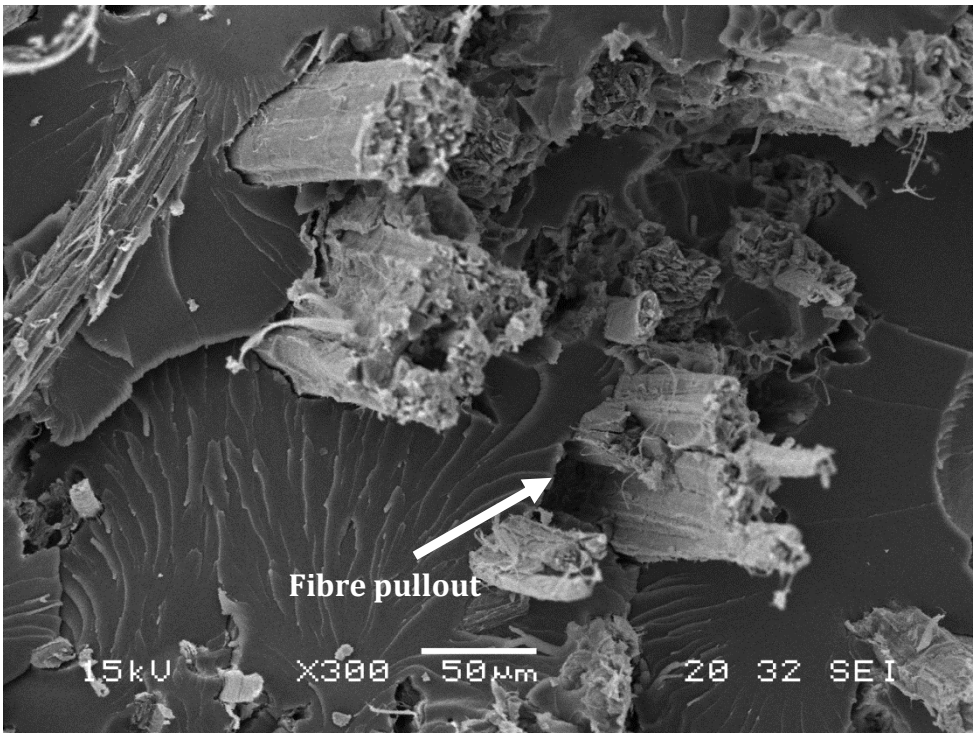

Figure 6.3. 300x SEM image of VE/hemp fibre composite.

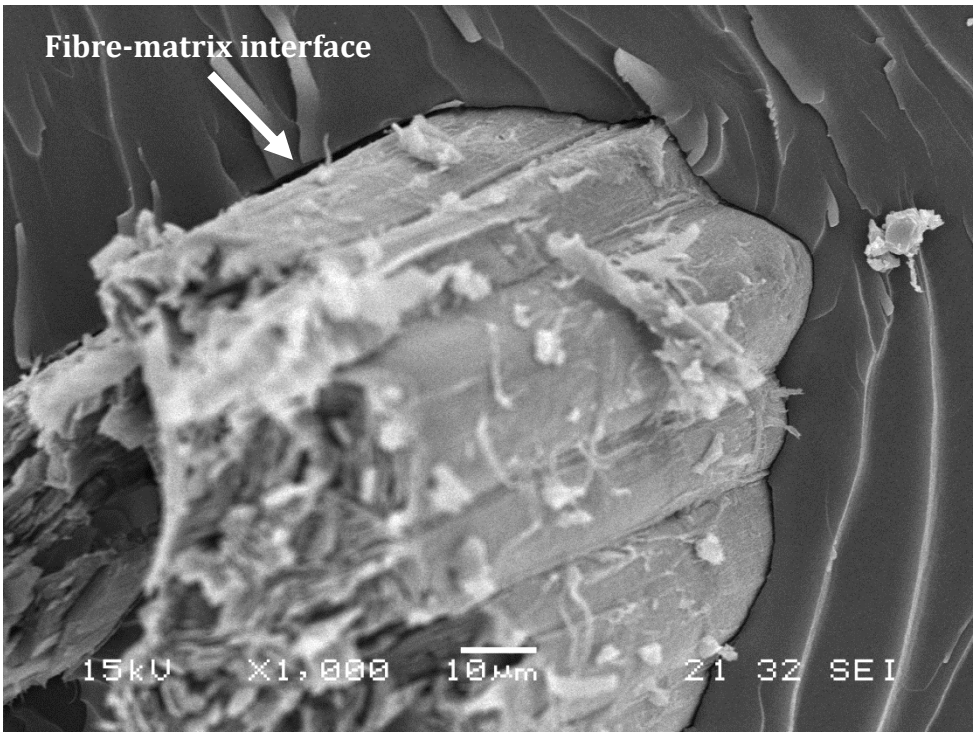

Figure 6.4. 1000x SEM image of AEHO/hemp fibre biocomposite.

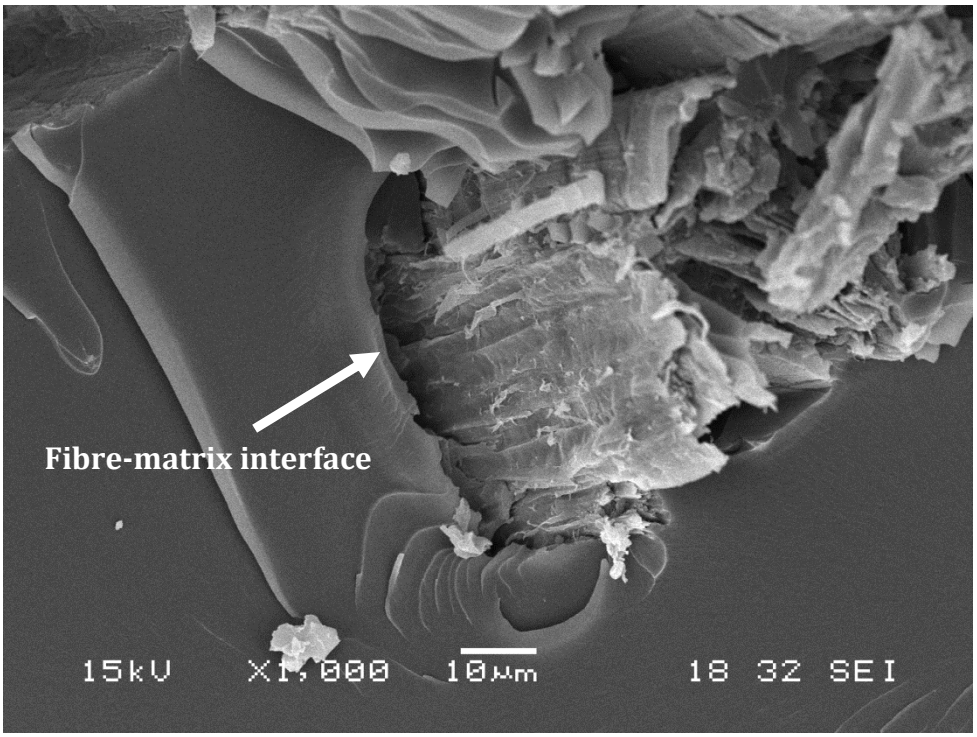

Figure 6.5. 1000x SEM image of VE/hemp fibre composite.

6.4.2 Interlaminar shear strength

The interlaminar shear strength of reinforced plastics is dependent upon on the fibre-matrix adhesion, resin strength, and moisture and void content in the composite itself (Agarwal & Broutman 1990; Halpin 1992; Kaw 1997; Reddy 2003; Wright 1991). ILSS has a strong influence on the structural performance of composites, since their strength is strongly influenced by factors weakening the interface. Petker (1965) reported that the ILSS increases with the increase in the matrix strength up to certain point whereby the influence of voids becomes increasingly important in the failure mechanism and the ILSS becomes constant despite further increases in resin strength.

From Figure 6.6 it is apparent that the interlaminar shear strength of the AEHO/hemp fibre biocomposites was 1.47 times higher than that of the VE/hemp fibre hybrid composites. During processing, styrene can form bubbles under high vacuum conditions due to its low vapour pressure, and these bubbles can sometimes be trapped in the fabric and remain as voids after the resin cures. However, the same fibre mat and processing conditions were used in the manufacture of the composite panels and the styrene content in the VE resin was the same as in the AEHO. For this reason, void content was almost identical in both composites.

Therefore, the ILSS results suggest that the hemp fibre-AEHO matrix interface is stronger than the hemp fibre-VE interface, since the strength of the VE resin is superior to that of the bioresin as discussed in section 6.4.3. The higher amount of hydroxyl groups present on the AEHO resin in comparison with the VE resin could be the reason for the better adhesion between fibres and resin in the biocomposites, since those functional groups interact with the hydroxyl groups present in the cellulose of the natural fibres to form strong hydrogen bonds.

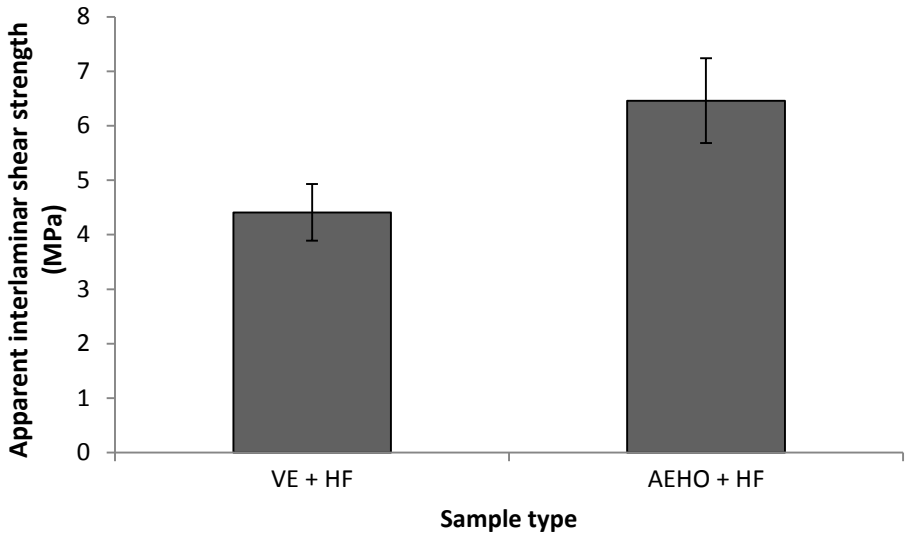

Figure 6.6. Interlaminar shear strength properties of AEHO based hemp fibre biocomposite.

6.4.3 Flexural properties

The flexural strength of the mentioned samples is shown in Figure 6.7. VE resin flexural strength was higher than that of the AEHO bioresin. No significant differences could be seen in the value of this property between the biocomposites and the hybrid composites. This is because while the biocomposite was 1.4 times stronger than the bioresin, the strength of the hybrid composite was found to be 40% lower than that of the neat VE resin. This behaviour was unexpected, since the tensile strength of hemp fibres (between 310-900 MPa (Dhakal et al. 2007; Zini & Scandola 2011)) is higher than the strength of the VE resin (86 MPa).

The observed decrease in flexural strength of the hybrid composite may be caused by the weak fibre-matrix interfacial adhesion present in the hybrid composites, as observed in the SEM images and the ILSS results. Since the bonding between fibres and matrix is low, the load is not transferred properly from the resin to the fibres and therefore most of the load is withstood by the resin itself. In addition, as seen in the SEM images (Figures 6.3 and 6.5), empty space between the fibres and the matrix act as flaws in the resin, and initiate cracks at stresses lower than that of the resin failure stress. Conversely, the

biocomposites showed a higher flexural strength than the neat bioresin because the strength of this resin is relatively low and the interfacial adhesion with the hemp fibres is stronger than in the case of the hybrid composites.

It is difficult to compare the values of flexural strength and modulus obtained in this work to those obtained by other researchers, since the reinforcement architecture, fibre volume fraction, manufacturing method and fibre and resin type are different. However, other researchers found the same decrease in the flexural properties of petrochemical matrices when natural fibres were added and hybrid composites were produced. Chin-San Wu et al. (2011) reported that the flexural strength of PBT/Sisal composites decreased as the sisal content was increased, and attributed this behaviour to the poor dispersion and compatibility between the fibres and the polymer. After grafting the PBT with acrylic acid, the authors reported that compatibility was improved and the flexural strength of the composites increased with the fibre volume fraction.

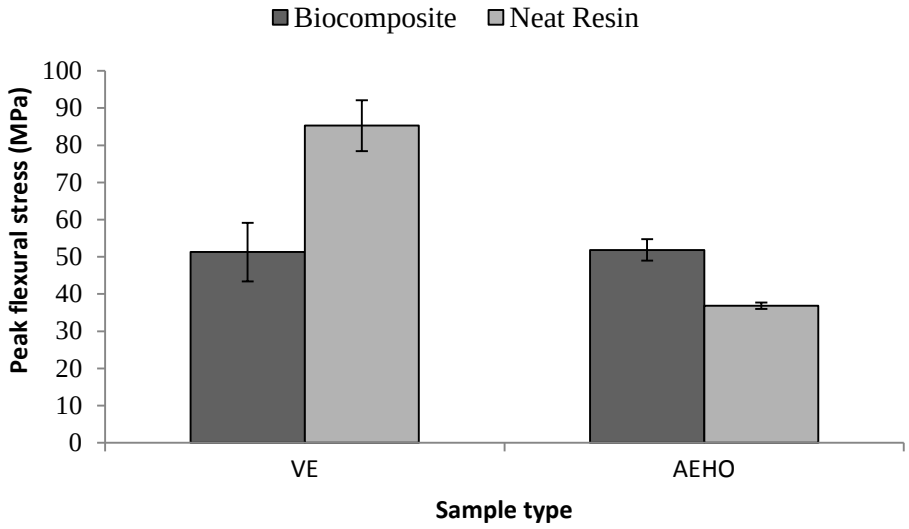

Figure 6.7. Peak flexural strength of AEHO based bioresin and biocomposite samples.

Figure 6.8 shows the flexural modulus of AEHO and VE resins as well as that of the biocomposites. This property was found to be three times higher in the VE resin than in the bioresin sample. Accordingly this is due to the lower crosslink density and the long fatty acid chains of the AEHO. Considering the results found for the biocomposites, it can be seen that the addition of the hemp fibre

reinforcement improved the flexural modulus found for the matrices by factors of 1.26 and 2.07 on VE and AEHO resins respectively. As a result, the biocomposite flexural modulus was just 23% lower than that of the hybrid composite.

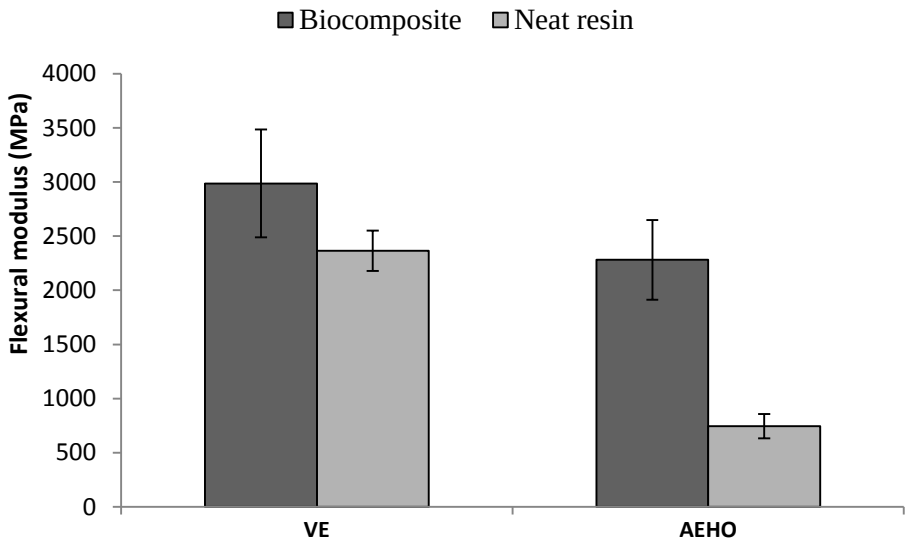

Figure 6.8. Flexural modulus of AEHO based bioresin and biocomposite samples.

6.4.4 Tensile properties

Despite the tensile strength and elastic modulus of the VE resin being higher than the AEHO bioresin no significant differences could be seen in the tensile behaviour of the biocomposites and the hybrid composites, as shown in Figure 6.9. Although the mean values of tensile strength and tensile modulus are 5% lower for the biocomposite, this difference falls within the error bars, thus no statement can be made regarding which one performs better in tensile behaviour. The high incompatibility of the hemp fibres with the VE resin is believed to be responsible for the low mechanical properties found in the hybrid composites, as seen previously in the flexural testing results, section 6.4.3. This incompatibility results in poor fibre-matrix adhesion which means compromised load transfer from the matrix to the fibres and the presence of flaws (empty space between fibre and resin, as seen in the SEM images). Therefore this hybrid composite is essentially behaving like a flawed VE resin.

In contrast however, the addition of hemp fibres improves the properties of the bioresin because these biocomposites present stronger fibre-matrix interfaces, as shown in the ILSS tests and SEM images. Consequently the tensile behaviour of hybrid composites and 100% hemp based biocomposites is similar.

The values of tensile strength and modulus obtained in this work for VE and AEHO/hemp fibre mat composites are similar to those obtained by Mehta et al. (2006) for polyester resin/hemp fibre mat (30% vol) compression moulded hybrid composites. The authors could improve these properties significantly by performing different treatments on the hemp mat (alkali, silane, UPE–MEKP, and acrylonitrile) showing the importance of treating natural fibre reinforcements to obtain good mechanical performance on the hybrid composites. In addition, compression moulded hybrid composites obtained by Mokhothu et al. (2011) and Chin-San Wu et al. (2011), showed lower tensile properties than those of the neat resin.

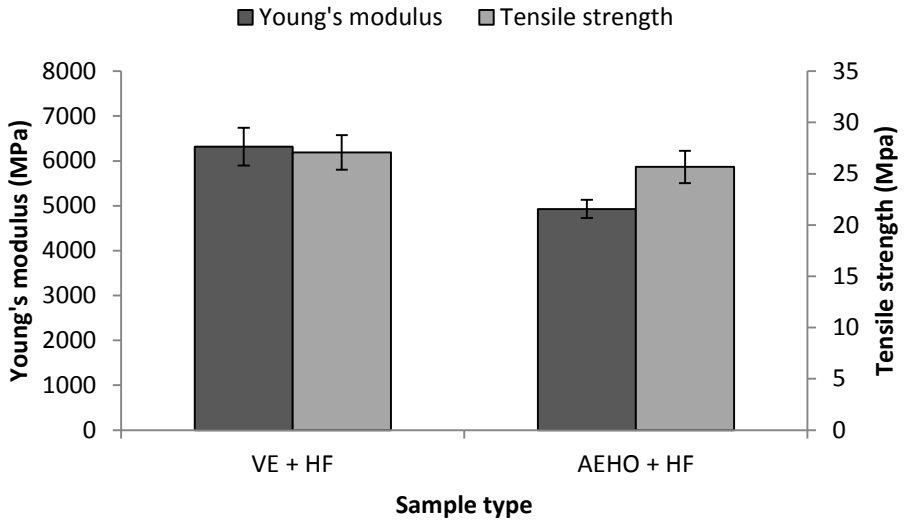

Figure 6.9. Tensile properties of AEHO based biocomposite samples.

6.4.5 Impact properties

As with all mechanical properties, the impact strength of composite materials is dependent upon the properties of matrix and fibres as well as the properties of the interface between them. Usually strong interfaces decrease the impact

strength of composites since energy-consumption mechanisms such as fibre pull out are inhibited and the fracture occurs in a brittle manner. In a Chapter 5, section 5.4.5 the Charpy impact strength for different synthetic epoxy/bioresin (based on EHO and ESO) blends was studied. Similarly in section 5.4.5 the Charpy impact strength of AEHO based jute reinforced biocomposites was also investigated. It was found that Charpy impact strength increased with increased bioresin concentration, be it EHO or AEHO based samples. This was attributed to the long fatty acid chains of the (AEVO) imparting flexibility and toughness to the matrix thereby increasing the energy required to break the biocomposite samples. For this reason, the impact strength of the VE resin is expected to be lower than that of the AEHO based bioresin, since the former is much less flexible, as shown in Figure 6.8. In addition, all of the results presented previously in this work (ILSS, tensile, flexural and SEM images) showed that the interface between the hemp fibres and the bioresin is stronger than the interface of the natural fibres with the synthetic VE resin. These two simultaneous effects are theorised as being responsible for the impact properties of VE hybrid composites to be lower than the value for the 100% hemp based biocomposites, as shown in figure 6.10.

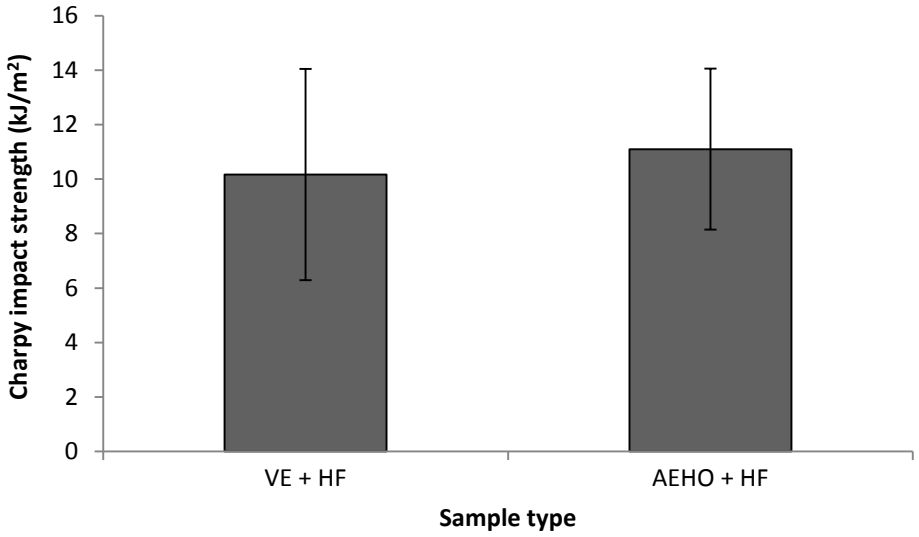

Figure 6.10. Charpy impact strength of AEHO based biocomposite samples.

6.4.6 Dynamic mechanical properties

DMA was performed on bioresin and biocomposite samples in order to characterize the viscoelastic behaviour of both VE and AEHO based neat bioresins and biocomposites. Figures 6.11 and 6.12 show the storage modulus plotted against temperature for the different bioresin and biocomposite samples. Table 6.1 summarises the storage modulus at 40 °C, T_g and crosslink density for both bioresin and biocomposite samples. As expected and consistent with the findings of the DMA of AEHO reinforced with jute fibre samples (section 5.4.6) VE based samples displayed higher storage modulus, T_g and crosslink density compared to AEHO based samples. Fibre reinforcement served to increase storage modulus, T_g and crosslink density for both sample types. Specifically, the addition of hemp fibre reinforcement resulted in an improvement in storage modulus by factors of approximately 1.37 and 2.34 for the VE and AEHO samples respectively. From examining Figure 6.11 it can be seen that the biocomposite samples have a less broad profile than those of the neat resin samples. Crosslink density was found to dramatically increase by factors of approximately 3.5 and 5.3 for the VE and AEHO samples respectively. Overall the behaviour and trends of this system are consistent with those found in section 5.4.6 for the jute fibre reinforced samples.

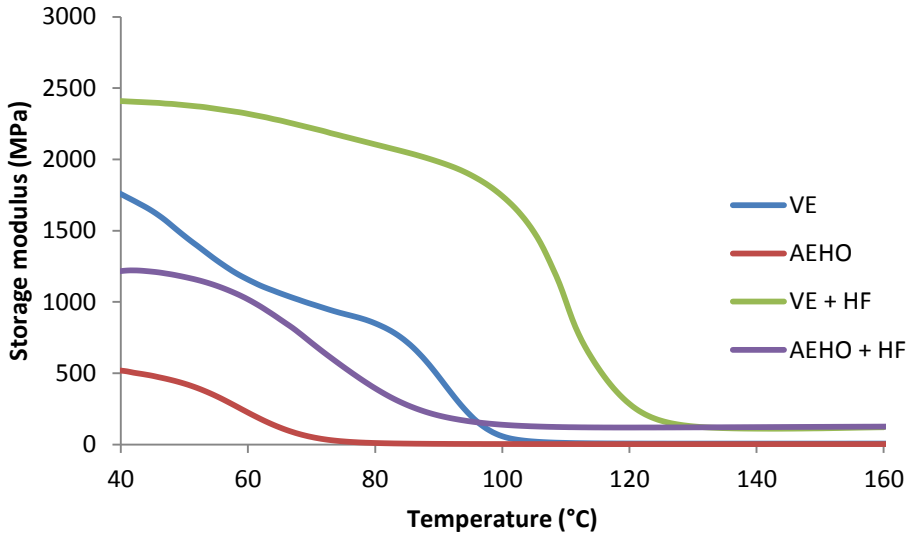

Figure 6.11. Storage modulus of AEHO based bioresins and biocomposites.

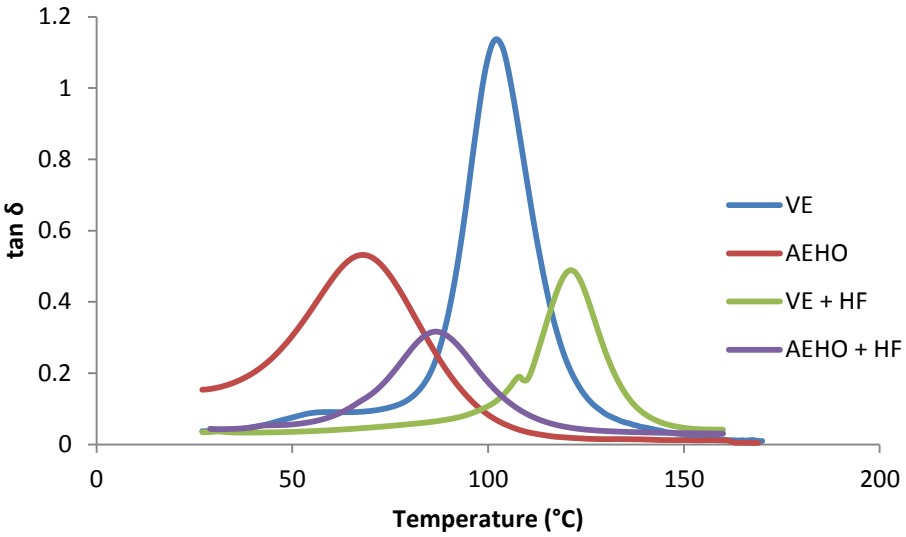

Figure 6.12. Tanδ of AEHO based bioresins and biocomposites.

Table 6.1. Dynamical mechanical properties of AEHO based bioresins and biocomposites.

Sample type	Storage modulus at 40 °C (MPa)	T_g (°C)	Crosslink density (mol/m³)
Neat bioresin			
VE	1757	102	6654
AEHO	519	68	4301
Biocomposite			
VE + HF	2409	121	23189
AEHO + HF	1216	87	22885

6.4.7 Moisture absorption

Figure 6.13 displays the moisture absorption behaviour for both VE and AEHO neat resin and hemp fibre reinforced samples. Table 6.2 summarises the diffusion coefficients and the saturation moisture content. It can be seen from the moisture absorption results that both the neat resin and biocomposite samples behaved consistent with a linear Fickian manner. After a rapid initial moisture absorption phase the samples began to slow in absorption until equilibrium was reached. As discussed previously in section 5.4.7 the transport mechanism was heavily dominated by the fibre reinforcement. This is apparent from both Figure 6.13 and Table 6.2 whereby it can be seen that the both the diffusion coefficient and saturation moisture content are markedly higher for the biocomposite samples compared with those of the neat resin. This is due to

the presence of the natural fibres in the biocomposites that have a characteristic hydrophilic nature and therefore absorb moisture. Biocomposite samples containing hemp fibre reinforcement exhibited higher diffusion coefficients and saturation moisture contents than those manufactured with jute fibre reinforcement. Although the manufacturing processes differ for the jute and hemp based samples it is thought that due to the vacuum infusion process some voids may be present in the hemp fibre samples. These voids provide additional transport and increase moisture absorption.

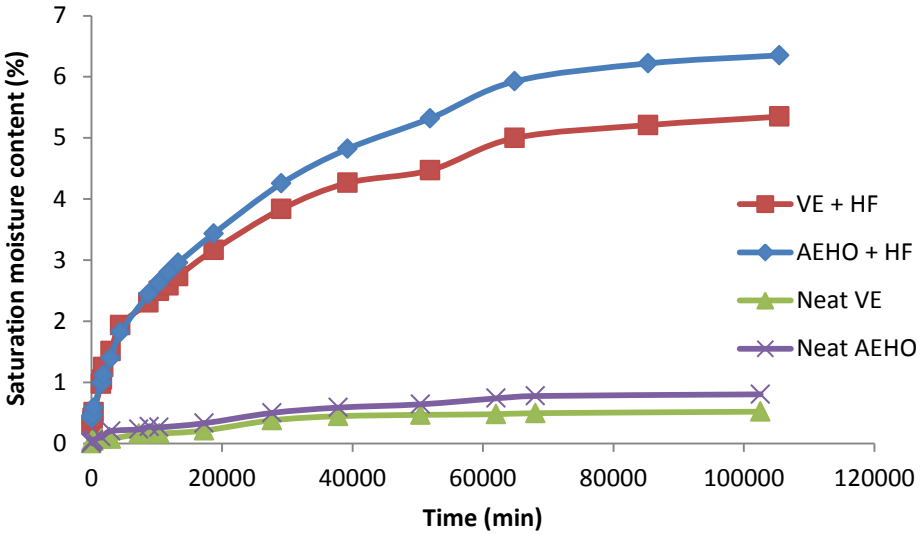

Figure 6.13. Moisture absorption of AEHO based bioresin and biocomposite samples.

Table 6.2. Water absorption properties of AEHO based bioresins and biocomposites.

Sample type	Diffusion coefficient $\times 10^{-6}$ (mm^2/s)	Saturation moisture Content (%)
Bioresin samples		
VE	0.801	0.52
AEHO	0.958	0.80
Jute fibre samples		
VE	9.14	5.35
AEHO	9.68	6.35

6.5 Conclusions

In this chapter, the mechanical performance (tensile, flexural, ILSS and impact) and the water absorption properties of 100% hemp based biocomposite panels were investigated and compared to those of a VE hybrid composite. The test samples were cut from panels manufactured by the vacuum infusion technique, using a hemp fibre mat as reinforcement and two different matrices: a commercial VE resin and an AEHO based bioresin synthesised in our laboratories.

Results showed that, except for the flexural modulus which was 23% higher in the case of the hybrid composite, no significant differences exist in the mechanical performance of both tested materials. The higher fibre/matrix compatibility of the biocomposites led to stronger fibre/matrix interfaces compensating the lower mechanical performance of the neat bioresin with respect to the VE. Therefore both biocomposites and hybrid composite showed to have similar flexural and tensile properties. In regards to the impact tests, it was observed that the higher impact strength of the neat bioresin combined with the stronger fibre/matrix adhesion led to a biocomposite material with similar impact strength than the panels made with the synthetic VE resin (VE/HF), which has lower impact strength than the bioresin.

Moisture absorption tests showed that AEHO based biocomposite samples displayed both higher diffusion coefficient and saturation moisture content than their equivalents with synthetic VE resin, where the presence of the natural fibre reinforcement was the dominant factor in the diffusion and absorption process.

VE based composite samples were found to display higher dynamical mechanical properties compared with AEHO based samples. Storage modulus and crosslink density were found to drastically increase with the addition of hemp fibre reinforcement. The value of the T_g temperature was also found to increase although to a lesser extent than the other properties.

This work demonstrated that if no chemical treatments are performed on natural reinforcements, plant oil based bioresins can be used instead of petrochemical resins since the final properties are very similar in both type of composites (hybrid composites and biocomposites), and therefore the environmental impact would be reduced. As a future work, the effect of different fibre treatments on 100% biocomposites and hybrid composites is proposed to be studied, with the aim of establishing the maximum mechanical properties that can be obtained in each case and see if the use of a petrochemical based matrix is ultimately justified.

Chapter 7

CONCLUSIONS AND RECOMENDATIONS FOR FUTURE RESEARCH

7.1 Summary

Currently the materials utilised within the civil engineering and construction industries, including fibre composites are predominately produced from non-renewable resources. There is therefore a requirement to increase the sustainability of these materials by incorporating those of a more biobased origin such as those investigated in the present study. Biocomposites produced with plant oil based resins and plant based fibres are one class of materials that has the potential to be used in a sustainable manner within these industries. A comprehensive review of the literature indicated that there is a requirement to research and develop novel plant oil based bioresins and biocomposites such as those based on hemp oil.

This research was the first to investigate the synthesis of hemp oil based bioresins and applying them to biocomposites. However, there are still several key challenges that need to be addressed for hemp oil based bioresins to become a viable alternative to commercially produced petrochemical based resins. The conclusions gathered from the different studies and chapters of this work have contributed to the understanding of hemp oil based bioresins and

their associated biocomposite performance and issues. Recommendations for further research are suggested in order to facilitate the adoption and implementation of hemp oil based bioresins for use in biocomposite applications.

The primary aim of this thesis was to assess the viability of using hemp oil as a precursor for biobased polymer resins. And if possible, develop and characterise novel types of bioresins based on hemp oil (EHO and AEHO) and assess the viability of using these bioresins as polymeric matrices for biocomposites. The primary aim of this thesis was addressed through research conducted in order to meet the following objectives:

1. Synthesise and characterise hemp oil (EHO and AEHO) based bioresins.

2. Develop curing kinetic parameters and models for EHO and AEHO based bioresins.
3. Determine and investigate the thermo-mechanical properties of neat cured EHO and AEHO based bioresins.

4. Determine and investigate the thermo-mechanical properties of EHO and AEHO based biocomposites (with natural fibre reinforcement).

5. Study the moisture absorption behaviour of EHO and AEHO based bioresins and biocomposites.

All five objectives were addressed throughout this thesis and are discussed in the following sections.

7.2 Primary conclusions from the study

7.2.1 Synthesis and characterisation of hemp oil based bioresins

EHO was successfully synthesised through the *in situ* epoxidation of hemp oil and resulted in an EHO and AEHO bioresin yields of approximately 75% by volume. AEHO was also synthesised from the EHO via *in situ* acrylation. Viscosities of hemp oil, EHO and AEHO were determined and compared with commercial ESO, synthetic epoxy and VE. Characterisation was performed on both EHO and AEHO to determine the number of C=C, the degree of epoxidation and the degree of acrylation. Numerous techniques were employed to achieve these specific objectives such as titrations, FTIR and ^{1}H-NMR.

Specifically the degree of C=C in the hemp oil and EHO was quantified by determining the iodine values, which respectively were 122 and 21 for hemp oil and EHO. Due to these values the conversion relative to iodine value was calculated as approximately 89.4%. FTIR was used to monitor the epoxidation and acrylation reactions by analysing the peaks pertinent to C=C consumption and epoxide and acrylate formation.

To determine the degree of epoxidation and the number of epoxy groups per triglyceride, titrations and ^{1}H-NMR were employed. EHO exhibited an oxirane oxygen content of approximately 8.3% and a relative conversion to oxirane of 89.4%. Similarly from ^{1}H-NMR spectroscopy analysis the oxirane oxygen content was calculated as approximately 8.6% and a relative to conversion to oxirane of 92%. Furthermore, according to the ^{1}H-NMR spectrum for hemp oil and EHO there are approximately 5.1 epoxy groups per triglyceride which compares favourably to those found for other oils.

According to the ^{1}H-NMR analysis of AEHO, acrylate peaks were present and were of the magnitude of approximately 4.1 acrylates per triglyceride. As per

the literature AESO and AELO were found to contain 3.4 and 5.7-5.8 acrylates per triglyceride respectively. Some epoxide homopolymerisation was found to occur in the synthesis of AEHO as represented by peaks 3.26-4.2 ppm. As a result of this epoxide homopolymerisation, conversion to AEHO was limited to approximately 81%. Overall this study has demonstrated that EHO and AEHO can be successfully synthesised and are in turn, comparable in quality to other plant oil based bioresins such as ECO, ESO, AESO, ELO and AELO.

7.2.2 Curing analysis and cure kinetic modelling of hemp oil based bioresins

EHO based samples

An EHO based bioresin system cured with two different systems; TETA and TETA/IPD was studied and compared. Cure kinetic analysis was performed using two dynamic models; Kissinger and Ozawa-Flynn-Wall and one autocatalytic model developed by Kamal modified to account for diffusion post-vitrification. It was found that the total heats of reaction were slightly influenced by the addition of IPD. From the observed dynamic activation energies the bioresin system containing IPD exhibited activation energies approximately 10% lower than the TETA system.

Both bioresin systems displayed autocatalytic mechanisms with the system containing IPD being characterised as heavily influenced by n^{th} order mechanicsms. Maximum conversions of the TETA/IPD system were consistently higher than those of the TETA system throughout the entire temperature range. Cure kinetic parameters where obtained for both systems with k_1 and k_2 increasing and decreasing respectively as temperature increased. The observed decrease in k_2 is thought to be due to an unidentified competive reaction. The total order of the reaction was found to decrease with an increase in temperature for both systems. An autocatalytic model developed by Kamal, modified to account for diffusion post-vitrification was found to satisfactorily

describe the cure behaviour of both bioresin/hardener systems. It was found that IPD increased the curing rate of the EHO bioresin systems.

AEHO based samples

The cure behaviour of AEHO based bioresins was investigated by dynamic and isothermal DSC. As expected, the maximum degree of cure increased as the cure temperature increased. The conversion was found to be 0.81 at the lowest temperature used in the DSC tests (50˚C) while the highest conversion was 0.92 at the highest cure temperature used (80˚C). The AEHO showed an autocatalytic behaviour and the vitrification phenomenon prevented the conversion reaching full conversion. Therefore, a modified expression of the autocatalytic Kamal's model that takes into account vitrification was used for the kinetic model. This model accurately fitted the experimental kinetic values for all temperatures, enabling it to be used in further numerical modelling of the curing of AEHO bioresins and biocomposites containing AEHO.

The activation energies estimated from dynamic and isothermal measurements were found to be similar. They were calculated from dynamic DSC data using the Kissinger (58.87 kJ/mol) and Ozawa-Flynn-Wall (62.02 kJ/mol) models, and from isothermal DSC data using the Arrhenius-type dependence of the reaction rate constants, k_1 and k_2, with temperature (58.94 kJ/mol and 45.32 kJ/mol respectively). The value of k_2 was found to be higher than the value of k_1 for all temperatures, suggesting that the curing behaviour of this bioresin is more influenced by autocatalytic mechanisms than by *n*th order mechanisms.

7.2.3 Thermo-mechanical properties of hemp oil based bioresins and jute fibre reinforced biocomposites

EHO based samples

EHO based bioresins and jute fibre reinforced biocomposites were prepared and compared with ESO based samples in terms of SEM, mechanical, dynamic mechanical and moisture absorption properties. EHO based biocomposite samples were found to display higher tensile stress, modulus of elasticity, flexural stress, flexural modulus and interlaminar shear strength than ESO based samples. Mechanical performance decreased for both EHO and ESO bioresins and biocomposites with increased bioresin loading. A significant reduction occurred after 30% bioresin concentration. As expected, synthetic epoxy control samples displayed superior mechanical performance compared with both EHO and ESO samples. From the SEM analysis it was confirmed that fibre-matrix interfacial adhesion was negatively affected with increasing bioresin content.

In terms of DMA, EHO based bioresin and biocomposite samples exhibited higher glass transition temperature (T_g), storage modulus, flexural properties and crosslink density than ESO bioresin and biocomposite samples. Moreover the addition of EHO/ESO bioresins to the synthetic epoxy resulted in a reduction of the T_g, the storage modulus and the crosslink density values. With an EHO/ESO concentration greater than 30% a significant reduction in properties was observed. The addition of jute fibre reinforcement resulted in higher crosslink densities than the neat resin samples primarily due to higher storage modulus values. The change in T_g for the bioresin compared to the biocomposite samples was found to be negligible.

Moisture absorption tests showed that synthetic control samples exhibited the lowest diffusion coefficient and saturation moisture content of all samples. The moisture absorption of the epoxy bioresin blends and biocomposite samples

was found to increase with increased bioresin loading. EHO based samples displayed lower diffusion coefficient and saturation moisture content than ESO based samples although the difference is minimal. The type of fibre reinforcement in the biocomposites, in particularly jute fibre, proved to be the dominant moisture absorption factor.

Overall this study has shown that EHO based bioresins when applied to jute fibre reinforced biocomposites can compete with commercially produced ESO in terms of mechanical performance, dynamic mechanical properties and water absorption characteristics. However the general, realistic conclusion is that both EHO and ESO are indeed best suited to a plasticizing role rather than complete bioresin matrices. Although it was shown that EHO can be used in higher concentrations than ESO, thereby resulting in more sustainable biocomposites.

AEHO based samples

ILSS was found to increase with increasing AEHO content suggesting that the fibre-matrix interfacial adhesion is stronger for the AEHO based samples compared with the VE based samples. This was confirmed to be the case with SEM analysis. In terms of flexural performance the flexural strength of the neat bioresins were found to be higher than those of the biocomposite samples. The VE based neat resin samples showed markedly higher flexural stress than samples containing AEHO. However when jute fibre reinforcement was incorporated, all three systems exhibited similar flexural performance. Flexural modulus was found to increase for all three biocomposite types over the bioresin samples. This was expected due to the addition of the relatively stiff jute fibres. VE samples displayed the highest flexural moduli for both neat bioresin and biocomposite samples however the difference was marginal in the case of the biocomposites. AEHO based jute reinforced biocomposites were subjected to tensile test. It was observed that VE based samples exhibited the highest tensile strength with the addition of AEHO resulting in a slight reduction in performance. Young's modulus was found to be similar for all three sample

types Charpy impact properties of all three samples were similar in nature, especially accounting for the standard deviation.

DMA was performed in order to characterise the visco-elastic behaviour of the AEHO based bioresins and biocomposites. Specifically VE based samples were found to have higher $T_{g,}$ storage modulus and crosslink density than AEHO based samples. As the AEHO content increased $T_{g,}$ storage modulus and crosslink density were found to decrease. The addition of jute fibre reinforcement resulted in a marginal increase in T_g, for the VE samples however a noticeable increase was observed for AEHO based samples. Similarly to the EHO/ESO samples the crosslink density was found to significantly increase with the addition of jute fibre reinforcement. In studying the moisture absorption of AEHO based bioresins and biocomposites it was found that increasing AEHO content resulted in increasing saturation moisture content and diffusion coefficient. Also as previously found with the EHO based samples overall the moisture absorption was heavily dominated by fibre addition rather than resin type.

7.2.4 Production and characterisation of 100% hemp based biocomposites

The mechanical performance (tensile, flexural, ILSS and impact) and the moisture absorption properties of 100% hemp based biocomposite panels were investigated and compared to those of a VE hybrid composite. The test samples were cut from panels prepared by the vacuum infusion technique, using a hemp fibre mat as reinforcement and two different matrices: a commercial VE resin and an AEHO based bioresin synthesised in our laboratories.

Results showed that, except for the flexural modulus that was 23% higher in the case of the hybrid composite, no significant differences exist in the mechanical performance of both tested materials. The higher fibre/matrix compatibility of the biocomposites led to stronger fibre/matrix interfaces compensating the

lower mechanical performance of the neat bioresin with respect to the VE. Therefore both biocomposites and hybrid composite showed to have practically the same flexural and tensile properties. Exactly the opposite happened in the impact tests, where the higher impact strength of the bioresin combined with the stronger fibre/matrix adhesion led to a composite material with similar impact strength than the one made with the vinyl ester resin, which has lower impact strength than the bioresin.

Moisture absorption tests showed that AEHO based samples displayed both higher diffusion coefficient and saturation moisture content however fibre reinforcement was the dominant transfer mechanism.

VE based samples were found to display higher dynamical mechanical properties compared with AEHO based samples. Storage modulus and crosslink density were found to drastically increase with the addition of hemp fibre reinforcement, as expected. T_g was also found to increase although to a lesser extent than the other properties.

This work showed that if no chemical treatments are performed on natural reinforcements, plant oil based bioresins should be used instead of petrochemical based resins since the final properties are very similar in both type of composites, and the environmental impact would be reduced. As a future work, the effect of different fibre treatments on 100% biocomposites and hybrid composites is to be studied, to investigate the maximum mechanical properties that can be obtained in each case and see if the use of a petrochemical based matrix is justified.

7.3 Recommendations for future research

The overall process of undertaking and completing this fundamental research into hemp oil based bioresins has brought to the fore certain limitations,

challenges and consequently opportunities for future research directions. It is expected that by focusing on these key areas it will help future researchers to realise the goal of 100% biobased biocomposites. The following section outlines the recommendations for future work.

7.3.1 Renewable hardeners and catalysts

Throughout the literature and indeed in this thesis synthetic non-renewable hardeners and catalysts are utilised for the curing of bioresins. So as to improve the sustainability of the bioresins and therefore the biocomposites it is essential to also utilise biobased hardeners and catalysts. Recently preliminary investigations from the CEEFC indicate that epoxy/EHO blends are able be cured with a cashew nut shell liquid (CNSL)-amine curing agent, PAA5012 (Satya Cashew Chemicals). Therefore future work should investigate the effects of using PAA5012 on the fundamental properties such as curing kinetics, thermo-mechanical and moisture absorption of epoxy/EHO bioresins and biocomposites. Researchers have developed systems for reducing or replacing styrene monomers in acrylated biopolymers through the use of fatty acid-based monomers (Campanella, La Scala & Wool 2009; La Scala, JJ et al. 2004). However biobased alternatives to synthetic catalysts for AEHO need to also be investigated and developed.

7.3.2 Fibre-matrix interfacial adhesion of hemp oil based matrices and natural fibres

This dissertation concluded that if no chemical treatments are performed on natural plant based fibre reinforcement, AEHO should be used instead of petrochemical based resins because the final properties are very similar in both type of composites and the environmental impact would be reduced. Therefore as a future work, the effect of different fibre treatments on 100% biocomposites and hybrid composites should be studied to investigate the maximum

mechanical properties that can be obtained in each case and see if the use of a petrochemical matrix and/or fibre treatments are justified.

7.3.3 Life cycle analysis of hemp oil bioresins and biocomposites

Although the hemp oil based bioresins and biocomposites studied in this dissertation offer sustainability it is central that they be subjected to life-cycle analysis (LCA). In order to compare these materials with those of which they aim to replace and/or complete LCA should be conducted to ascertain the full life-cycle cost, and also include for example; bioresin and biocomposite manufacturing, production and transportation of natural fibres and oils and reclamation and or end-of life recyclability. Currently this work is nonexistent for hemp based biopolymers and biocomposites and is a fundamental requirement for commercial production.

A.1 Composite processing techniques

There are numerous well established composite processing techniques present both throughout industry and the literature. Processing techniques are largely dependent upon factors such as number of components, cost and shape for example. Techniques may vary from highly technical automated methods used to service industry to simple labour intensive methods suited to laboratory sized samples such as hand lay-up. Some of the most common processing techniques are: vacuum infusion compression moulding, hand lay-up, film stacking and vacuum bagging. Of these techniques of interest to this dissertation are hand lay-up and vacuum infusion.

A.1.1 Hand lay-up

Hand lay-up is a simple, yet laborious composite processing technique. Typically a mould is used that has been treated with a gel coat, wax or mould release agent. Liquid thermosetting polymer is prepared and added to the fibre reinforcement. A roller is used to ensure even impregnation of the fibre reinforcement by the polymer resin, Figure A.1. It is important to use resins with a sufficient gel time. Modest capital outlay is required as it is a simple technique. Generally mechanical properties are not optimal as low fibre volumes of 30% or less are able to be used. Hand lay-up was used for the majority of the biocomposites produced in this work.

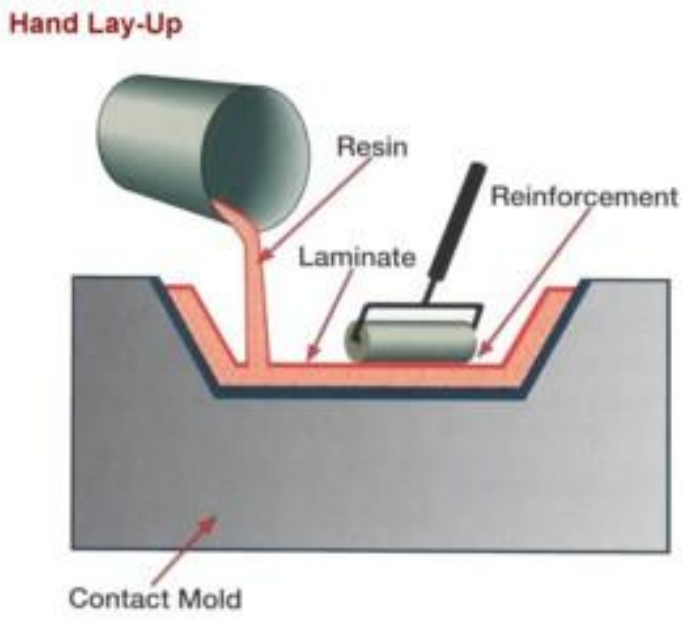

Figure A.1. Hand lay-up composite processing (Unknown).

A.1.2 Vacuum infusion

Liquid composite moulding (LCM) techniques, such as resin transfer moulding (RTM) or vacuum infusion (VI), Figure A.2 seem to be a good choice for processing biocomposites. They make it possible to obtain high quality laminates, repeatability, high surface finish and dimensional tolerances and because of the low processing temperatures, fibres do not suffer thermo-mechanical degradation as in some thermoplastic processing techniques. In LCM techniques a catalysed resin is forced through a mould which contains the dry reinforcement. In RTM, the preform (a stack of several layers of the fabric used as reinforcement) is compacted between two rigid mould faces. In VI a flexible vacuum bag is used as the upper part of the mould. When it became available, VI was used to manufacture the biocomposite panels due to the lower tooling cost required in this work. The main disadvantages of this technique are that it does not allow constant thickness along the panel and high surface finish in both sides of the part to be obtained.

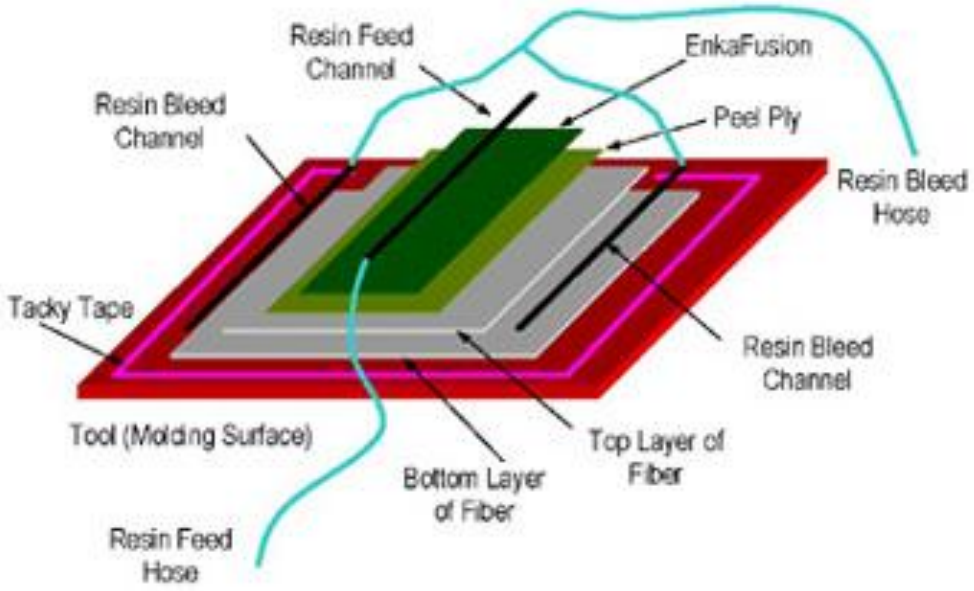

Figure A.2. vacuum infusion composite processing (Unknown).

References

ABC 2012, 'More oilseeds in Australia and around the world', viewed 26/04/2012, <http://www.abc.net.au/rural/news/content/201203/s3446491.htm>.

Adekunle, K, Åkesson, D & Skrifvars, M 2010a, 'Biobased composites prepared by compression molding with a novel thermoset resin from soybean oil and a natural-fiber reinforcement', *Journal of Applied Polymer Science*, vol. 116, no. 3, pp. 1759-65.

Adekunle, K 2010b, 'Synthesis of reactive soybean oils for use as a biobased thermoset resins in structural natural fiber composites', *Journal of Applied Polymer Science*, vol. 115, no. 6, pp. 3137-45.

Agarwal, BD & Broutman, LJ 1990, *Analysis and performance of fiber composites*, Wiley.

Agrawal, R, Saxena, NS, Sharma, KB, Thomas, S & Sreekala, MS 2000, 'Activation energy and crystallization kinetics of untreated and treated oil palm fibre reinforced phenol formaldehyde composites', *Materials Science and Engineering A*, vol. 277, no. 1-2, pp. 77-82.

Akil, HM, Cheng, LW, Mohd Ishak, ZA, Abu Bakar, A & Abd Rahman, MA 2009, 'Water absorption study on pultruded jute fibre reinforced unsaturated polyester composites', *Composites Science and Technology*, vol. 69, no. 11–12, pp. 1942-8.

Anwar, F, Latif, S & Ashraf, M 2006, 'Analytical characterization of hemp (*Cannabis sativa*) seed oil from different agro-ecological zones of Pakistan', *Journal of the American Oil Chemists' Society*, vol. 83, no. 4, pp. 323-9.

ASTM 2011, *Standard Test Method for Determination of the Iodine Value of Fats and Oils*, American Society for Testing and Materials.

Australian Oilseeds Federation 2010, *February Crop Report* Australian Oilseeds Federation.

Badrinarayanan, P, Lu, Y, Larock, RC & Kessler, MR 2009, 'Cure characterization of soybean oil - Styrene - Divinylbenzene thermosetting copolymers', *Journal of Applied Polymer Science*, vol. 113, no. 2, pp. 1042-9.

Bahl, OP, Shen, Z, Lavin, JG & Ross, RA 1998, *Manufacture of Carbon Fibers*, 3rd edn, Marcel Dekker Inc, New York.

Barral, L, Cano, J, López, J, López-Bueno, I, Nogueira, P, Abad, MJ & Ramírez, C 2000, 'Kinetic studies of the effect of ABS on the curing of an epoxy/cycloaliphatic amine resin', *Journal of Polymer Science Part B: Polymer Physics*, vol. 38, no. 3, pp. 351-61.

Beckermann, G 2007, 'Performance of Hemp-Fibre Reinforced Polypropylene Composite Materials ', PhD thesis, Univeristy of Waikato.

Behera, D & Banthia, AK 2008, 'Synthesis, characterization, and kinetics study of thermal decomposition of epoxidized soybean oil acrylate', *Journal of Applied Polymer Science*, vol. 109, no. 4, pp. 2583-90.

Bledzki, AK & Gassan, J 1999, 'Composites reinforced with cellulose based fibres', *Progress in Polymer Science*, vol. 24, no. 2, pp. 221-74.

Bogoeva-Gaceva, G, Avella, M, Malinconico, M, Buzarovska, A, Grozdanov, A, Gentile, G & Errico, ME 2007, 'Natural fiber eco-composites', *Polymer Composites*, vol. 28, no. 1, pp. 98-107.

Borden, G 1975, *Radiation curable compositions of acrylated epoxidized soybean oil amine compounds useful as inks and coatings and methods of curing same*, patent, USA.

Bos, H, Van Den Oever, M & Peters, O 2002, 'Tensile and compressive properties of flax fibres for natural fibre reinforced composites', *Journal of Materials Science*, vol. 37, no. 8, pp. 1683-92.

Bouchareb, B & Benaniba, MT 2008, 'Effects of epoxidized sunflower oil on the mechanical and dynamical analysis of the plasticized poly(vinyl chloride)', *Journal of Applied Polymer Science*, vol. 107, no. 6, pp. 3442-50.

Bunsell, AR & Renard, J 2005, *Fundamentals of fibre reinforced composite materials*, 1st edn, Taylor & Francis, USA.

Burgueño, R, Quagliata, MJ, Mehta, GM, Mohanty, AK, Misra, M & Drzal, LT 2005, 'Sustainable Cellular Biocomposites from Natural Fibers and Unsaturated Polyester Resin for Housing Panel Applications', *Journal of Polymers and the Environment*, vol. 13, no. 2, pp. 139-49.

Burgueño, R, Quagliata, MJ, Mohanty, AK, Mehta, G, Drzal, LT & Misra, M 2004, 'Load-bearing natural fiber composite cellular beams and panels', *Composites Part A: Applied Science and Manufacturing*, vol. 35, no. 6, pp. 645-56.

Burgueño, R 2005a, 'Hierarchical cellular designs for load-bearing biocomposite beams and plates', *Materials Science and Engineering A*, vol. 390, no. 1-2, pp. 178-87.

Burgueño, R 2005b, 'Hybrid biofiber-based composites for structural cellular plates', *Composites Part A: Applied Science and Manufacturing*, vol. 36, no. 5, pp. 581-93.

Cai, C, Dai, H, Chen, R, Su, C, Xu, X, Zhang, S & Yang, L 2008, 'Studies on the kinetics of *in situ* epoxidation of vegetable oils', *European Journal of Lipid Science and Technology*, vol. 110, no. 4, pp. 341-6.

Callaway, J 2004, 'Hempseed as a nutritional resource: An overview', *Euphytica*, vol. 140, no. 1, pp. 65-72.

Campanella, A & Baltanás, MA 2005, 'Degradation of the oxirane ring of epoxidized vegetable oils with hydrogen peroxide using an ion exchange resin', *Catalysis Today*, vol. 107-108, pp. 208-14.

Campanella, A, La Scala, JJ & Wool, RP 2009, 'The use of acrylated fatty acid methyl esters as styrene replacements in triglyceride-based thermosetting polymers', *Polymer Engineering & Science*, vol. 49, no. 12, pp. 2384-92.

Can, E, Wool, RP, Küsefo, S, gbreve & lu 2006a, 'Soybean- and castor-oil-based thermosetting polymers: Mechanical properties', *Journal of Applied Polymer Science*, vol. 102, no. 2, pp. 1497-504.

Can, E 2006b, 'Soybean and castor oil based monomers: Synthesis and copolymerization with styrene', *Journal of Applied Polymer Science*, vol. 102, no. 3, pp. 2433-47.

Canché-Escamilla, G, Cauich-Cupul, JI, Mendizábal, E, Puig, JE, Vázquez-Torres, H & Herrera-Franco, PJ 1999, 'Mechanical properties of acrylate-grafted henequen cellulose fibers and their application in composites', *Composites Part A: Applied Science and Manufacturing*, vol. 30, no. 3, pp. 349-59.

Chandrashekhara, K, Flanigan, V, Berring, N & Unser, J 2002, 'Pultrudable resin from soybean oil', in *44th International SAMPE Symposium*, pp. 1857-65.

Chandrashekhara, K, Sundararaman, S, Flanigan, V & Kapila, S 2005, 'Affordable composites using renewable materials', *Materials Science and Engineering: A*, vol. 412, no. 1-2, pp. 2-6.

Chen, J, Soucek, MD, Simonsick, WJ & Celikay, RW 2002, 'Epoxidation of partially norbornylized linseed oil', *Macromolecular Chemistry and Physics*, vol. 203, no. 14, pp. 2042-57.

Chen, W-Y, Wang, Y-Z & Chang, F-C 2004, 'Study on curing kinetics and curing mechanism of epoxy resin based on diglycidyl ether of bisphenol a and melamine phosphate', *Journal of Applied Polymer Science*, vol. 92, no. 2, pp. 892-900.

Chern, CS & Poehlein, GW 1987, 'A kinetic model for curing reactions of epoxides with amines', *Polymer Engineering & Science*, vol. 27, no. 11, pp. 788-95.

Cole, KC 1991, 'A new approach to modeling the cure kinetics of epoxy/amine thermosetting resins. 1. Mathematical development', *Macromolecules*, vol. 24, no. 11, pp. 3093-7.

Cooney, T 2009, 'Epoxidised resins from natural renewable resources', USQ Honours research project thesis.

Cooney, T, Cardona, F & Tran-Cong, T 2011, 'Kinetics of in situ epoxidation of hemp oil under heterogeneous reaction conditions: an overview with preliminary results', in *eddBE2011: 1st International Postgraduate Conference on Engineering, Designing and Developing the Built Environment for Sustainable Wellbeing*, Brisbane, pp. 106-11.

Cowles, G 2013, *Industrial hemp in Queensland*, Department of Agriculture, Fisheries and Forestry, viewed 28th April 2013 2013, <http://www.daff.qld.gov.au/26_14356.htm>.

Czub, P 2006a, 'Application of Modified Natural Oils as Reactive Diluents for Epoxy Resins', *Macromolecular Symposia*, vol. 242, no. 1, pp. 60-4.

Czub, P 2006b, 'Characterization of an Epoxy Resin Modified with Natural Oil-Based Reactive Diluents', *Macromolecular Symposia*, vol. 245-246, no. 1, pp. 533-8.

Dash, BN, Rana, AK, Mishra, HK, Nayak, SK, Mishra, SC & Tripathy, SS 1999, 'Novel, low-cost jute-polyester composites. Part 1: Processing, mechanical properties, and SEM analysis', *Polymer Composites*, vol. 20, no. 1, pp. 62-71.

Datta, C, Basu, D & Banerjee, A 2002, 'Mechanical and dynamic mechanical properties of jute fibers–Novolac–epoxy composite laminates', *Journal of Applied Polymer Science*, vol. 85, no. 14, pp. 2800-7.

Davey, SW 2004, 'A foundational investigation of vinyl ester / cenosphere composite materials for civil and structural engineering', PhD thesis, University of Southern Queensland.

Dhakal, HN, Zhang, ZY, Richardson, MOW & Errajhi, OAZ 2007, 'The low velocity impact response of non-woven hemp fibre reinforced unsaturated polyester composites', *Composite Structures*, vol. 81, no. 4, pp. 559-67.

Dickison, W 2000, *Integrative plant anatomy*, Academic Press, Burlington.

Dinda, S, Patwardhan, AV, Goud, VV & Pradhan, NC 2008, 'Epoxidation of cottonseed oil by aqueous hydrogen peroxide catalysed by liquid inorganic acids', *Bioresource Technology*, vol. 99, no. 9, pp. 3737-44.

Du, S, Guo, Z-S, Zhang, B & Wu, Z 2004, 'Cure kinetics of epoxy resin used for advanced composites', *Polymer International*, vol. 53, no. 9, pp. 1343-7.

Dupuy, J, Leroy, E & Maazouz, A 2000, 'Determination of activation energy and preexponential factor of thermoset reaction kinetics using differential scanning calorimetry in scanning mode: Influence of baseline shape on different calculation methods', *Journal of Applied Polymer Science*, vol. 78, no. 13, pp. 2262-71.

Dweib, MA, Hu, B, O'Donnell, A, Shenton, HW & Wool, RP 2004, 'All natural composite sandwich beams for structural applications', *Composite Structures*, vol. 63, pp. 147-57.

Dweib, MA, Hu, B, Shenton Iii, HW & Wool, RP 2006, 'Bio-based composite roof structure: Manufacturing and processing issues', *Composite Structures*, vol. 74, no. 4, pp. 379-88.

Ebbing, D & Gammon, S 2005, *General chemistry*, 8th edn, Houghton Mifflin.

Ecofibre 2010, *Hemp seed oil*, Ecofibre Industries Operations, viewed 6th September 2010, <http://www.ecofibre.com.au/hemp-seed-oil>.

Espinoza-Pérez, J, Haagenson, D, Pryor, S, Ulven, C & Wiesenborn, D 2009, 'Production and characterization of epoxidized canola oil', *ASABE* vol. 52, no. 4, pp. 1289-97.

Espinoza-Pérez, J, Wiesenborn, D, Haagenson, D & Ulven, C 2008, 'Study of the process parameters of the canola oil epoxidation', in *2008 ASABE Annual International Meeting*, Providence, Rhode Island.

Espinoza-Pérez, J, Wiesenborn, D, Kristi, T, Ulven, C & Tatlari, M 2007, 'Preparation and partial characterization of canola-based epoxy resins for bio-based plastic composites', in *2007 ASABE Annual International Meeting*, Minneapolis, Minnesota.

Espinoza-Pérez, J, Wiesenborn, D, Tostenson, K, Haagenson, D, Ulven, C, Tatlari, M & Gustafson, C 2007, 'Canola-based epoxy resins applied to plastic composites', in *2007 ASABE/CSBE North Central Intersectional Conference*, Fargo, North Dakota, USA.

Espinoza-Pérez, J, Wiesenborn, D, Ulven, C, Haagenson, D & Brudvik, R 2009, 'Epoxy resins from high-oleic oils applied to composites', in *2009 ASABE Annual International Meeting*, Reno, Nevada.

Flory, PJ 1953, *Polymer Chemistry*, Cornell University Press.

Flynn, JH & Wall, LA 1966, 'General treatment of the thermogravimetry of polymers', *Journal of Research of the National Bureau of Standards, Section A: Physics and Chemistry*, vol. 70A, no. 6, pp. 487-523.

Fowler, PA, Hughes, JM & Elias, RM 2006, 'Biocomposites: technology, environmental credentials and market forces', *Journal of the Science of Food and Agriculture*, vol. 86, no. 12, pp. 1781-9.

Francucci, G, Rodríguez, ES & Vázquez, A 2012, 'Experimental study of the compaction response of jute fabrics in liquid composite molding processes', *Journal of Composite Materials*, vol. 46, no. 2, pp. 155-67.

Fu, L, Yang, L, Dai, C, Zhao, C & Ma, L 2010, 'Thermal and mechanical properties of acrylated expoxidized-soybean oil-based thermosets', *Journal of Applied Polymer Science*, vol. 117, no. 4, pp. 2220-5.

Gassan, J & Bledzki, AK 1999, 'Possibilities for improving the mechanical properties of jute/epoxy composites by alkali treatment of fibres', *Composites Science and Technology*, vol. 59, no. 9, pp. 1303-9.

George, J, Sreekala, MS & Thomas, S 2001, 'A review on interface modification and characterization of natural fiber reinforced plastic composites', *Polymer Engineering & Science*, vol. 41, no. 9, pp. 1471-85.

Ghaemy, M, Barghamadi, M & Behmadi, H 2004, 'Cure kinetics of epoxy resin and aromatic diamines', *Journal of Applied Polymer Science*, vol. 94, no. 3, pp. 1049-56.

Ghaemy, M, Rostami, A & Omrani, A 2006, 'Isothermal cure kinetics and thermodynamics of an epoxy-nickel-diamine system', *Polymer International*, vol. 55, no. 3, pp. 279-84.

Gibbons, WS, Patel, HM & Kusy, RP 1997, 'Effects of plasticizers on the mechanical properties of poly(vinyl chloride) membranes for electrodes and biosensors', *Polymer*, vol. 38, no. 11, pp. 2633-42.

Gillard, E 2010, *Bio-based industrial products*, viewed 11th December 2012 2012.

Goldstein, H 1996, 'Catching up on composites', *American society of civil engineers*, vol. 66, no. 3, pp. 47-9.

Goldsworthy, B 1995, 'Composites - Just another building material - Only better', in *40th International SAMPE Symposium*, Covina.

González-Romero, VM & Casillas, N 1989, 'Isothermal and temperature programmed kinetic studies of thermosets', *Polymer Engineering & Science*, vol. 29, no. 5, pp. 295-301.

Goud, V, Patwardhan, A, Dinda, S & Pradhan, N 2007, 'Epoxidation of karanja (*Pongamia glabra*) oil catalysed by acidic ion exchange resin', *European Journal of Lipid Science and Technology*, vol. 109, no. 6, pp. 575-84.

Goud, V, Patwardhan, A & Pradhan, N 2006, 'Kinetics of *in situ* Epoxidation of Natural Unsaturated Triglycerides Catalyzed by Acidic Ion Exchange Resin', *Industrial & Engineering Chemistry Research*, vol. 46, no. 10, pp. 3078-85.

Goud, V, Pradhan, N & Patwardhan, A 2006, 'Epoxidation of karanja (*Pongamia glabra*) oil by H_2O_2', *Journal of the American Oil Chemists' Society*, vol. 83, no. 7, pp. 635-40.

Goud, VV, Dinda, S, Patwardhan, AV & Pradhan, NC 2010, 'Epoxidation of Jatropha (*Jatropha curcas*) oil by peroxyacids', *Asia-Pacific Journal of Chemical Engineering*, vol. 5, no. 2, pp. 346-54.

Goud, VV, Patwardhan, AV, Dinda, S & Pradhan, NC 2007, 'Kinetics of epoxidation of jatropha oil with peroxyacetic and peroxyformic acid catalysed by acidic ion exchange resin', *Chemical Engineering Science*, vol. 62, no. 15, pp. 4065-76.

Goud, VV, Patwardhan, AV & Pradhan, NC 2006, 'Studies on the epoxidation of mahua oil (*Madhumica indica*) by hydrogen peroxide', *Bioresource Technology*, vol. 97, no. 12, pp. 1365-71.

Govignon, Q, Bickerton, S & Kelly, P 2012, 'Experimental investigation into the post-filling stage of the resin infusion process', *Journal of Composite Materials*.

Grishchuk, S & Karger-Kocsis, J 2010, 'Hybrid thermosets from vinyl ester resin and acrylated epoxidized soybean oil (AESO)', *eXPRESS Polymer Letters*, vol. 5, no. 1, pp. 2-11.

Gunstone, FD 1996, *Fatty Acid and Lipid Chemistry*, Springer.

Hallstar 2011a, *Plasthall ELO MSDS*, Hallstar Company

Hallstar 2011b, *Plasthall ESO MSDS*, Hallstar Company

Halpin, JC 1992, *Primer on Composite Materials Analysis*, Second edn, CRC PressINC.

Haman, K, Badrinarayanan, P & Kessler, MR 2009, 'Cure characterization of the ring-opening metathesis polymerization of linseed oil-based thermosetting resins', *Polymer International*, vol. 58, no. 7, pp. 738-44.

Han, CD & Lee, D-S 1987, 'Curing behavior of unsaturated polyester resin with mixed initiators', *Journal of Applied Polymer Science*, vol. 34, no. 2, pp. 793-813.

Harper, CA 2002, *Handbook of Plastics, Elastomers & Composites* 4th edn, McGraw-Hill.

Helfferich, FG 2004, *Kinetics of multistep reactions*, 2nd edn, Elsevier, Amsterdam.

Ho, M-p, Wang, H, Lee, J-H, Ho, C-k, Lau, K-t, Leng, J & Hui, D 2012, 'Critical factors on manufacturing processes of natural fibre composites', *Composites Part B: Engineering*, vol. 43, no. 8, pp. 3549-62.

Hong, CK & Wool, RP 2005, 'Development of a bio-based composite material from soybean oil and keratin fibers', *Journal of Applied Polymer Science*, vol. 95, no. 6, pp. 1524-38.

Horie, K, Hiura, H, Sawada, M, Mita, I & Kambe, H 1970, 'Calorimetric investigation of polymerization reactions. III. Curing reaction of epoxides with amines', *Journal of Polymer Science Part A-1: Polymer Chemistry*, vol. 8, no. 6, pp. 1357-72.

Hu, B, Dweib, M, Wool, RP, Shenton, HW & Iii 2007, 'Bio-Based Composite Roof for Residential Construction', *Journal of Architectural Engineering*, vol. 13, no. 3, pp. 136-43.

Imam, SH, Greene, RV & Zaidi, BR 1999, *Biopolymers: utilizing nature's advanced materials*, American Chemical Society.

Islam, MS 2008, 'The Influence of Fibre Processing and Treatments on Hemp Fibre/Epoxy and Hemp Fibre/PLA Composites ', PhD thesis, The University of Waikato.

Islam, MS, Pickering, KL & Foreman, NJ 2009, 'Curing kinetics and effects of fibre surface treatment and curing parameters on the interfacial and tensile properties of hemp/epoxy composites', *Journal of Adhesion Science and Technology*, vol. 23, no. 16, pp. 2085-107.

Jacob, M, Francis, B, Thomas, S & Varughese, KT 2006, 'Dynamical mechanical analysis of sisal/oil palm hybrid fiber-reinforced natural rubber composites', *Polymer Composites*, vol. 27, no. 6, pp. 671-80.

Jacob, M, Varughese, KT & Thomas, S 2006, 'A study on the moisture sorption characteristics in woven sisal fabric reinforced natural rubber biocomposites', *Journal of Applied Polymer Science*, vol. 102, no. 1, pp. 416-23.

Jin, F-L & Park, S-J 2008, 'Thermomechanical behavior of epoxy resins modified with epoxidized vegetable oils', *Polymer International*, vol. 57, no. 4, pp. 577-83.

John, MJ & Thomas, S 2008, 'Biofibres and biocomposites', *Carbohydrate Polymers*, vol. 71, no. 3, pp. 343-64.

Joseph, K, Thomas, S & Pavithran, C 1996, 'Effect of chemical treatment on the tensile properties of short sisal fibre-reinforced polyethylene composites', *Polymer*, vol. 37, no. 23, pp. 5139-49.

Joseph, K, Varghese, S, Kalaprasad, G, Thomas, S, Prasannakumari, L, Koshy, P & Pavithran, C 1996, 'Influence of interfacial adhesion on the mechanical properties and fracture behaviour of short sisal fibre reinforced polymer composites', *European Polymer Journal*, vol. 32, no. 10, pp. 1243-50.

Joshi, SV, Drzal, LT, Mohanty, AK & Arora, S 2004, 'Are natural fiber composites environmentally superior to glass fiber reinforced composites?', *Composites Part A: Applied Science and Manufacturing*, vol. 35, no. 3, pp. 371-6.

Jústiz-Smith, NG, Virgo, GJ & Buchanan, VE 2008, 'Potential of Jamaican banana, coconut coir and bagasse fibres as composite materials', *Materials Characterization*, vol. 59, no. 9, pp. 1273-8.

Kabir, MM, Wang, H, Lau, KT, Cardona, F & Aravinthan, T 2012, 'Mechanical properties of chemically-treated hemp fibre reinforced sandwich composites', *Composites Part B: Engineering*, vol. 43, no. 2, pp. 159-69.

Kahraman, MV, Kayaman-Apohan, N, Ogan, Ae & Güngör, A 2006, 'Soybean oil based resin: A new tool for improved immobilization of α-amylase', *Journal of Applied Polymer Science*, vol. 100, no. 6, pp. 4757-61.

Kamal, MR 1974, 'Thermoset characterization for moldability analysis', *Polymer Engineering & Science*, vol. 14, no. 3, pp. 231-9.
Karbhari, V 1997, 'Application of composite materials to the renewal of twenty-first century infrastructure', in *11th International Conference on Composite Materials*, Melbourne, Australia.

Karkanas, PI & Partridge, IK 2000, 'Cure modeling and monitoring of epoxy/amine resin systems. I. Cure kinetics modeling', *Journal of Applied Polymer Science*, vol. 77, no. 7, pp. 1419-31.

Kaw, A 1997, *Mechanics of composite materials*, 1st edn, CRC-Press, Tampa, Florida, USA.

Kenny, JM 1994, 'Determination of autocatalytic kinetic model parameters describing thermoset cure', *Journal of Applied Polymer Science*, vol. 51, no. 4, pp. 761-4.

Kenny, JM & Trivisano, A 1991, 'Isothermal and dynamic reaction kinetics of high performance epoxy matrices', *Polymer Engineering & Science*, vol. 31, no. 19, pp. 1426-33.

Khot, SN, Lascala, JJ, Can, E, Morye, SS, Williams, GI, Palmese, GR, Kusefoglu, SH & Wool, RP 2001, 'Development and application of triglyceride-based polymers and composites', *Journal of Applied Polymer Science*, vol. 82, no. 3, pp. 703-23.

Kissinger, HE 1957, 'Reaction Kinetics in Differential Thermal Analysis', *Analytical Chemistry*, vol. 29, no. 11, pp. 1702-6.

Klempner, D, Sendijarevi′c, V, Sendijarevic, V & Aseeva, RM 2004, *Polymeric Foams And Foam Technology*, Hanser.

La Scala, JJ & Wool, RP 2002, 'Effect of FA composition on epoxidation kinetics of TAG', *Journal of the American Oil Chemists' Society*, vol. 79, no. 4, pp. 373-8.

La Scala, JJ & Wool, RP 2005, 'Property analysis of triglyceride-based thermosets', *Polymer*, vol. 46, no. 1, pp. 61-9.

La Scala, JJ 2002, 'The effects of triglyceride structure on the properties of plant oil-based resins', PhD thesis, University of Delaware.

La Scala, JJ, Sands, JM, Orlicki, JA, Robinette, EJ & Palmese, GR 2004, 'Fatty acid-based monomers as styrene replacements for liquid molding resins', *Polymer*, vol. 45, no. 22, pp. 7729-37.

La Scala, JJ & Wool, R 2002, 'The effect of fatty acid composition on the acrylation kinetics of epoxidized triacylglycerols', *Journal of the American Oil Chemists' Society*, vol. 79, no. 1, pp. 59-63.

La Scala, JJ & Wool, RP 2005, 'Rheology of chemically modified triglycerides', *Journal of Applied Polymer Science*, vol. 95, no. 3, pp. 774-83.

Laate, EA 2012, *Industrial Hemp Production in Canada*, Alberta Agriculture and Rural Development, viewed 24th April 2013 2013, <http://www1.agric.gov.ab.ca/>.

Le Troedec, M, Sedan, D, Peyratout, C, Bonnet, JP, Smith, A, Guinebretiere, R, Gloaguen, V & Krausz, P 2008, 'Influence of various chemical treatments on the composition and structure of hemp fibres', *Composites Part A: Applied Science and Manufacturing*, vol. 39, no. 3, pp. 514-22.

Lee, JH & Lee, JW 1994, 'Kinetic parameters estimation for cure reaction of epoxy based vinyl ester resin', *Polymer Engineering & Science*, vol. 34, no. 9, pp. 742-9.

Leizer, C, Ribnicky, D, Poulev, A, Dushenkov, S & Raskin, I 2000, 'The Composition of Hemp Seed Oil and Its Potential as an Important Source of Nutrition', *Journal of Nutraceuticals, Functional & Medical Foods*, vol. 2, no. 4, pp. 35-53.

Lem, K-W & Han, CD 1984, 'Thermokinetics of unsaturated polyester and vinyl ester resins', *Polymer Engineering & Science*, vol. 24, no. 3, pp. 175-84.

Li, X, Tabil, L & Panigrahi, S 2007, 'Chemical Treatments of Natural Fiber for Use in Natural Fiber-Reinforced Composites: A Review', *Journal of Polymers and the Environment*, vol. 15, no. 1, pp. 25-33.

Li, Y, Fu, L, Lai, S, Cai, X & Yang, L 2010, 'Synthesis and characterization of cast resin based on different saturation epoxidized soybean oil', *European Journal of Lipid Science and Technology*, vol. 112, no. 4, pp. 511-6.

Liang, G & Chandrashekhara, K 2006, 'Cure kinetics and rheology characterization of soy-based epoxy resin system', *Journal of Applied Polymer Science*, vol. 102, no. 4, pp. 3168-80.

Liang, G, Garg, A, Chandrashekhara, K, Flanigan, V & Kapila, S 2005, 'Cure Characterization of Pultruded Soy-based Composites', *Journal of Reinforced Plastics and Composites*, vol. 24, no. 14, pp. 1509-20.

Liu, KS 1997, *Soybeans: Chemistry, Technology and Utilization*, Springer.

Lu, J, Khot, S & Wool, RP 2005, 'New sheet molding compound resins from soybean oil. I. Synthesis and characterization', *Polymer*, vol. 46, no. 1, pp. 71-80.

Lu, J & Wool, RP 2006, 'Novel thermosetting resins for SMC applications from linseed oil: Synthesis, characterization, and properties', *Journal of Applied Polymer Science*, vol. 99, no. 5, pp. 2481-8.

Lu, M, Shim, M & Kim, S 1999, 'Dynamic DSC Characterization of Epoxy Resin by Means of the Avrami Equation', *Journal of Thermal Analysis and Calorimetry*, vol. 58, no. 3, pp. 701-9.

Malik, M, Choudhary, V & Varma, IK 2000, 'Current Status of Unsaturated Polyester Resins', *Journal of Macromolecular Science, Part C: Polymer Reviews*, vol. 40, no. 2-3, pp. 139-65.

Martini, DdS, Braga, BA & Samios, D 2009, 'On the curing of linseed oil epoxidized methyl esters with different cyclic dicarboxylic anhydrides', *Polymer*, vol. 50, no. 13, pp. 2919-25.

Mathew, D, Nair, CPR, Krishnan, K & Ninan, KN 1999, 'Catalysis of the cure reaction of bisphenol A dicyanate. A DSC study', *Journal of Polymer Science Part A: Polymer Chemistry*, vol. 37, no. 8, pp. 1103-14.

Matthews, FL & Rawlings, RD 1999, *Composite Materials: Engineering and Science*, Reprint edn, Chapman & Hall.

Mehta, G, Drzal, LT, Mohanty, AK & Misra, M 2006, 'Effect of fiber surface treatment on the properties of biocomposites from nonwoven industrial hemp fiber mats and unsaturated polyester resin', *Journal of Applied Polymer Science*, vol. 99, no. 3, pp. 1055-68.

Meier, MAR, Metzger, JO & Schubert, US 2007, 'Plant oil renewable resources as green alternatives in polymer science', *Chemical Society Reviews*, vol. 36, pp. 1788-802.

Meyer, P, Techaphattana, N, Manundawee, S, Sangkeaw, S, Junlakan, W & Tongurai, C 2008, 'Epoxidation of soybean oil and jatropha oil', *Thammasat International Journal of Science and Technology*, vol. 13.

Mishra, HK, Dash, BN, Tripathy, SS & Padhi, BN 2000, 'A study on mechanical performance of jute-epoxy composites', *Polymer-Plastics Technology and Engineering*, vol. 39, no. 1, pp. 187-98.

Miyagawa, H, Misra, M, Drzal, LT & Mohanty, AK 2005, 'Fracture toughness and impact strength of anhydride-cured biobased epoxy', *Polymer Engineering & Science*, vol. 45, no. 4, pp. 487-95.

Miyagawa, H, Mohanty, A, Misra, M & Drzal, L 2004, 'Thermo-physical and impact properties of epoxy containing epoxidized linseed oil - Amine-cured epoxy', *Macromolecular Materials and Engineering*, vol. 289, no. 7, pp. 636-41.

Miyagawa, H, Mohanty, AK, Burgueño, R, Drzal, LT & Misra, M 2007, 'Novel biobased resins from blends of functionalized soybean oil and unsaturated polyester resin', *Journal of Polymer Science Part B: Polymer Physics*, vol. 45, no. 6, pp. 698-704.

Mohanty, AK & Misra, M 1995, 'Studies on Jute Composites—A Literature Review', *Polymer-Plastics Technology and Engineering*, vol. 34, no. 5, pp. 729-92.

Mohanty, AK, Misra, M & Hinrichsen, G 2000, 'Biofibres, biodegradable polymers and biocomposites: An overview', *Macromolecular Materials and Engineering*, vol. 276-277, no. 1, pp. 1-24.

Mohanty, AK, Wibowo, A, Misra, M & Drzal, LT 2004, 'Effect of process engineering on the performance of natural fiber reinforced cellulose acetate biocomposites', *Composites Part A: Applied Science and Manufacturing*, vol. 35, no. 3, pp. 363-70.

Mokhothu, TH, Guduri, BR & Luyt, AS 2011, 'Kenaf fiber-reinforced copolyester biocomposites', *Polymer Composites*, vol. 32, no. 12, pp. 2001-9.

Mooleki, S, McVicar, R, Brenzil, C, Panchuk, K, Pearse, P, Hartley, S, Hanks, A & Friesen, K 2006, *Hemp Production in Saskatchewan*, Saskatchewan Ministry of Agriculture, Saskatchewan.

Morye, SS & Wool, RP 2005, 'Mechanical properties of glass/flax hybrid composites based on a novel modified soybean oil matrix material', *Polymer Composites*, vol. 26, no. 4, pp. 407-16.

Mungroo, R, Pradhan, N, Goud, V & Dalai, A 2008, 'Epoxidation of Canola Oil with Hydrogen Peroxide Catalyzed by Acidic Ion Exchange Resin', *Journal of the American Oil Chemists' Society*, vol. 85, no. 9, pp. 887-96.

Murphy, S 2012, 'The hemp comeback', *Landline, ABC*.

O'Donnell, A, Dweib, MA & Wool, RP 2004, 'Natural fiber composites with plant oil-based resin', *Composites Science and Technology*, vol. 64, no. 9, pp. 1135-45.

Olsen, JK 2004, *An information paper on industrial hemp (industrial cannabis)*, Department of Primary Industries and Fisheries, Queensland Government. .

Omrani, A, Simon, LC, Rostami, AA & Ghaemy, M 2008, 'Cure kinetics, dynamic mechanical and morphological properties of epoxy resin-Im6NiBr2 system', *European Polymer Journal*, vol. 44, no. 3, pp. 769-79.

Ozawa, T 1965, 'A new method of analysing thermogravimetric data', *Bulletin of the Chemical Society of Japan*, vol. 38, no. 11, pp. 1881-6.

Park, S-J, Jin, F-L & Lee, J-R 2004, 'Synthesis and Thermal Properties of Epoxidized Vegetable Oil', *Macromolecular Rapid Communications*, vol. 25, no. 6, pp. 724-7.

Parzuchowski, PG, Jurczyk-Kowalska, M, Ryszkowska, J & Rokicki, G 2006, 'Epoxy resin modified with soybean oil containing cyclic carbonate groups', *Journal of Applied Polymer Science*, vol. 102, no. 3, pp. 2904-14.

Patel, PS, Shah, PP & Patel, SR 1986, 'Differential scanning calorimetry investigation of curing of bisphenolfurfural resins', *Polymer Engineering & Science*, vol. 26, no. 17, pp. 1186-90.

Pelletier, H, Belgacem, N & Gandini, A 2006, 'Acrylated vegetable oils as photocrosslinkable materials', *Journal of Applied Polymer Science*, vol. 99, no. 6, pp. 3218-21.

Petker, I 1965, 'The influence of resin strength and defects on the interlaminar shear strength of filament-wound composites', *Polymer Engineering & Science*, vol. 5, no. 1, pp. 49-58.

Petrovic, ZS, Zlatanic, A, Lava, CC & Sinadinovic-Fiscaroner, S 2002, 'Epoxidation of soybean oil in toluene with peroxoacetic and peroxoformic acids - kinetics and side reactions', *European Journal of Lipid Science and Technology*, vol. 104, no. 5, pp. 293-9.

Peyser, P & Bascom, WD 1977, 'Kinetics of epoxy resin polymerization using differential scanning calorimetry', *Journal of Applied Polymer Science*, vol. 21, no. 9, pp. 2359-73.

Plate, A 2006, 'Queensland leads nation's hemp industry with new plant', *ABC Rural*, 7th July 2006.

Prime, RB, Michalski, C & Neag, CM 2005, 'Kinetic analysis of a fast reacting thermoset system', *Thermochimica Acta*, vol. 429, no. 2, pp. 213-7.

Puglia, D, Biagiotti, J & Kenny, JM 2005, 'A Review on Natural Fibre-Based Composites - Part II', *A Review on Natural Fibre-Based Composites—Part II*, vol. 1, no. 3, pp. 23-65.

Puig, G 2006, 'Biobased Thermosets from Vegetable Oils. Synthesis, Characterization, and Properties ', PhD thesis, UNIVERSITAT ROVIRA I VIRGILI.

Queensland State Government 2012, *Agricultural overview*, Queensland Government, viewed 11th December 2012 2012, <http://www.business.qld.gov.au/industry/agriculture/agriculture>.

Rahman, MM, Zainuddin, S, Hosur, MV, Robertson, CJ, Kumar, A, Trovillion, J & Jeelani, S 'Effect of NH2-MWCNTs on crosslink density of epoxy matrix and ILSS properties of e-glass/epoxy composites', *Composite Structures*, no. 0.

Ramírez, C, Rico, M, Barral, L, Díez, J, García-Garabal, S & Montero, B 2007, 'Organic/inorganic hybrid materials from an epoxy resin cured by an amine silsesquioxane', *Journal of Thermal Analysis and Calorimetry*, vol. 87, no. 1, pp. 69-72.

Ramos, JA, Pagani, N, Riccardi, CC, Borrajo, J, Goyanes, SN & Mondragon, I 2005, 'Cure kinetics and shrinkage model for epoxy-amine systems', *Polymer*, vol. 46, no. 10, pp. 3323-8.

Ray, D, Sarkar, BK & Bose, NR 2002, 'Impact fatigue behaviour of vinylester resin matrix composites reinforced with alkali treated jute fibres', *Composites Part A: Applied Science and Manufacturing*, vol. 33, no. 2, pp. 233-41.

Reddy, JN 2003, *Mechanics of composite materials and shells-theory and analysis*, CRC Press, Boca Raton.

Rong, MZ, Zhang, MQ, Liu, Y, Yang, GC & Zeng, HM 2001, 'The effect of fiber treatment on the mechanical properties of unidirectional sisal-reinforced epoxy composites', *Composites Science and Technology*, vol. 61, no. 10, pp. 1437-47.

Rosu, D, Mititelu, A & Cascaval, CN 2004, 'Cure kinetics of a liquid-crystalline epoxy resin studied by non-isothermal data', *Polymer Testing*, vol. 23, no. 2, pp. 209-15.

Saheb, DN & Jog, JP 1999, 'Natural fiber polymer composites: A review', *Advances in Polymer Technology*, vol. 18, no. 4, pp. 351-63.

Sanders, T & Lewis, F 2007, *Review of Nutritional Attributes of GOOD OIL (Cold Pressed Hemp Seed Oil)*, King's College London, London.

Shabeer, A, Chandrashekhara, K & Schuman, T 2007, 'Synthesis and characterization of soy-based nanocomposites', *Journal of Composite Materials*, vol. 41, no. 15, pp. 1825-49.

Shenton, H & Wool, RP 2004, 'Bio-based composite material for whole house design: Potential applications and research needs', in *NSF-PATH housing research agenda workshop*, vol. 2, pp. 327-33.

Sinadinović-Fišer, S, Janković, M & Petrović, Z 2001, 'Kinetics of *in situ* epoxidation of soybean oil in bulk catalyzed by ion exchange resin', *Journal of the American Oil Chemists' Society*, vol. 78, no. 7, pp. 725-31.

Singh, B & Gupta, M 2005, 'Natural fiber composites for building applications', in *Natural fibers, Bioploymers and Biocomposites*, CRC Press, pp. 261-90.

Singh, B, Gupta, M & Verma, A 2000, 'The durability of jute fibre-reinforced phenolic composites', *Composites Science and Technology*, vol. 60, no. 4, pp. 581-9.

Sourour, S & Kamal, MR 1976, 'Differential scanning calorimetry of epoxy cure: isothermal cure kinetics', *Thermochimica Acta*, vol. 14, no. 1–2, pp. 41-59.

Souza, AGd, Santos, JCO, Conceição, MM, Silva, MCD & Prasad, S 2004, 'A thermoanalytic and kinetic study of sunflower oil', *Brazilian Journal of Chemical Engineering*, vol. 21, pp. 265-73.

Stevenson, JK 1986, 'Free radical polymerization models for simulating reactive processing', *Polymer Engineering & Science*, vol. 26, no. 11, pp. 746-59.

Takahashi, T, Hirayama, K-i, Teramoto, N & Shibata, M 2008, 'Biocomposites composed of epoxidized soybean oil cured with terpene-based acid anhydride and cellulose fibers', *Journal of Applied Polymer Science*, vol. 108, no. 3, pp. 1596-602.

Tan, SG & Chow, WS 2010, 'Thermal Properties, Fracture Toughness and Water Absorption of Epoxy-Palm Oil Blends', *Polymer-Plastics Technology and Engineering*, vol. 49, no. 9, pp. 900 - 7.

Tatlari, M 2008, 'Vegetable oil-based epoxy resin for structural composite material manufacturing', North Dakota State University.

Tellez, G, Vigueras-Santiago, E, Hernández-López, S & Bilyeu, B 2008, 'Synthesis and thermal cross-linking study of partially-aminated epoxidized linseed Oil', *Designed Monomers and Polymers*, vol. 11, pp. 435-45.

Thomsen, AB, Thygesen, A, Bohn, V, Nielsen, KV, Pallesen, B & Jørgensen, MS 2006, 'Effects of chemical-physical pre-treatment processes on hemp fibres for reinforcement of composites and for textiles', *Industrial Crops and Products*, vol. 24, no. 2, pp. 113-8.

Thygesen, A 2006, 'Properties of hemp fibre polymer composites -An optimisation of fibre properties using novel defibration methods and fibre characterisation', PhD thesis, PhD thesis, The Royal Agricultural and Veterinary University of Denmark.

Trecker, D, Borden, G & Smith, O 1976a, *Acrylated epoxidized soybean oil amine compositions and method*, patent, USA.

Trecker, D 1976b, *Method for curing acrylated epoxidized soybean oil amine compositions*, patent, USA.

Tripathy, SS, Di Landro, L, Fontanelli, D, Marchetti, A & Levita, G 2000, 'Mechanical properties of jute fibers and interface strength with an epoxy resin', *Journal of Applied Polymer Science*, vol. 75, no. 13, pp. 1585-96.

Unknown *Composite Fabrication Method* viewed 10th December 2012, <http://www.flexidynamic.com/method.htm>.

Unknown *What is Vacuum Infusion Processing (VIP)?*, viewed 10th December 2012 2012, <http://www.structuralcd.com.au/composite-fabrication/vacuum-infusion-process.php>.

Valadez-Gonzalez, A, Cervantes-Uc, JM, Olayo, R & Herrera-Franco, PJ 1999, 'Effect of fiber surface treatment on the fiber-matrix bond strength of natural fiber reinforced composites', *Composites Part B: Engineering*, vol. 30, no. 3, pp. 309-20.

Van Erp, G & Ayers, S 2004, 'A fair dinkum approach to fibre composites in civil engineering', in *2nd international conference advanced polymer composites for structural applications in construction*, Guildford, UK.

Van Erp, G & Rogers, D 2003, 'Development of sunflower oil resins for fibre composite applications', in *14th Australian Sunflower Association Conference*, Gold Coast, Queensland.

Vilas, JL, Laza, JM, Garay, MT, Rodríguez, M & León, LM 2001, 'Unsaturated polyester resins cure: Kinetic, rheologic, and mechanical-dynamical analysis. I. Cure kinetics by DSC and TSR', *Journal of Applied Polymer Science*, vol. 79, no. 3, pp. 447-57.

Vlček, T & Petrović, Z 2006, 'Optimization of the chemoenzymatic epoxidation of soybean oil', *Journal of the American Oil Chemists' Society*, vol. 83, no. 3, pp. 247-52.

Vyazovkin, S & Sbirrazzuoli, N 1996, 'Mechanism and Kinetics of Epoxy−Amine Cure Studied by Differential Scanning Calorimetry', *Macromolecules*, vol. 29, no. 6, pp. 1867-73.

Vyazovkin, S 1999, 'Kinetic methods to study isothermal and nonisothermal epoxy-anhydride cure', *Macromolecular Chemistry and Physics*, vol. 200, no. 10, pp. 2294-303.

Wambua, P, Ivens, J & Verpoest, I 2003, 'Natural fibres: can they replace glass in fibre reinforced plastics?', *Composites Science and Technology*, vol. 63, no. 9, pp. 1259-64.

Williams, GI & Wool, RP 2000, 'Composites from natural fibers and soy oil resins', *Applied Composite Materials*, vol. 7, no. 5, pp. 421-32.

Wisanrakkit, G & Gillham, JK 1990, 'The glass transition temperature (Tg) as an index of chemical conversion for a high-Tg amine/epoxy system: Chemical and diffusion-controlled reaction kinetics', *Journal of Applied Polymer Science*, vol. 41, no. 11-12, pp. 2885-929.

Wool, RP & Khot, S 2001, 'Bio-based resins and natural fibers', in *ASM Handbook*, ASM International, vol. 21, pp. 184-93.

Wool, RP, Kusefoglu, S, Palmese, G, Khot, S & Zhao, R 2000, *High modulus polymers and composites from plant oils*, University of Delaware, Newark, Del., patent, 6121398.

Wool, RP & Sun, X 2005, *Bio-based polymers and composites*, 1st edn, Oxford: Academic.

Wright, WW 1991, 'Design with advanced composite materials. Edited by L. N. Phillips, The Design Council, (Springer-Verlag), Berlin, Heidelberg, London, 1989. pp. 365, price DM 118.00. ISBN 0-85072-238-1', *Polymer International*, vol. 26, no. 3, pp. 204-.

Wu, C-S, Yen, F-S & Wang, C-Y 2011, 'Polyester/natural fiber biocomposites: preparation, characterization, and biodegradability', *Polymer Bulletin*, vol. 67, no. 8, pp. 1605-19.

Yousefi, A, Lafleur, PG & Gauvin, R 1997, 'Kinetic studies of thermoset cure reactions: A review', *Polymer Composites*, vol. 18, no. 2, pp. 157-68.

Zakaria, S & Kok Poh, L 2002, 'Polystyrene-Benzoylated EFB Reinforced Composites', *Polymer-Plastics Technology and Engineering*, vol. 41, no. 5, pp. 951-62.

Zhan, M & Wool, RP 2010, 'Biobased composite resins design for electronic materials', *Journal of Applied Polymer Science*, vol. 118, no. 6, pp. 3274-83.

Zhu, J, Chandrashekhara, K, Flanigan, V & Kapila, S 2004, 'Curing and mechanical characterization of a soy-based epoxy resin system', *Journal of Applied Polymer Science*, vol. 91, no. 6, pp. 3513-8.

Zhu, J, Chandrashekhara, K, Flanigan, V & Kapila, S 2004, 'Manufacturing and mechanical properties of soy-based composites using pultrusion', *Composites Part A: Applied Science and Manufacturing*, vol. 35, no. 1, pp. 95-101.

Zini, E & Scandola, M 2011, 'Green composites: An overview', *Polymer Composites*, vol. 32, no. 12, pp. 1905-15.